

**MODELLING DRUG DELIVERY MECHANISMS FOR MICROENCAPSULATED
SUBSTANCES APPLIED ON TEXTILE SUBSTRACTS**

Dissertation:

To obtain the doctor's degree at the Universitat Politècnica de Catalunya

Textile Engineering Department

Directors: Dr. Manuel José Lis and Dr. Josep Valldeperas

by Núria Carreras Parera

Terrassa,

18 of May 2012

ACKNOWLEDGEMENTS

Firstly, I would like to thank all those people who have given their time and dedication to carry out some of the analytical tests and provide the necessary resources to develop the project. I thank Mercedes Escusa at the Department of Textile and Paper Engineering, she helped me taking pictures with the scanning electron microscope (SEM). I thank Dra. Meritxell Martí at the Spanish Council for Scientific Research Institute of Advanced Chemistry of Catalonia (CSIC-IQAC), for the analysis of particle size distribution in the characterization of the microcapsules. I thank Dr. Josep Valldeperas and Dr. Fernando Carrillo at the Textile and Chemical Technology Laboratory of INTEXTER, for their resources that enabled me to make the impregnation of the microcapsules on textiles by using the technique of the pad-dry. I thank Dr. Jose Luis Parra, Dra. M^a Lluïsa Coderch, Dra. Cristina Alonso and Dra. Meritxell Martí again, at the Spanish Council for Scientific Research Institute of Advanced Chemistry of Catalonia (CSIC-IQAC), who led me use other techniques, which were necessary for the validation of the microencapsulated system; such as their *in vitro* technique by Franz diffusion cells, which has enabled the kinetic study of drug delivery system through the skin, using different exposure times. Furthermore, I want to thank the Ghent University, namely Dra. Lieva Van Langenhove, Dr. Vincent Nierstrasz, Karen de Clerck and Lucy Van Ciera at the Textile Department, who have allowed me to work for four months in one of his European projects, called (NOT BUG: Novel Bio-based release system and utilities for mosquito Repellent Garments and textiles (Seventh Framework Programme, Theme 4). Thanks to this stay, I will be able to get an International PhD.

I also would like to thank my two thesis supervisors, Dr. Manel Lis and Dr. Josep Valldeperas, for their support, motivation and reviews during all the doctorate process.

I acknowledge the financial support of a scholarship from the Association of Industrial Engineers of Catalonia (Col·legi d'Enginyers Industrials de Catalunya) for the Doctoral Thesis with the support of Socio-cultural Association of Industrial Engineers of Catalonia (Agrupació Sòcio-Cultural dels Enginyers Industrials de Catalunya).

Also, I would like to Mrs. Judith Diaz, the person responsible of the lab and a friend of mine as well, who has always been available to assist me in anything I have needed. In addition, I want to thank the students for their effort and assistance, who have worked in their final project of the degree and have collaborated with me. And, I would also like to thank Manon Trouche, Alicia Camacho, Ignacio Parés and Víctor Acuña. as a working team, for the hard work carried out during this time.

Finally, I would like to thank all the people who have always been close to me, who have allowed me to get where I have wanted, and therefore, have given me the opportunity to try and achieve the goal of a doctorate. Firstly, my family, my parents, each of my six siblings and my fourteen nephews and nieces. I also include in this group all the friends who have never failed to me and have always appreciated my work and have given me great support to achieve my challenges. And above all this, I want to thank Matthias, my partner, for his comprehension,

help, support and strength along over these past months.

TABLE OF CONTENTS

CHAPTER 1: INTRODUCTION	9
1.1 MICROENCAPSULATION	9
1.2 TECHNIQUES OF MICROENCAPSULATION	11
1.3 APPLICATIONS OF MICROENCAPSULATION.....	12
1.4 TEXTILE INDUSTRY	13
1.5 MODELLING OF DRUG RELEASE	14
1.5.1 POLYMERS IN CONTROLLED DRUG RELEASE	15
1.5.2 ACTIVE COMPOUNDS.....	21
1.5.2.1 CAFFEINE	21
1.5.2.2 IBUPROFEN	22
1.5.2.3 GALLIC ACID.....	22
1.5.3 RELEASE MECHANISMS	24
1.5.4 MODELS OF DRUG RELEASE	26
1.5.4.1 THEORETICAL MECHANISMS OF DRUG RELEASE.....	28
1.5.4.2 POWER LAW.....	29
1.5.4.3 HIGUCHI EQUATION.....	30
1.5.4.4 KORSENMEYER-PEPPAS EQUATION APPROXIMATION	30
1.6 TRANSDERMAL DRUG RELEASE.....	31
1.6.1 ANIMAL MODEL OF SKIN DELIVERY – PIG.....	33
1.6.2 <i>IN VITRO</i> TECHNIQUES	34
1.6.3 DRUG PERMEATION THROUGH MEMBRANES.....	34
1.6.3.1 DRUG DISSOLUTION	35
1.6.3.2 DRUG DISPERSION IN A LIQUID PHASE	38
1.6.3.3 POLYMERIC MATRIX CONTAINING DRUG.....	40
1.6.3.4 DRUG SOLUTION RESERVOIR.....	42
CHAPTER 2: RESEARCH APPROACH	44
2.1 ABSTRACT.....	44
2.2 OBJECTIVES OF THE THESIS	44
2.3 EXPERIMENTAL STRUCTURE	45
2.4 MATERIALS.....	46
2.4.1 BIOCOMPATIBLE POLYMERS AND ACTIVE AGENTS.....	46
2.4.2 TEXTILE SUBSTRATES	47
2.4.3 SKIN PERMEATION	47
2.5 EXPERIMENTAL METHODS AND TECHNIQUES.....	47
2.5.1 PREPARATION OF MICROSPHERES	47
2.5.2 CHARACTERIZATION OF MICROSPHERES.....	49
2.5.2.1 SCANNING ELECTRON MICROSCOPY (SEM).....	49
2.5.2.2 ENCAPSULATION EFFICIENCY	50
2.5.2.3 FOURIER TRANSFORM INFRARED SPECTROSCOPY (FTIR).....	51
2.5.2.4 PARTICLE SIZE DISTRIBUTION	51
2.5.3 IMPREGNATION OF MICROSPHERES ON TEXTILE SUBSTRATE	52

2.5.4	ANALYSIS OF DRUG RELEASE	53
2.5.5	OBTAINING A MASS TRANSPORT MODEL THROUGH THE SKIN.....	53
CHAPTER 3: PREPARATION OF MICROSPHERES AND THEIR CHARACTERIZATION		57
.....		
3.1	PREPARATION OF MICROSPHERES	57
3.1.1	PLGA-MICROSPHERES WITH CAFFEINE	57
3.1.2	PCL-MICROSPHERES WITH IBUPROFEN	58
3.1.3	PCL-MICROSPHERES WITH GALLIC ACID	59
3.2	CHARACTERIZATION OF MICROSPHERES.....	60
3.2.1	SCANNING ELECTRON MICROSCOPY (SEM).....	60
3.2.2	ENCAPSULATION EFFICIENCY	60
3.2.3	FOURIER TRANSFORM INFRARED SPECTROSCOPY (FTIR)	61
3.2.4	PARTICLE SIZE DISTRIBUTION	61
3.3	RESULTS AND DISCUSSION.....	62
3.3.1	SEM – PLGA-MICROSPHERES WITH CAFFEINE	62
3.3.2	SEM – PCL-MICROSPHERES WITH IBUPROFEN	63
3.3.3	SEM-PCL MICROSPHERES WITH GALLIC ACID.....	63
3.3.4	ENCAPSULATION EFFICIENCY – PLGA-MICROSPHERES WITH CAFFEINE .	64
3.3.5	ENCAPSULATION – PCL-MICROSPHERES WITH IBUPROFEN	64
3.3.6	ENCAPSULATION EFFICIENCY – PCL-MICROSPHERES WITH GALLIC ACID	65
3.3.7	FTIR – PLGA-MICROSPHERES WITH CAFFEINE	65
3.3.8	FTIR – PCL-MICROSPHERES WITH IBUPROFEN.....	67
3.3.9	FTIR – PCL-MICROSPHERES WITH GALLIC ACID	69
3.3.10	PARTICLE SIZE DISTRIBUTION – PLGA-MICROSPHERES WITH CAFFEINE.	71
3.3.11	PARTICLE SIZE DISTRIBUTION – PCL-MICROSPHERES WITH IBUPROFEN	72
3.3.12	PARTICLE SIZE DISTRIBUTION – PCL-MICROSPHERES WITH GALLIC ACID	73
3.4	CONCLUSIONS.....	73
CHAPTER 4: IMPREGNATION OF MICROSPHERES ON TEXTILE SUBSTRATE		75
4.1	PAD-DRY TECHNIQUE.....	75
4.2	RESULTS AND DISCUSSION.....	75
4.2.1	PAD-DRY TECHNIQUE – PLGA-MICROSPHERES WITH CAFFEINE	75
4.2.2	PAD-DRY TECHNIQUE – PCL-MICROSPHERES WITH IBUPROFEN	77
4.2.3	PAD-DRY TECHNIQUE – PCL-MICROSPHERES WITH GALLIC ACID	78
4.3	CONCLUSIONS.....	79
CHAPTER 5: ANALYSIS OF DRUG RELEASE		80
5.1	DRUG RELEASE ESSAY.....	80
5.3	RESULTS AND DISCUSSION.....	80
5.4	THEORETICAL MECHANISMS OF DRUG RELEASE.....	80
5.4.1	THEORETICAL MECHANISMS – PLGA-MICROSPHERES WITH CAFFEINE...	80
5.4.2	THEORETICAL MECHANISMS – PCL-MICROSPHERES WITH IBUPROFEN ..	83
5.4.3	THEORETICAL MECHANISMS – PCL-MICROSPHERES WITH GALLIC ACID .	86
5.5	POWER LAW	88

5.5.1	POWER LAW – PLGA-MICROSPHERES WITH CAFFEINE	88
5.5.2	POWER LAW – PCL-MICROSPHERES WITH IBUPROFEN.....	90
5.5.3	POWER LAW – PCL-MICROSPHERES WITH GALLIC ACID.....	91
5.6	KORSENMEYER-PEPPAS EQUATION APPROXIMATION AND HIGUCHI MODEL..	93
5.6.1	KORSENMEYER-PEPPAS EQUATION APPROXIMATION AND HIGUCHI MODEL – PLGA-MICROSPHERES WITH CAFFEINE	93
5.6.2	KORSENMEYER-PEPPAS EQUATION APPROXIMATION AND HIGUCHI MODEL – PCL-MICROSPHERES WITH IBUPROFEN.....	94
5.6.3	KORSENMEYER-PEPPAS EQUATION APPROXIMATION AND HIGUCHI MODEL – PCL-MICROSPHERES WITH GALLIC ACID	95
5.7	CONCLUSIONS.....	96
CHAPTER 6: MASS TRANSPORT MODEL THROUGH THE SKIN.....		97
6.1	PERCUTANEOUS ABSORPTION ESSAY	97
6.2	RESULTS AND DISCUSSION - MASS TRANSPORT MODEL THROUGH THE SKIN 99	
6.3	CONCLUSIONS.....	103
CHAPTER 7: CONCLUSIONS AND FUTURE OUTLOOK		104
7.1	FINAL CONCLUSIONS	104
7.2	FUTURE OUTLOOK	105
CHAPTER 8: STAY ABROAD (GHENT UNIVERSITY).....		106
8	STAY ABROAD (GHENT UNIVERSITY)	106
8.1	BACTERIAS INCORPORATED IN FIBERS BY ELECTROSPINNING TECHNIQUE	106
REFERENCES.....		107
ANNEX		118

1.1 MICROENCAPSULATION







Microencapsulation is a coating technology based on solid small particles, drops of liquids, or gaseous components, with protective membranes – microparticle walls. These particles are known as microparticles. [1]

Microparticles are tiny particles with diameters in the range of nanometres or millimetres which consist of core materials and covering membranes. The most important feature of microparticles is their little size, providing large effective surface or interface area. Depending on the selection of the covering materials and the core substances, microparticles can be endowed with a wide range of functions.

Covering materials are generally chosen to highlight microencapsulation effects. Therefore, the synthetic and natural polymers are used to produce microparticles, as well as lipids and inorganic materials. [2]

Due to the development and specialisation of microencapsulation technologies and applications, microencapsulation products differ in structure and terminology (Table 1). [1]

Table 1. Terminology of microencapsulation products [1]

Terminology	Description	Size range	Schematic illustration
Microcapsules (narrow sense of meaning)	Products of coating liquid nuclei with solid walls.	μm	
Nanocapsules	Same structure as microcapsules, but smaller.	nm	
Microspheres or microparticles	The cores and walls are both solid. Often, there is no clear distinction between them: the thick solid wall functions as a porous matrix where active substances are embedded.	μm	
Nanospheres or nanoparticles	Same structure as microspheres, but smaller.	nm	
Liposomes	Lipid wall, often made of phospholipids and cholesterol. Subtypes: unilamellar (one lipid layer) and multilamellar (several lipid layers).	μm to nm	
Niosomes	Similar to liposomes but their membranes are made of synthetic amphiphilic molecules (detergents).		

There are several reasons and interesting advantages to use microencapsulation, which are as follows:

1. Controlled release of encapsulation active agents.
2. Protection of the encapsulated materials against oxidation or deactivation due to reaction in the environment.
3. Masking of odour and/or taste of encapsulating materials.
4. Isolation of encapsulating materials from undesirable phenomena.
5. Easy handling, specially the powder-like materials. [2]

1.2 TECHNIQUES OF MICROENCAPSULATION

The main interest of microencapsulation consists of separating the active principle from its environment through the occlusion in the cavity of microparticles surrounded by a polymer.

Microencapsulation techniques are mainly based on the emulsion of the active principle in a solution of polymer used to surround the droplets formed. The “solidification” of the particles is obtained by modifying the continuous medium of solution, either changing physical-chemical parameters, or by incorporating a chemical agent.

There are different types of emulsions depending on the composition and morphology of the dispersed phase and continuous phase. Two groups are known basically:

1. Emulsions where water is the internal dispersed phase and the continuous phase is oil, are termed water-in-oil emulsions (W/O).
2. Emulsions where oil is the dispersed phase and the continuous phase is water, are known as oil-in-water emulsions (O/W).

More complex systems where one emulsifier is further dispersed into another continuous phase are called double or multiple emulsions (W/O/W or O/W/O emulsions) (Figure 1). [3]

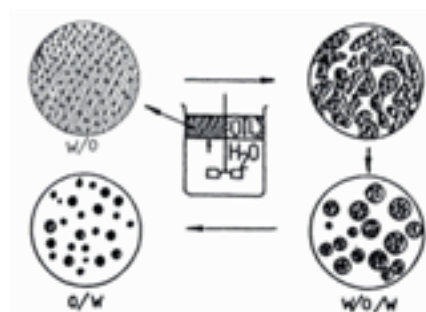


Figure 1. Possible sequence of events leading to the final formation of an O/W emulsion via a transient (W/O/W) emulsion, when hydrophilic surfactant is initially located in the oil phase. [3]

Various techniques are available for the encapsulation of core materials. The choice of the appropriate technique depends on the core material properties, the involved manufacturing conditions and the user requirements of the final product. The physical nature of the core substance to be encapsulated, will determine the technique to be used. In general terms, methods are divided into three main types (see different types of microencapsulation techniques listed in Table 2). [1,4-6]

1. **Chemical methods.** The membrane of the capsule is directly formed by the polycondensation of two reactive monomers surrounding the dispersed core material. You can get the same effect with a previous dissolution, with two immiscible liquids but soluble in the same phase.
2. **Physico-chemical methods.** These processes are based on the control of the solubility and precipitation conditions of the polymers under the influence of several factors that tend to reduce the solvation on the solvent.
3. **Physico-mechanical methods.** These methods are similar to the coating techniques in general.

Table 2. Different techniques used for microencapsulation. [4]

Chemical processes	Physico-chemical processes	Physico-mechanical process
Interfacial polymerization	Coacervation and phase separation	Spray drying and congealing
In situ polymerization	Sol-gel encapsulation	Fluid bed coating
Poly condensation	Supercritical CO ₂ assisted microencapsulation	Pan coating
		Solvent evaporation

1.3 APPLICATIONS OF MICROENCAPSULATION

The introduction of microencapsulation techniques for industrial purposes was at the end of the 1950s to produce pressure sensitive copying papers with hydrophobic solutions of leuco dyes encapsulated (Fanger, 1974).

Since then, the microencapsulation has been constantly improved, modified and adapted for a variety of purposes and applications. As a result, it has become a relevant example of a knowledge-intensive and dynamic technology (Boh and Kardos, 2003), characterised by a rapid growth of patent applications, reflecting industrial research and development, as well as an increase of the number of new scientific articles, deriving from the basic research (Figure 2).

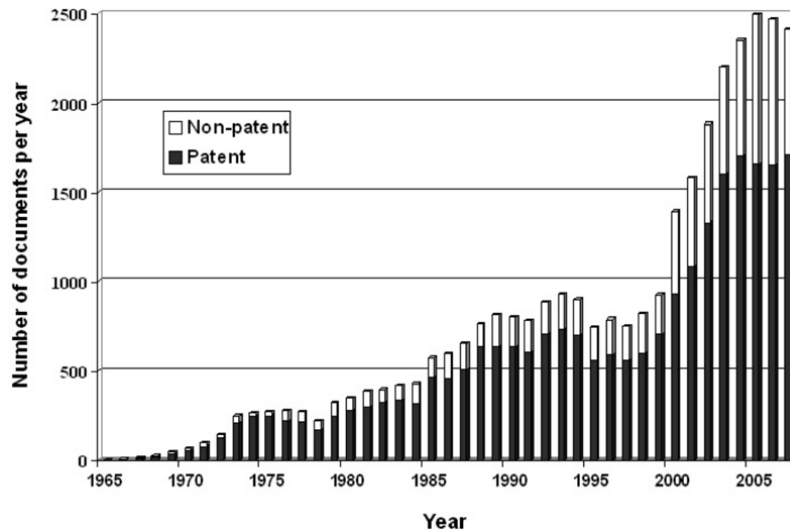


Figure 2. Growth of new patent documents and scientific articles on microencapsulation. [1]

Apart from the graphic and printing industries, microencapsulation has been vastly used for pharmaceutical and medical purposes in cosmetic and food products, agricultural formulations, in chemical and construction materials industries, biotechnology, photography, electronics, and waste treatment. However, their introduction in the textile industry is pretty new.

The microcapsule composition for textile purposes will depend on the required effect. Sophisticated shell materials and technologies have already been developed and an extremely wide variety of functionalities can now be achieved through microencapsulation. [1,7]

1.4 TEXTILE INDUSTRY

The textile industry has been slow to react to the possibilities of microencapsulation, although by the beginning of the 1990s a few commercial applications were appearing with many more at the research and development stage (Nelson, 1991).

The microencapsulation technology applied on textiles was firstly used in the early 1980s by the US National Aeronautics and Space Administration (NASA) with the aim of managing the thermal barrier properties of garments, especially in space suits. They encapsulated phase-change materials (PCMs) with the aim of reducing the impact of extreme variations in temperature during space missions by astronauts.

As the industry moves into the 21st century the number of commercial applications of microencapsulation in the textile industry keeps on growing, particularly in Western Europe, Japan and North America. The decision of the most developed countries is to introduce into fabrics new properties with added value, specially medical textiles and technical textiles.[8]

Textile manufacturers show increasing interest in the application for durable fragrances in textiles, as well as in skin softeners. Other potential applications include insect repellents, cosmetics, dyes, antimicrobials, phase change materials, fire retardants, counterfeiting, polychromic and thermochromic effects, in specific medical applications and antibiotics. [7]

The methods for applying microparticles on fabrics are basically two: either they can be incorporated directly into the fiber during the spinning process, or they can be added at the finishing process (Figure 3).

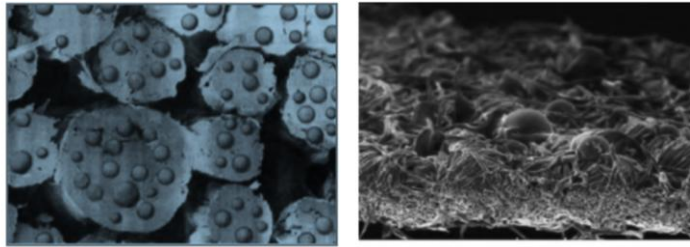


Figure 3. PCM microcapsules incorporated directly into the fibers. PCM microcapsules applied on textile by a finishing process. [9]

The encapsulation process allows the active compound to be integrated in textile finishing, by textile impregnation (Pad-dry technique) by exhaust bath, or directly incorporated in different artificial fibres (spinning). The microparticles will remain effective as long as the coating or fibres remain intact. [9-11]

All common coating processes, such as knife over roll, knife over air, or screen printing, can be adapted to apply microcapsules to fabric. The method for manufacturing coating composition has been widely described in technical literature. Nevertheless, few papers published in technical literature give account of the formulation of coating, finishing of fabrics, and they neither offer a waste evaluation of their characteristics, such as thermal and durability properties. However, the choice of the process influences the microencapsulated fabric behaviour and the efficiency of the system tissue-microparticles [9-12].

1.5 MODELLING OF DRUG RELEASE

The science of drug release may be described as the application of chemical and biological principles to control the *in vivo* temporal and spatial location of drug molecules for clinical benefit. When drugs are delivered (oral or jet injection delivery), only a very small portion of the dose actually hits the relevant receptors or sites of action, and a considerable part of the dose is actually wasted because it is taken up into the “wrong” tissue, removed from the “right” tissue too quickly, or destroyed on the way before its reception. [13-15]

The design and implementation of systems for controlled drug dosage and management systems located in the activity of a given drug is currently one of the most important aspects in

the development of new ways of drug delivery [16]. The main objective of the controlled release is simple, it consists on getting the right amount of active agent, at the right time and in the right place. This release method is commonly used to extend the therapeutic dosage and to remove or reduce the concentrations exceeding the therapeutic requirements [17].

Drug delivery is becoming an extremely demanding science. The reasons are essentially threefold:

1. The emergence of the more challenging low molecular weight molecules and biomacromolecules with poor aqueous solubility, poor tissue permeation, or with both.
2. The increased use of biological materials with poorly understood physical properties or questionable shelf life issues.
3. When determining the portion of the precise dose it has to be directed to the specific aim. This way toxic side effects would become less frequent, thus improving the therapeutic index.

The emerging areas of tissue engineering or tissue reconstruction have harnessed the properties of the polymers as drug delivery systems. These matrix systems effectively hold up the diffusion of active agents, trapping them within a three-dimensional network of polymer chains. Therefore, their mechanical properties have to be taken into account in the fabrication process of these systems. Specifically, there should be a good match between tissue and polymer properties, being a main requirement to achieve the final aim of the system [13].

1.5.1 POLYMERS IN CONTROLLED DRUG RELEASE

The introduction of the controlled release from polymers happened on the 1960s through the employment of silicone rubber (Folkman and Long, 1964) and polyethylene (Desai et al., 1965) with the aim to improve the effectiveness of drug therapy. But it is necessary to go further in its research, because the lack of degradability in these systems implies the requirement of eventual surgical removal and restricts their applicability. In the 1970s, biodegradable polymers were suggested as appropriate drug delivery materials circumventing the requirement of removal (Jalil and Nixon, 1990).

The idea of polymer microcapsules as delivery systems was reported at early 60s (Chang, 1964) and degradation was incorporated by Mason et al. (1976) through the employment of a degradable polymer coating, the topic was reviewed by Marty and Oppenheim (1977).

Recent literature shows that biodegradable systems of microencapsulation can be employed for sustained drug release at desirable doses, by implantation and without surgical procedures.

Biocompatibility can be achieved by the use of natural polymers such as cellulose, chitin, and chitosan or using polymers made from naturally occurring monomers such as lactic and glycolic acids. However, polymers derived from synthetic monomers also show excellent delivery properties. The wide range of polymers used in controlled release applications based on backbone compositions is shown in Table 3. [18-20]

Table 3. Summary of Polymer Structures based on backbone composition. [19]

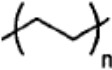
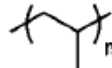
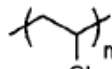
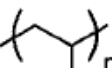
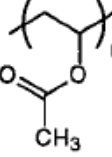
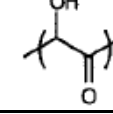
Backbone Structure	Examples	Notes
C-C	<p>Poly(ethylene)</p> <p>(PE)</p> 	<p>Zero-order temporal control achieved by diffusion from matrices.</p> <p>Tetanus toxoid released by pulsatile kinetics.</p> <p>Prolonged pseudo-first order release of acetoaminophen in gastrointestinal tract.</p>
	<p>Poly(propylene)</p> <p>(PP)</p> 	<p>Biocompatibility improved by albumin grafting to surface.</p> <p>Ophthalmic drug delivery applications.</p> <p>Accurel® used to release agents active in vapour state.</p>
Vinyl-based C-C	<p>Poly(vinyl chloride)</p> <p>(PVC)</p> 	<p>Membrane devices formulated to release volatile agents into air and non-volatile agents into aqueous solutions.</p>
	<p>Poly(vinyl alcohol)</p> <p>(PVA)</p> 	<p>Water-soluble copolymer of vinyl alcohol and vinyl acetate is formed by hydrolyzing poly(vinyl acetate).</p> <p>Surface stabilizer in microsphere formulation.</p> <p>Bioadhesive hydrogels.</p>
Vinyl-based C-C	<p>Poly(ethylene-vinyl acetate)</p> <p>p(EVAc)</p> 	<p>Employed as rate controlling membrane in Ocusert®.</p> <p>Drug permeability tailored by ratio of vinyl acetate present.</p> <p>Used in magnetically controlled temporal release, ultrasound-stimulated release, subcutaneous implant for cancer pain relief, and chemotherapeutic agents.</p>
	<p>Poly(enol-ketone)</p> <p>(PEK)</p> 	<p>Produced by controlled oxidation of PVA.</p>

Table 3. Continued [19]

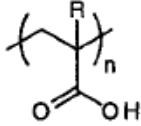
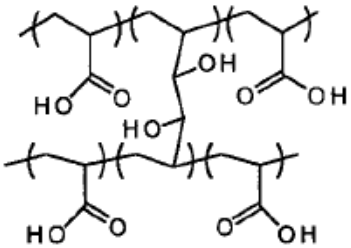
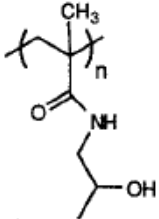
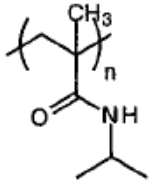
Backbone Structure	Examples	Notes
	<p>Poly(acrylic acid) (PAA)</p>  <p>R = H (acrylic) = CH₃ (methacrylic)</p>	<p>Bioadhesive polymer. Hydrogels of PAA reversibly swell as function of pH.</p>
	<p>Poly(carbophil)</p> 	<p>PAA-based hydrogel loosely cross-linked with divinyl glycol. Mucoadhesive properties allow temporal and distribution control.</p>
<p>Vinyl-based C-C</p>	<p>Poly(acrylamides) e.g., poly(N-(2-hydroxypropyl) methacrylamide) p(HPMA)</p> 	<p>Plasma expander used as polymer-drug conjugate for distribution control. Enzyme cleavable side chains employed to target release at colon. Hydrolytically degradable hydrogels produced by cross-linking with N,O-dimethacryloyl hydroxylamine linker. Component of photosensitive delivery system.</p>
	<p>Poly(N-isopropyl acrylamide) e.g., p(NIPAAm)</p> 	<p>Pronounced negative thermosensitivity. Used in stimuli sensitive systems.</p>

Table 3. Continued [19]

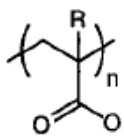
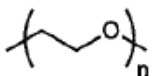
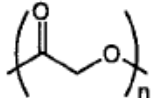
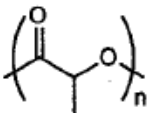
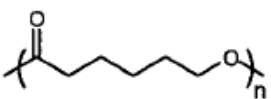
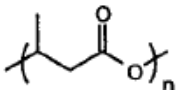
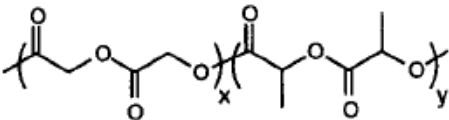
Backbone Structure	Examples	Notes
	<p>Poly(acrylates)</p>  <p>R = H (acrylic) = CH₃ (methacrylic) = CN (cyanoacrylate)</p>	<p>Employed as surgical adhesive due to polymerization in water at room temperature. Controlled drug release applications reported in polymer-drug conjugate and topical applications. Bone cements with hydrophilicity tailored to facilitate protein release.</p>
C-O	<p>Poly(ethylene glycol) (PEG)</p> 	<p>Also termed poly(ethylene oxide) (PEO). Used as diffusion-limited tablet formulation, cross-linked hydrogels, and polymer-drug conjugates. Employed as a component of block copolymer systems.</p>
C-O, C=O	<p>Poly(glycolic acid) (PGA)</p>  <p>Poly(lactic acid) (PLA)</p>  <p>Poly(ε-caprolactone) (PCL)</p>  <p>Poly(3-hydroxybutyrate)</p> 	<p>Copolymer: Poly(lactic acid-co-glycolic acid) (PLGA)</p>  <p>Biosynthetic poly(ester) often employed as copolymer with hydroxyvalerate monomer.</p>

Table 3. Continued [19]

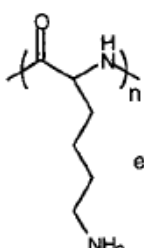
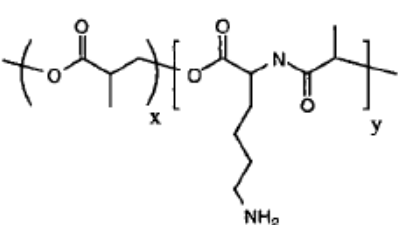
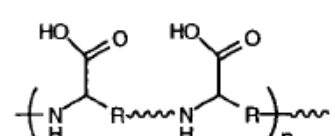
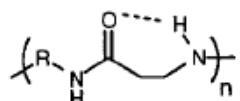
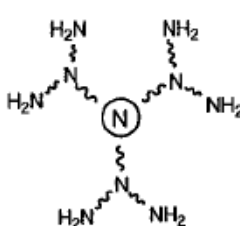
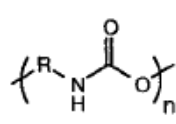
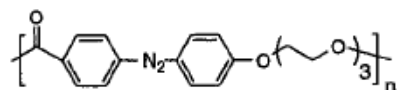
Backbone Structure	Examples	Notes
C-N, C=O	<p style="text-align: center;">Poly(amino acids)</p>  <p style="text-align: center;">e.g., poly(lysine)</p>	<p style="text-align: center;">Poly(lactic acid-co-lysine) (PLAL)</p> 
	<p style="text-align: center;">pseudo-poly(amino acids)</p> 	
C-N, C=O	<p style="text-align: center;">Poly(amide-enamines)</p> 	Hydrolyzable polymer with hydrophilic and hydrophobic segments. Potential for diffusion controlled drug release.
	<p style="text-align: center;">Poly(amido amines) (PAMAM) dendrimers</p> 	Complexes with DNA to form conjugates for gene therapy.
C-N, C-O, C=O	<p style="text-align: center;">Poly(urethanes)</p> 	Hard and soft segment polymers containing PEG for temporal controlled release. Azo-containing polymers used to control site of polymer-drug conjugate degradation. Anti-infectious biomaterials containing antibiotics.
	<p style="text-align: center;">Azopolymer poly(ether-ester)</p> 	Azo bond degraded by bacteria in colon thereby generating colon-specific delivery of chemotherapeutic and other drugs.

Table 3. Continued [19]

Backbone Structure	Examples	Notes
Silicon-based Si-O	<p>Poly(dimethylsiloxane)</p> $\left(\begin{array}{c} \text{CH}_3 \\ \\ \text{---Si---O---} \\ \\ \text{CH}_3 \end{array} \right)_n$	Temporal controlled release of rifampicin from shunt. Bone infections treated with crosslinked matrix.
Phosphorus-based P=N, P-O	<p>Poly(phosphazenes)</p> $\left(\begin{array}{c} \text{R} \\ \\ \text{---N=P---} \\ \\ \text{R} \end{array} \right)_n$	Amino acid side chains generate flexible materials that degrade to amino acid, phosphate and ammonia poly[bis(glycine ethyl ester)phosphazene]. PEG-modified nanoparticles for site-specific drug delivery.

The most attractive and commonly used biodegradable polymers are polyesters such as poly(lactic acid) (PLA), poly(lactic-co-glycolic acid) (PLGA) and poly(ϵ -caprolactone) (PCL) (Table 3). These materials are commercially available in different compositions and molecular weights, allowing the control of the polymer degradation.

The term degradation designates the process of polymer chain cleavage which leads to a loss in molecular weight (inducing to the subsequent erosion of the material). For biodegradable polymers two different erosion mechanisms can be suggested: homogeneous or bulk erosion, and heterogeneous or surface erosion. The difference between both is that, in the case of the bulk erosion, degradation is observed all over their cross-section because the penetration of water into the polymer bulk is faster than degradation of polymer. However, in surface eroding polymers, the degradation is faster than the penetration of water into the bulk. As a consequence, these polymers erode mainly from their surface. But normally, for most polymers, erosion follows both mechanisms.

The erosion mechanism has consequences for the mechanism of drug release which has been classified into diffusion, swelling and erosion-controlled. A biodegradable polymer device might release the active agent by all three mechanisms and the fastest mechanism dominates. In the case of biodegradable polyesters, based on monomers connected to each other by ester bonds, degradation starts after penetration of water into the device. The breakage of ester bonds occurs randomly via hydrolytic ester cleavage and leads to the subsequent erosion of the device. The hydrolysis rate is influenced by molecular weight, copolymer ratio, polydispersity and crystallinity, and all these factors can be used to control drug release. For example, poly(ϵ -caprolactone), which is a highly hydrophobic and crystalline polyester, degrades very slowly compared to amorphous less hydrophobic PLGA. [19]

Depending on these variables, the degradation time varies from several weeks up to years and allows the release of drugs over this time period. However, the achievement of controlled drug release from polyester-based delivery systems is difficult because these polymers undergo bulk erosion which changes the polymer matrix and influences drug release. As a consequence,

drug release is controlled by swelling, drug diffusion and polymer erosion, which is not straight forward to predict [19-23].

1.5.2 ACTIVE COMPOUNDS

The active compounds that have been tested in this project are: caffeine, ibuprofen and gallic acid. Caffeine and gallic acid are cosmetic compounds that have functions as anti-cellulite and antioxidant, respectively. And Ibuprofen as an anti-inflammatory pharmaceutical compound.

1.5.2.1 CAFFEINE

Caffeine, $C_8H_{10}N_4O_2$ is a natural alkaloid appear in more than 60 species of plants. It is part of the daily diet contained in drinks such as coffee or tea, chocolate and some soft drinks. It could be considered one of the most widely consumed stimulant substances and it is socially accepted worldwide.

Caffeine is an odourless, colourless and bitter powder or white, long and silky needles, which easily agglomerate and shape fluffy and light masses. It is very soluble in boiling water, in which crystallizes with a water molecule (in water at 25 °C is 16 mg/mL).

Friedrich Ferdinand Runge extracted it from the coffee in 1819 and from the tea in 1827, but its chemical structure was not described until 1875 by E. Fischer. Caffeine (1,3,7-trimethylxanthine) and other methylxanthine alkaloids (Figure 4), as theobromine (3,7-dimethylxanthine) and theophylline (1,3-dimethylxanthine), come from the group of xanthines, which, at the same time, come from purines. They are pharmacologically related to psychostimulants. Methylxanthines are common ingredients used in cellulite products, such as, caffeine, aminophylline, theophylline, etc. and are used because of their suggested effect on adipocyte lipolysis via inhibition of phosphodiesterase, and increasing cyclic adenosine monophosphate (AMP) levels [14,24,25].

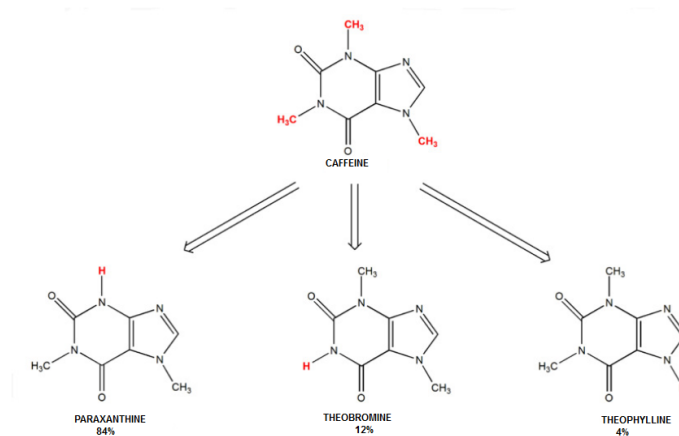


Figure 4. Metabolites of Caffeine. [25]

1.5.2.2 IBUPROFEN

Ibuprofen ($C_{13}H_{18}O_2$) (Figure 5) was derived from propionic acid by the research of Boots Group during the 1960's. It was discovered by Andrew RM Dunlop with the colleagues Stewart Adams, John Nicholson, Jeff Wilson and Colin Burrows and was patented in 1961. The drug was launched as a treatment for rheumatoid arthritis in the UK in 1969, and in the United States in 1974.

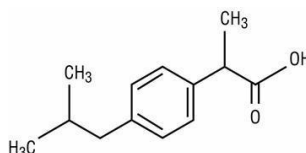


Figure 5. Chemical structure of Ibuprofen.

It is a nonsteroidal anti-inflammatory drug (NSAID) used to relieve the symptoms of arthritis, fever, as an analgesic (pain reliever), especially where there is an inflammatory component, and dysmenorrhea. Ibuprofen is known to have an antiplatelet effect, though it is relatively mild and somewhat short-lived when compared with aspirin or other better-known antiplatelet drugs. In general, ibuprofen also acts as a vasoconstrictor, having been shown to constrict coronary arteries and some other blood vessels mainly because it inhibits the vasodilating prostacyclin produced by cyclooxygenase 2 enzymes. Ibuprofen is poorly soluble in water, its solubility at 25°C in water is 0.14 mg/mL, however, it is much more soluble in solutions alcohol / water [26].

1.5.2.3 GALLIC ACID

Gallic acid is an important component of iron gall ink, the standard European writing and drawing ink from the 12th to 19th century. Pliny the Elder (23-79 AD) described his experiments with it and wrote that it was used to produce dyes. It was discovered by French chemist and pharmacist Henri Braconnot (1780–1855) in 1818 and studied by French chemist Théophile-Jules Pelouze (1807–1867).

Gallic acid is an organic acid polyphenolic acid also known as 3,4,5-trihydroxybenzoic, found in a wide variety of plants. Its chemical formula is $C_6H_2(OH)_3COOH$ (Figure 6). It is a white crystalline powder or pale. It is soluble in acetone, ethyl acetate, alcohol, slightly soluble in cold water and insoluble in benzene or chloroform. Its solubility in water at 25 °C is 11.50 mg/mL.

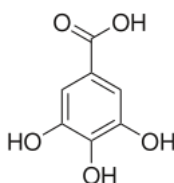


Figure 6. Chemical structure of gallic acid.

Gallic acid is found both in free form or as part of tannins. Salts and esters of gallic acid are called gallates. Gallic acid is obtained by hydrolysis of tannic acid with sulfuric acid or enzymes.

It has astringent, antiseptic and antioxidant properties. It helps to protect the cells against oxidative damage. It is used to treat diabetes and also for some other treatments such as psoriasis and external haemorrhoids containing this active agent [27].

1.5.3 RELEASE MECHANISMS

The release of the encapsulated agent can be achieved by several methods, according to three types of systems (Figure 7): [16,20]

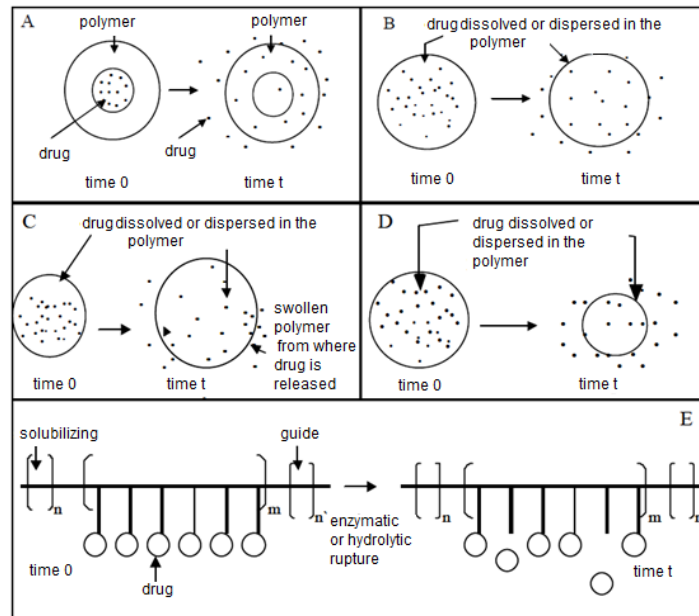


Figure 7. Systems of controlled drug release from a polymeric matrix. A) Systems of controlled release of bioactive agent inner core, B) monolithic controlled release system, C) Monolithic controlled release system by swelling, D) bioerodible system, E) controlled release system with side chains. [18]

1. Diffusion of active agents through polymers.

The release behaviour of active agents is the result of the phenomenon of diffusion in the polymer through the molecules network and mass transfer restrictions in the interphase polymer/liquid. Thus, the modification or the design of a controlled release system requires prior knowledge of the mechanism of diffusion of the solute through the polymeric material .

2. Controlled dosage by physical mechanisms.

Polymeric systems of drug release can be classified according to the way that drug molecules have been incorporated to the matrix. In the case of systems with physical bonds between the polymer and the active agent, depending on the mechanism of action, the systems can be controlled by diffusion, either in reservoirs (membranes), in matrices (monolithic) or controlled by the solvent (controlled by swelling or osmotic systems).

2.1. Systems controlled by diffusion.

The amount of active compound that reaches a particular area is controlled by the phenomenon of diffusion, it could be directly through the molecular structure of the polymer or through macro/micropores. However, the most common one is a combination of both mechanisms.

- a) Systems with reservoir or systems with inner core that contains the drug.
This consists of a core of the active agent surrounded by a homogeneous, non-porous and thin membrane. The active compound is contained within a polymeric coating, which can swell or not in the biological medium where is applied.
- b) Matrices or monolithic devices.
In these systems the active compound is uniformly distributed in a support of solid polymer. Drug can be dissolved in the polymeric matrix or dispersed, depending on if its solubility is greater than the solubility limit.

2.2. Systems controlled by the solvent.

These are polymeric matrices or systems with reservoir where the release is controlled by the penetration of a solvent, via osmosis or swelling.

- a) Systems controlled by swelling.
These are monolithic systems in which the active compound is dissolved or dispersed in a support of hydrophilic polymer, cross-linked or not, which swells without dissolving when it is in contact with an aqueous medium. These polymeric systems are named hydrogels and have achieved great interest, at least theoretically, because they can achieve a constant rate of release.
- b) Osmotic systems.
These are systems with a drug core surrounded by a polymeric membrane that is selective to the pass of water. The membrane allows water molecules to pass but it does not allow drugs to get through. These devices are like pressurized chambers containing aqueous solutions of the drug, this pressure is relieved by the flow of the solution out of the delivery device.

3. Dosage controlled in a chemical way.

Such method where the dosage is controlled by chemical means, the release of the active compound is produced by a chemical mechanism, which can be either a hydrolytic or enzymatic attack to a weak bond, or by ionization or protonation.

3.1. Bioerodible systems.

The active compound is dispersed into a polymeric material which gets eroded as time passes, this allows the drug release. In the specific case of the surgical suture (one of the most important applications), this method does not require surgical removal, since the biodegradable polymers are gradually absorbed by the organism. However, the resulting products may be toxic, immunogenic or carcinogenic.

3.2. Systems with side chains.

The drug molecule is chemically bonded by a polymeric chain and it is released by hydrolytic or enzymatic rupture.

1.5.4 MODELS OF DRUG RELEASE

There are many devices providing several mechanisms to control drug release; mechanisms such as polymer swelling, drug dissolution, drug diffusion or combinations of them.

The physicochemical characteristics and the geometry of each device determine the resulting governing processes. As for the mathematical modelling of the microencapsulation systems release, one must identify the most important transport phenomenon for the investigated device and leave other processes aside, otherwise the mathematical model becomes too complex to be used. [28]

The kinetic models of drug release in biological medium, are generally governed by zero order or first order. The following table shows the kinetic models of drug release (Table 4) [29].

Table 4. Kinetic models of Drug Release.

% Q: Percentage of dissolved drug; F: Fraction of released drug; α : Parameter that defines the process time; β : parameter that defines the shape of the matrix. [29]

MODEL	EQUATION	APPLICATION
Baker and Lonsdale	$\frac{3}{2} [1 - (1 - F)^{2/3}] - F = k_{b1}t$	Describe the drug release from spherical matrices.
First order	$\% Q = 100 (1 - e^{-kt})$	The amount of drug released depends on the diffusion and/or dissolution.
Higuchi	$\% Q = k_H \cdot t^{0.5}$	It is a release model controlled by diffusion from homogeneous matrices and granular matrices.
Hixson-Crowell (Root cubic Law)	$1 - (1 - F)^{1/3} = k_{hc} \cdot t$	Kinetic model for dissolution of powder; is used to describe the release from erodible isometric matrices (eg, spheres and cubes).
Jorgensen and Christensen model	$F = [1 - (1 - (1 - n)k(t - t_0)^{1/1-n})]$	Multiparticles systems (individual particles, assembly particles and tablets).
Combination between Higuchi and zero order models	$\% Q = k_0 \cdot t + k_H \cdot t^{0.5}$	Indicative of controlled release by diffusion and membrane that acts as a barrier for itself.
Equation of Peppas and Korsenmeyer (Power Law)	$M_t / M_0 = k \cdot t^n$	Polymeric systems with swelling, n depends on the geometry of the system and its value is indicative of the release mechanism.
Weibull	$\% Q = 100 [1 - e^{-(t-t_0/\beta)^\alpha}]$	Describes exponential curves and sigmoidal forms.
Zero Order	$\% Q = k_0 \cdot t$	Constant release rate; erodible systems with constant surface area and systems with membranes that control the diffusion with constant concentration gradient over the membrane.

1.5.4.1 THEORETICAL MECHANISMS OF DRUG RELEASE

There is relevant coherence between current results and the assorted model release curves in some portion of the release curve, but there often significant deviations. Release of core material from a non-erodible microcapsule can be observed in several ways. Figure 8 shows four theoretical curves (A, B, C, and D) which describe four types of release behaviour. All curves are plotted as percent of drug released versus time.

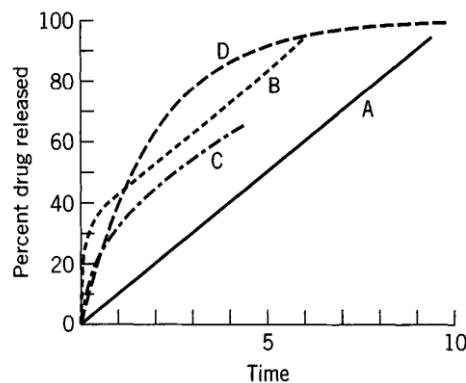


Figure 8. Theoretical release curves expected for different types of non erodible delivery systems. A, Membrane reservoir-type free of lag time and burst effects; B, same as A, with burst effects; C, matrix or monolithic sphere with square root time-release; D, system with first-order release. [30]

In Figure 8, curve A represents the release behaviour of a perfect, non-erodible, spherical microcapsule which releases the encapsulated material by steady-state diffusion through a coating of uniform thickness. The rate of release remains constant as long as the internal and external concentrations of core material and the concentration gradient through the membrane are constant. If a finite time is needed to establish the initial, constant concentration gradient in the capsule wall membrane then there is a time lag in core material release. Curve A displays a system with no time lag. If some of the encapsulated material migrates through the microcapsule membrane during storage, a burst effect occurs, as represented by Curve B. If the microcapsule acts as an inert matrix particle in which core material is dispersed (a microsphere), the Higuchi model is valid up to 60% release (equation (3)). In this case, a plot of percent drug released versus square-root time is linear, as shown by Curve C in Figure 8. First-order release is represented by Curve D. The curve is linear if log percent core material left in the capsule is plotted versus time. [30]

1.5.4.2 POWER LAW

Several kinetic equations have been used to study drug release for different systems (Table 4). Thus, the Power Law (1) is used to measure the coupled effects of Fickian diffusion and viscoelastic relaxation in polymer systems, including both processes,

$$\frac{M_t}{M_\infty} = kt^n \quad (1)$$

where M_t amount of drug released at time t , M_∞ the maximal amount of the released drug at infinite time (equilibrium), k is the rate constant of drug release, n is a release exponent depends on the system geometry and its value is indicative of the release mechanism of the active principle.

It is clear from Eq. (1) that when the exponent n takes a value of 1.0, the drug release rate is not linked to time. This case corresponds to zero-order release kinetics. For slabs, the mechanism that creates the zero-order release is known among polymer scientists as case-II transport. Here the relaxation process of the macromolecules occurring upon water imbibition into the system is the rate-controlling step. Water acts as a plasticizer and decreases the glass transition temperature of the polymer. Once the T equals the temperature of the system, the polymer chains undergo the transfer from the glassy to the rubbery state, with increasing mobility of the macromolecules and volume expansion.

Thus, Eq. (1) has two distinct physical realistic meanings in the two special cases of $n=0.5$ (indicating diffusion-controlled drug release) and $n=1.0$ (indicating swelling-controlled drug release). Values of n between 0.5 and 1.0 can be regarded as an indicator for the superposition of both phenomena (anomalous transport). It has to be kept in mind that the two extreme values for the exponent n , 0.5 and 1.0, are only valid for slab geometry. For spheres and cylinders different values have been derived, as listed in Table 5 [28,31-41].

Table 5. Drug delivery models based on the parameter n .

Exponent n			
Plane surface	Cylinder	Sphere	Drug Delivery Systems
0,5	0,45	0,43	Fickian Diffusion Mechanism
$0,5 < n < 1,0$	$0,45 < n < 0,89$	$0,43 < n < 0,85$	Anomalous Diffusion
1,0	0,89	0,85	Non-Fickian Diffusion Mechanism

1.5.4.3 HIGUCHI EQUATION

Higuchi probably published the most famous and most often used mathematical equation to describe the release rate of drugs from matrix systems. It was initially valid only for planar matrix, but it was later modified and extended to consider different geometries and matrix characteristics. The classical Higuchi equation was derived under pseudo-steady state assumptions and generally cannot be applied to real controlled release systems.

An important advantage of these equations is their simplicity. However, when applying them to controlled drug delivery systems, the assumptions of the Higuchi derivation should carefully be kept in mind: [31-41]

1. The initial drug concentration in the system is much higher than the solubility of the drug. This assumption is very important, because it provides the basis for the justification of the applied pseudosteady state approach.
2. Mathematical analysis is based on one-dimensional diffusion. Thus, edge effects must be negligible.
3. The suspended drug is in a fine state such that the particles are much smaller in diameter than the thickness of the system.
4. Swelling or dissolution of the polymer carrier is negligible.
5. The diffusivity of the drug is constant.
6. Perfect sink conditions are maintained.

This equation can be expressed as:

$$\frac{M_t}{M_\infty} = K\sqrt{t} \quad (2)$$

1.5.4.4 KORSENMEYER-PEPPAS EQUATION APPROXIMATION

In addition, a proportionality between the fractional amount of drug released and the square root of time can as well be derived from an exact solution of Fick's second Law. So the diffusion of the active compound can be studied as a plane surface for short times of liberation, where D is the diffusion coefficient of drug release, and δ is the thickness of thin films under perfect sink conditions, it can be expressed as follows [28,42-47]:

$$\frac{M_t}{M_\infty} = 4 \left(\frac{Dt}{\pi\delta^2} \right)^{1/2} = K\sqrt{t} \quad (3)$$

Thus, a proportionality between the fraction of drug released and the square root of time can also be based on these physical circumstances which are substantially different from those studied by Higuchi from the derivation of his classical equation.

1.6 TRANSDERMAL DRUG RELEASE

The transdermal drug release is a viable administration route for powerful, low-molecular weight therapeutic agents, which has to be precise in their control of drug distribution. This strategy is specially recommended for many drugs that are difficult to be taken since they must be delivered slowly over a prolonged period to have a beneficial effect. However, there is still necessary to research in this field. For instance, the drug release modelling of biodegradable polymeric systems by encapsulation technology in textiles has not progressed much yet, due to its high complexity.

Skin drug delivery can be divided into topical and transdermal. In a topical administration, the drug is meant to act at skin level, this is indicated for the treatment of skin diseases such as follicle-related disorders (for example, acne and alopecias). And the aim of transdermal administration is getting a systemic release, and in this case the skin acts as a barrier and not as a target. It is logic that the topical administration shows far less problems than the transdermal one for the use of drug delivery system. However, transdermal administration has several interesting advantages over other systemic administration routes such as:

- a) The reduction of first-pass drug degradation as the liver is initially bypassed.
- b) The reduction of over dosage peaks that can appear in oral administration.
- c) The existence of variable delivery conditions, typical of the gastrointestinal tract.

Transdermal administration also can take advantage of chemical and physical strategies that can improve skin permeability and allow to drug penetration [47-54]. Specifically, the transdermal drug delivery is a good viable administration route for powerful, low-molecular weight therapeutic agents which either can or cannot withstand the hostile environment of the gastrointestinal tract are subject to considerable first-pass metabolism by the liver [55]. Regardless of the necessity or not of physical-chemical enhancing, for a reliable and effective designing of transdermal delivery systems it is fundamental prerequisite the knowledge of skin structure and its properties [58].

The human skin is composed of three layers (Figure 9), the outer layer is the epidermis. This is put in contact with the dermis by the so-called dermo-epidermic junction (as permeable area). The dermis is constituted by a connective tissue layer of mesenchymal origin. Finally, the inner layer is represented by the hypodermis, mainly constituted by connective tissue. The different layers of the skin are crossed by nerve endings and blood vessels. Additionally, hair follicles and glands, non uniformly distributed throughout the skin, are present. The total human skin weight

is more than 3 kg and the total surface is of 1.5–2 m². The peripheral blood flow through the skin in the extremities and torso is 0.3 mL/h/cm³. The fluxes through the skin cheeks, front, fingers, foot–sole, or palms are somewhat higher. The total surface area of the intracutaneous blood vessels, available for the direct passage of drugs into the systemic circulation, amounts to 100%–200% of the skin area [55].

For that reason, the drug release to the skin surface and its transport to the systemic circulation are studied as a multistep process which involves:

- dissolution within and release from the drug formulation,
- partitioning into the skin's outermost layer, the stratum corneum (SC),
- diffusion through the SC, principally via a lipidic intercellular pathway, (i.e., the rate-limiting step for most compounds),
- partitioning from the SC into the aqueous viable epidermis,
- diffusion through the viable epidermis and into the upper dermis, and
- uptake into the local capillary network and eventually the systemic circulation (Figure 9).

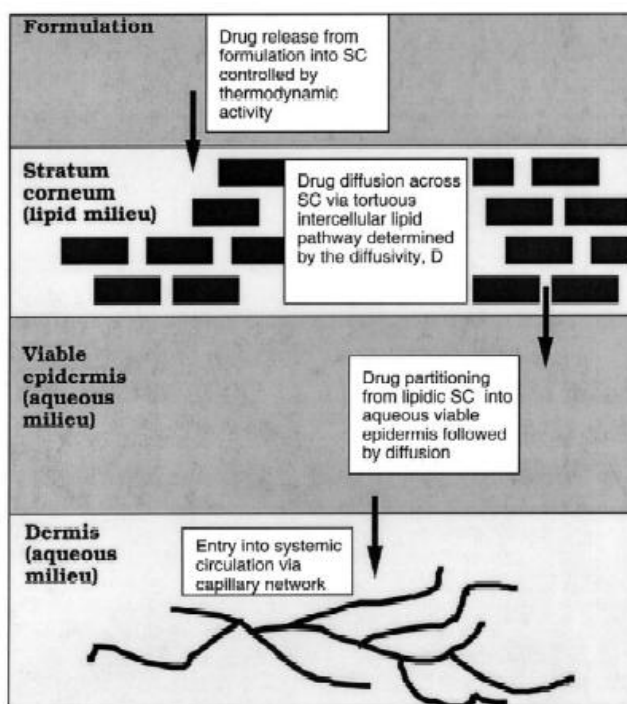


Figure 9. Schematic representation of the transport processes involved in drug release from the formulation up to its uptake through the dermal capillaries. [55]

Therefore, an ideal drug candidate would have sufficient lipophilicity to partition into the SC, but also sufficient hydrophilicity to enable the second partitioning step into the viable epidermis and eventually the systemic circulation.

A transdermal drug release is a formulation or device (for example, a transdermal patch) that maintains the blood concentration of the drug for therapeutic purposes. It should ensure that drug levels neither fall below the minimum effective concentration nor exceed the minimum toxic

dose [55].

1.6.1 ANIMAL MODEL OF SKIN DELIVERY – PIG

Detailed information about skin absorption and percutaneous permeation is of utmost relevance for skin pharmacological and toxicological research or other products.

It is important to progress /go forward in these fields, since the availability of alternative methods to human experimentation is a current need. *In vitro* methods, using human or animal skin, can meet the purpose. However, sometimes without a reliable *in vivo* animal model, definitive conclusions are difficult to be reached. Thus, animal models have been widely considered. Pig model is one of particular interest. The common anatomical and physiological characteristics between man and pig indicate that pig skin represents a reliable model to study percutaneous permeation in man.

Pigs, like men, have a median body size, large enough to collect multiple samples (body fluids, biopsies) and, at the same time, it is not too large to be conveniently handled in standard laboratory animal facilities. Another important similarity is that the skin of both is only sparsely covered with hair. Therefore, it is possible to select pig strains with different amounts of hair. Man and pig skins are both characterized by a sparse hair coat and a thick epidermis, which, by parameters of tissue turnover time and the characterization of keratinous proteins are comparable. Additionally, swine SC contains protein fractions grossly similar to human and presents a filament density and areas of cell overlapping comparable as well. The epidermal–dermal junction is also similar in the pig and man. Dermis is comparable between man and pig where it is characterized by a well differentiated papillary body and a large content of elastic tissue. Moreover, the structure of collagen fibres and fibre bundles in the dermis of pig, generally corresponded to those observed in human skin, including the thickness of collagen fibrils. Finally, biochemical similarities were also observed studying glycosphingolipids and ceramides in human and pig epidermis as well as the enzyme patterns.

But, some differences have been observed with regard to the amount of vessels which are more abundant in man than in pig, and also differences have been revealed in skin glands. The pig has only apocrine glands however, human have mostly eccrine sweat over the body surface.

Percutaneous absorption in man varies depending on the area of the body on which the chemical resides as well as on the age and sex. Most of the percutaneous permeation studies conducted in pigs were performed on their back, the ear, the flank, or the abdomen. The selection of a specific skin site of the pig, when matching it to the human skin, determines the result of the test. *In vivo* studies involving classified chemical agents and stimulant agent showed that the back skin of weanling pigs were closely approximated to human forearm skin with regard to its resistance to permeation.

Also permeation tests substantially confirm the similarities. For instance, *in vitro* skin permeation to water revealed that human and porcine skins were similar, as well as other compounds. Anatomical and biochemical analysis and permeation tests definitely confirm the similarities between pig and man and therefore, the possibility to use the pig as a transdermal model [56,57].

1.6.2 IN VITRO TECHNIQUES

An experimental apparatus (Franz diffusion Cells) aimed to measure skin permeability as an *in vitro* technique was proposed in mid-1970s by Franz. Simply, Franz Cell is a double-walled beaker characterized by a top donor chamber separated from the receiver chamber by skin. While thermostatic fluid flows inside the beaker double wall (constant temperature), sampling receiver takes place from the sampling port (Figure 10). Skin permeability is evaluated on the basis of drug concentration increase in the receiver environment. *In vivo* tests are usually conducted on human, rodent, and pig skin, which are the closest to human skin. Monkey skin is also used [58-62].

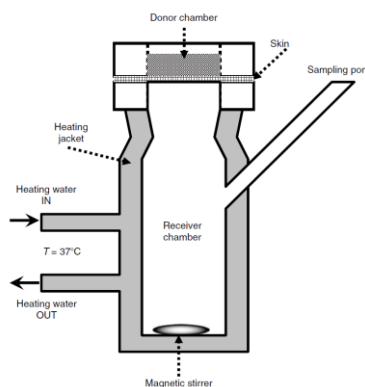


Figure 10. Schematic representation of Franz Diffusion Cell. [57]

1.6.3 DRUG PERMEATION THROUGH MEMBRANES

Historically speaking, the first mathematical model of drug permeation phenomenon through skin is the one proposed by Higuchi. Then, many other authors developed excellent research studies on this topic, finding several models based on the changes on active principle concentrations.

These models can be divided into two main groups: empirical and mechanistic models. Although mechanistic models should be further used as they can provide very useful information about the relative importance of several phenomena concurring in the determination of skin permeability, empirical ones can overcome inaccuracies of mechanistic models (due to uncertainties) providing better predictions from the practical point of view.

Mechanistic models are divided into two categories: Analysis based on simple diffusion models (Fick's diffusion law, Quantitative structure-activity relationship (QSAR) methods) and Analysis based on heterogeneous diffusion models. Empirical analysis of skin permeation of drugs is based on molecular structures such as a Neural network modelling to predict of skin permeability [63-69].

Complex situations may happen in the drug release. They can be summarized in four simple conditions concerning release properties of the formulation :

- a) Formulation can match drug dissolution.
- b) Formulation can show drug dispersion in a liquid phase [70].
- c) A polymeric matrix containing the drug in a dissolved or an undissolved form.
- d) Drug solution reservoir separated from the skin by a matrix.

1.6.3.1 DRUG DISSOLUTION

When formulation consists of a well-stirred drug solution, skin acts as a unique barrier characterized by proper, constant diffusion (D_{skin}) and partition (K_{skin}) coefficients. In that way drug transport can be approached according to Fick's second law considering the diffusion in only in one direction [71]

$$\frac{\partial C_{\text{skin}}}{\partial t} = \frac{\partial}{\partial X} \left(D_{\text{skin}} \frac{\partial C_{\text{skin}}}{\partial X} \right) \quad (4)$$

where t is time, X is the abscissa, and $C_{\text{skin}}(t, X)$ is drug concentration inside the skin. Assuming that initial drug concentration in the solution C_{d0} is constant and that drug concentration in $X=h_{\text{skin}}$ (skin thickness) is always zero, equation (4) must be solved with the following initial and boundary conditions:

initial:

$$C_{\text{skin}}(X) = 0, \quad 0 < X < h_{\text{skin}} \quad (5)$$

boundary:

$$C_{\text{skin}} = k_{\text{skin}} C_{d0}, \quad X = 0; \quad C_{\text{skin}} = 0, \quad X = h_{\text{skin}} \quad (6)$$

where equation (5) states that the skin is initially drug free, while equation (6) states the partitioning conditions at the formulation/skin interface (left equation) and sink conditions in the receiver environment (right equation). Equation (5) holds in the presence of a wide solution

volume, while equation (6) holds in the presence of a wide receiver volume. Equation (7) analytical solution reads

$$M_t = Sh_{\text{skin}}k_{\text{skin}}C_{d0} \left(\frac{D_{\text{skin}}}{h_{\text{skin}}^2} t - \frac{1}{6} - \frac{2}{\pi^2} \sum_{i=1}^{\infty} \frac{(-1)^i}{i^2} e^{-\left(\frac{D_{\text{skin}}i^2\pi^2t}{h_{\text{skin}}^2}\right)} \right) \quad (7)$$

M_t as the drug amount permeated at time t and S is the permeation area. This equation can be used as a model both *in vitro* and *in vivo* experiments, even if the assumption of zero drug concentration in $X=h_{\text{skin}}$ (Figure 11) is more reasonable for *in vivo* conditions, as systemic drug concentration is lowered by drug remove or metabolization.

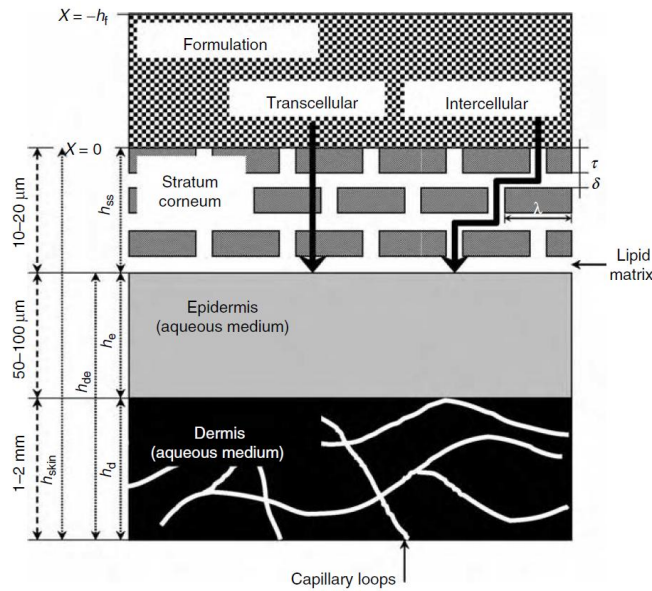


Figure 11. Schematic representation of human skin and most important geometric characteristics [63].

On the contrary, the assumption of pure one-dimension diffusion is much more reasonable *in vitro* set up than in *in vivo* experiments. D_{skin} is the skin effective diffusion coefficient accounting for skin heterogeneity (follicles, sweat gland, SC, epidermis, dermis). Interestingly, equation (8), for very long periods of time, can be designated as

$$M_t = Sh_{\text{skin}}k_{\text{skin}}C_{d0} \left(\frac{D_{\text{skin}}}{h_{\text{skin}}^2} t - \frac{1}{6} \right) \quad (8)$$

Consequently, drug flux J (mass/(surface \times time)) is given by

$$J = k_{\text{skin}} C_{\text{d0}} \frac{D_{\text{skin}}}{h_{\text{skin}}} = C_{\text{d0}} P_{\text{skin}} \quad (9)$$

where P_{skin} is skin permeability. Michaels et al. [70] (equation (9)) assuming that skin resistance is substantially due to SC, developed a simple model that can also account for permeation of dissociating compounds. They assume that SC is made up of parallel array of thin plates (constituted by proteins) regularly dispersed in a lipid homogeneous continuous matrix (Figure 11). As a result, drug diffusion behaves according to two different mechanisms: (a) solely through the continuous, tortuous lipid matrix, or (b) alternatively crossing the continuous and dispersed phase. Thus, J will be the sum of both contributions (J_a and J_b) and the problem shifts on their evaluation which, in turn, implies the determination of the corresponding permeability P_a and P_b . The plates are assumed as rectangles characterized by length λ and thickness T and that they are equidistantly separated by nearest neighbours by an interstitial channel of thickness δ (Figure 11), $h_{\text{skin}} = n(\delta + T)$ (n =layers number) while the thickness of lipidic and plate phases will be $h_L = n\delta$ and $h_P = nT$, respectively. Thus, P_b can be evaluated assuming that the diffusive resistance of a layered membrane is given by the sum of the resistances belonging to each layer.

$$\frac{1}{P_b} = R_L + R_P = \frac{n\delta}{k_{\text{pL}}D_L} + \frac{n\tau}{k_{\text{pP}}D_P} = \frac{n(\delta + \tau) \left(\frac{\beta}{\sigma} \frac{D_P}{D_L} + 1 \right)}{(\beta + 1)k_{\text{pP}}D_P}$$

$$\beta = \frac{\delta}{\tau}; \quad \sigma = \frac{k_{\text{pL}}}{k_{\text{pP}}} \quad (10)$$

P_a is estimated considering that the surface fraction (according to the diffusion direction) belonging to the lipid phase is $2\beta / \alpha$ and that the effective path length through the lipid channels is $1 + (\alpha + \beta) / 2(1 + \beta)$. Consequently, P_a is

$$P_a = \frac{k_{\text{pL}}D_L \frac{2\beta}{\alpha}}{n(\delta + \tau) \left(1 + \frac{\alpha + \beta}{2(1 + \beta)} \right)}; \quad \alpha = \frac{\lambda}{\tau} \quad (11)$$

Finally, model can be expressed as follows:

$$M_t = S(J_a + J_b)t = SC_{\text{d0}}(P_a + P_b)t \quad (12)$$

1.6.3.2 DRUG DISPERSION IN A LIQUID PHASE

Coceani et al. [70] studied permeation of drug molecule. This consists of a liquid phase containing dispersed drug with a shape of equal spherical particles of initial radius R_0 . The model requires the solution, in one dimension, of Fick's second law inside the trilaminar made up by stratum corneum, dermis–epidermis and stagnant layer, provided that the initial and boundary conditions appropriate are considered. Fick's second law for stratum corneum, dermis–epidermis and stagnant layer reads, respectively [70,72,73]:

$$\frac{\partial C_{sc}}{\partial t} = \frac{\partial}{\partial X} \left(D_{sc} \frac{\partial C_{sc}}{\partial X} \right) \quad (13)$$

$$\frac{\partial C_{de}}{\partial t} = \frac{\partial}{\partial X} \left(D_{de} \frac{\partial C_{de}}{\partial X} \right) \quad (14)$$

$$\frac{\partial C_{ss}}{\partial t} = \frac{\partial}{\partial X} \left(D_{ss} \frac{\partial C_{ss}}{\partial X} \right) \quad (15)$$

where D_{sc} , D_{de} , D_{ss} , C_{sc} , C_{de} , and C_{ss} are, respectively, the drug effective diffusion coefficient and concentration in the SC, in the dermis–epidermis and in the stagnant layer. Equation (13) through equation (15) must accomplish the following boundary conditions (Figure 11):

$$V_d \frac{dnC_d}{dt} = V_d K_t (C_s - C_d) + D_{sc} S \frac{\partial C_{sc}}{\partial nX} \Big|_{X=0} \quad (16)$$

$$D_{sc} \frac{\partial C_{sc}}{\partial X} \Big|_{X=h_{sc}} = D_{de} \frac{\partial C_{de}}{\partial X} \Big|_{X=h_{sc}} \quad (17)$$

$$D_{de} \frac{\partial C_{de}}{\partial X} \Big|_{X=h_{sc}+h_{de}} = D_{ss} \frac{\partial C_{ss}}{\partial X} \Big|_{X=h_{sc}+h_{de}} \quad (18)$$

$$V_r \frac{dC_r}{dt} = -D_{ss} S \frac{\partial C_{ss}}{\partial X} \Big|_{X=h_{sc}+h_{de}+h_{ss}} \quad (19)$$

$$k_{p1} = \frac{C_{sc}}{C_d}; \quad k_{p2} = \frac{C_{de}}{C_{sc}}; \quad k_{p3} = \frac{C_{de}}{C_{ss}}; \quad k_{p4} = \frac{C_{ss}}{C_r} = 1 \quad (20)$$

and the following initial conditions:

$$C_d = C_{d0}; \quad C_r = C_{sc} = C_{de} = C_{ss} = 0; \quad M = M_0 \quad (21)$$

where V_d and V_r are the donor and receiver environment volumes, respectively, K_t is the dissolution rate constant, and C_d and C_r are drug concentration in the donor and receiver compartment. Respectively, C_{d0} and M_0 are the starting drug concentration in the donor compartment and the starting amount of undissolved drug in the donor compartment. C_s is drug solubility in the fluid filling the donor compartment, S is the permeation area, and K_{p1} , K_{p2} , K_{p3} , and K_{p4} are the partition coefficients.

Equation (16) shows the drug mass balance made up on the donor compartment: the first right-hand side term takes into account powder dissolution, whereas the second one takes into account the mass flux that leave from the donor through the SC.

Equation (17) and equation (18) impose, respectively, that it makes no difference whether accumulation occurs at the SC/dermis–epidermis interface ($X=h_{sc}$) or at the dermis–epidermis/stagnant layer interface ($X = h_{sc} + h_{de}$).

Equation (19) states that the increase in concentration of the receiver compartment depends on drug flux exiting from the stagnant layer.

Finally, equation (20) shows interfaces partitioning conditions while equation (21) states that, at the beginning, skin and receiver are drug free, while donor compartment contains a drug solution (initial concentration C_{d0}) and an amount M_0 of undissolved drug. Particles dissolution constant K_t is supposed to be time dependent, because particle radius decreases upon dissolution ($K_t = 4\pi R^2 k_d/V_d$).

As a result, once K_d (intrinsic drug dissolution constant) is known, K_t evaluation gives the knowledge of particle radius R reduction. For this purpose, A drug mass balance is created with the amount that reaches the skin, the donor and receiver compartments:

$$M = M_0 + V_d(C_{d0} - C_d) - V_r C_r - \int_0^{h_{sc}} C_{cs} S dX - \int_{h_{sc}}^{h_{sc}+h_{de}} C_{de} S dX - \int_{h_{sc}+h_{de}}^{h_{sc}+h_{de}+h_{ss}} C_{ss} S dX \quad (22)$$

where M is the drug amount not yet dissolved at time t . Bearing in mind the Hixon–Crowell equation:

$$R = R_0 \sqrt[3]{\frac{M}{M_0}} \quad (23)$$

it is possible to calculate R reduction and, thus, K_t reduction. Obviously, when the dissolution phenomenon implies a considerable variation of the particle radius, the effects of K_t decrease are more evident. In this case, the solid surface will be strongly reduced and, accordingly, the

drug flux feeding the donor compartment will decreased. Thus, the importance of K_t reduction should be more relevant for few big particles than for many small particles, the total particles mass remains the same.

Coceani et al. apply this model to study acyclovir permeation through male hairless rat skin at 37°C. In particular, they studied (Franz Diffusion cell apparatus) acyclovir permeation through the full skin and the dermis–epidermis layer after removing SC. [70]

Guy and Hadgraft [55,60] developed a mathematical model in order to investigate the effect of the variation of thickness during drug release through the skin. Accordingly, the experimental permeation data are fitted by the following equation, suitable to describe drug permeation through a thin membrane:

$$\frac{M_t}{M_\infty} = \left(1 - \exp\left(-\frac{D_s t}{KL_o L_s} \right) \right) \quad (24)$$

where M_t is the total amount of drug that passes through the layers of skin, L_s is stratum corneum thickness and L_o the formulation thickness, during period t . D_s is the diffusion coefficient of the drug through the different skin layers and K is a partition coefficient between skin layer and drug formulation (typically $K = \text{concentration in skin layer} / \text{concentration in vehicle}$).

1.6.3.3 POLYMERIC MATRIX CONTAINING DRUG

Fernandes et al. [74,75] proposes a very interesting analytical solution to the problem of skin (thought as a unique membrane) permeation when formulation is represented by a matrix containing dissolved drug. Taking this into account, , their model consists in the following equations:

$$\frac{\partial C_f}{\partial t} = \frac{\partial}{\partial X} \left(D_f \frac{\partial C_f}{\partial X} \right) \quad (25)$$

$$\frac{\partial C_{\text{skin}}}{\partial t} = \frac{\partial}{\partial X} \left(D_{\text{skin}} \frac{\partial C_{\text{skin}}}{\partial X} \right) \quad (26)$$

where $C_f(X)$ and $C_{\text{skin}}(X)$ represent, respectively, drug concentrations in the formulation and the skin, while D_f and D_{skin} are drug diffusion coefficients in the formulation and the skin, respectively. These equations are solved under the following initial and boundary conditions (see Figure 11):

initial conditions:

$$C_f = C_{f0} \quad -h_f < X < 0; \quad C_{\text{skin}} = 0 \quad 0 < X < h_{\text{skin}} \quad (27)$$

boundary conditions:

$$\left. \frac{\partial C_f}{\partial X} \right|_{X=-h_f} = 0 \quad (28)$$

$$D_f \left. \frac{\partial C_f}{\partial X} \right|_{X=0} = D_{\text{skin}} \left. \frac{\partial C_{\text{skin}}}{\partial X} \right|_{X=0} \quad (29)$$

$$C_{\text{skin}}(X = 0) = k_p C_f(X = 0) \quad (30)$$

$$C_{\text{skin}}(X = h_{\text{skin}}) = 0 \quad (31)$$

Although, initially, matrix (formulation) is uniformly loaded by the drug (concentration C_{f0}) (Equation (27)), skin is drug free.

Equation (28) imposes the existence of a drug impermeable wall on the matrix back while equation (29) excludes drug accumulation at the matrix/skin interface. Finally, Equation (30) imposes partitioning conditions at the matrix/skin interface and Equation (31) fixes to zero drug concentration in the blood circulation.

Model analytical solution reads

$$\frac{M_t}{M_\infty} = 1 + \beta p \sum_{i=1}^{\infty} \left\{ \frac{\text{sen}(\lambda_i/\sqrt{p})}{\text{Den}_i} e^{\left(-\lambda_i^2 \frac{D_{\text{skin}} t}{h_{\text{skin}}^2} \right)} \right\} \quad (32)$$

$$\text{Den}_i = \text{Den}_{i1} + \text{Den}_{i2} \quad (33)$$

$$\text{Den}_{i1} = -\frac{1}{2} \lambda_i \text{sen}(\lambda_i) \left[\sqrt{\frac{1}{p}} (k_p + \beta p) \lambda_i \cos\left(\frac{\lambda_i}{\sqrt{p}}\right) + 3k_p \text{sen}\left(\frac{\lambda_i}{\sqrt{p}}\right) \right] \quad (34)$$

$$\text{Den}_{i2} = \frac{1}{2} \lambda_i \cos(\lambda_i) \left[3\beta \sqrt{p} \cos\left(\frac{\lambda_i}{\sqrt{p}}\right) - \lambda_i (k_p + \beta) \text{sen}\left(\frac{\lambda_i}{\sqrt{p}}\right) \right] \quad (35)$$

$$\beta = \frac{D_{\text{skin}} h_f}{D_f h_{\text{skin}}}; \quad p = \frac{D_f h_{\text{skin}}^2}{D_{\text{skin}} h_f^2} \quad (36)$$

Where D_{en} is the diffusion corresponding to the enhancer and eigen-values λ_i are given by the solution of

$$\tan(\lambda_i) \tan\left(\frac{\lambda_i}{\sqrt{p}}\right) + \frac{\beta\sqrt{p}}{k} = 0 \quad (37)$$

1.6.3.4 DRUG SOLUTION RESERVOIR

The last configuration considered shows that the formulation is based on a drug solution reservoir separated from the skin by a matrix. Again, assuming that the skin as a one-layer membrane, mass transport in the matrix and in the skin is ruled by equation (25) and equation (26), respectively.

It obviously applies to different initial and boundary conditions:

initial conditions:

$$C_{res} = C_{res0} \quad (38)$$

$$C_f = k_p^{fr} C_{res0} \quad -h_f < X < 0; \quad C_{skin} = 0 \quad 0 < X < h_{skin} \quad (39)$$

boundary conditions:

$$V_{res} \frac{dC_{res}}{dt} = S_f D_f \left. \frac{\partial C_f}{\partial X} \right|_{X=-h_f} \quad (40)$$

$$D_f \left. \frac{\partial C_f}{\partial X} \right|_{X=0} = D_{skin} \left. \frac{\partial C_{skin}}{\partial X} \right|_{X=0} \quad (41)$$

$$C_{skin}(X=0) = k_p^{sf} C_f(X=0) \quad (42)$$

$$C_{skin}(X=h_{skin}) = 0 \quad (43)$$

where S is the surface area available for permeation, C_{res} is the drug concentration in the reservoir, C_{res0} is its initial value, k_p^{fr} and k_p^{sf} are matrix/reservoir and skin/matrix partition coefficients while V_{res} is the reservoir solution volume. Equation (39) implicitly assumes that, at test time, a drug equilibrium partitioning is fully established between the solution and the matrix whereas Equation (40) states that C_{res} reduction speed is equal to the drug flow crossing matrix surface in $X=0$.

It is worth mentioning that, to render skin permeation mathematical modelling closer to *in vivo* conditions, the boundary condition set in $X=h_{\text{skin}}$ should be modified. Indeed, if at an initial stage drug concentration can be set equal to zero, and it is also required to take the drug accumulation in the blood and drug released from the blood into account. As a consequence, the new boundary condition reads

$$V_b \frac{dC_b}{dt} = -S_{\text{skin}} D_{\text{skin}} \left. \frac{\partial C_{\text{skin}}}{\partial X} \right|_{X=h_{\text{skin}}} - k_e C_b \quad (44)$$

$$\left. \frac{C_{\text{skin}}}{C_b} \right|_{X=h_{\text{skin}}} = k_p^{\text{sb}} \quad (45)$$

where S_{skin} is the area available for permeation, V_b and C_b are, respectively, blood volume and drug concentration in blood, k_e is the drug elimination constant while k_p^{sb} is the skin/blood drug partition coefficient. Equation (45) simply affirms that C_b variation depends on drug flow crossing the skin and on drug elimination (here supposed, for the sake of simplicity, a first-order kinetics process) [76,77].

CHAPTER 2: RESEARCH APPROACH

2.1 ABSTRACT

Mathematical drug release modelling of biodegradable polymeric systems by microencapsulation technology in textiles has not progressed much yet, because it is generally too complex. The release of a therapeutic agent from a formulation applied to the skin surface and its transport to the systemic circulation has a multistep process.

The transdermal drug released is a feasible administration route for powerful, low-molecular weight therapeutic agents, which has to be accurate in their control of drug distribution. Moreover, many drugs are difficult to handle because they must be delivered slowly over a prolonged period to have a beneficial effect.

In the present work, several examples of practical applications of mathematical models, developed through experimental drug release data, are given. For those involved in the design and development of biodegradable drug delivery systems, it will be useful to choose the generic mathematical model for several specific drug release problems. This transport model is based on the appropriate solution to Fick's second law of diffusion and can be used to explain drug release kinetics into this complex biological membrane.

Keywords: Microencapsulation; Active compound; Biodegradable polymers; Drug release; Mathematic model; Smart Textiles;

2.2 OBJECTIVES OF THE THESIS

Current technology of microencapsulation has enabled the production of biofunctional textiles. These textiles are able to release drugs or cosmetics to the skin. This technology is based on empirical procedure which is limited to high added-value applications, such as the ones in medicine field. A quantitative analysis based on physico-chemical principles could allow the generation of new technologies.

The main objective of this study is to create smart textiles which allow a controlled drug release for any active compound/substance. Such objective will allow the control of the textiles drug release in such a way that the active compound is released in the right quantity, at the right time and at the right place.

The steps to be followed in order to get to the objective are as per below:

1. Handling and characterization of microspheres.
2. Impregnation of microspheres on textile substrate
3. Analysis of drug release.
4. Find and check a Mass Transport Model through the skin.

2.3 EXPERIMENTAL STRUCTURE

The experimental structure is adapted to the project steps. These steps are summarized in the Figure 12.

Microspheres containing active principles were prepared using a solvent evaporation procedure with poly(vinyl alcohol) as surfactant in the external aqueous phase. Several biodegradable microspheres of biocompatible polymers, taken as delivery systems for active agent, have been studied.

Polymers were PLGA (Poly(lactide-co-glycolide)) and PCL (poly(ϵ -caprolactone)). The active compounds chosen were cosmetics and drugs, such as gallic acid, caffeine and ibuprofen. The microspheres obtained were characterized by the measure of encapsulation efficiency. The surface morphology and chemical structure of the micro particles were investigated using scanning electron microscopy (SEM) and Fourier transform infrared spectroscopy (FT-IR). Nanosizer was used for particle size distribution.

The application of the microspheres in the fabrics was carried out using Pad-Dry technique, since it is a simple and efficient technology and its working conditions are harmless to the system.

The drug release system was analyzed, through samples of the treated fibre (cotton, polyamide, acrylic and polyester) in order to study the drug delivery behaviour in different media, deionized water and physiological saline ($T=37^{\circ}\text{C}$).

The skin penetration profile by *in vitro* technique for different active principles was determined using pigskin. The release experiments are performed resorting to the Franz Diffusion cells apparatus (Lara-Spiral, Courtenon, France) consisting of two thermostatic chambers, the upper donor and the lower receptor chamber, divided by a skin biopsy.

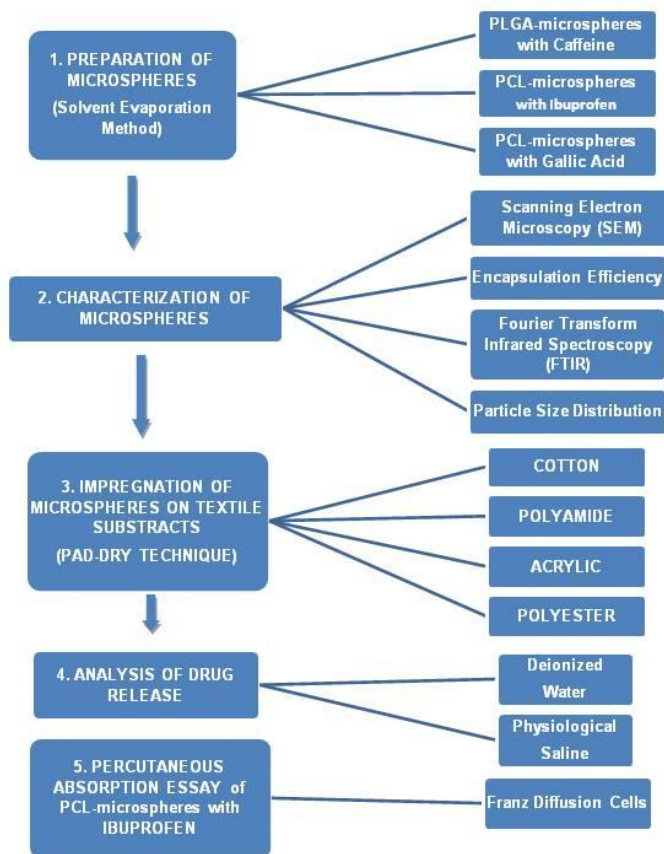


Figure 12. Scheme of the experimental structure of the project.

2.4 MATERIALS

2.4.1 BIOCOMPATIBLE POLYMERS AND ACTIVE AGENTS

The most important materials used to prepare microspheres were the ones from polymeric matrix, PLGA (Poly(lactide-co-glycolide)) with a copolymer ratio (lactic acid/glycolic acid) of 75/25 and a molecular mass (M_w) range of 5,000-15,000 from Aldrich and PCL (poly(ϵ -caprolactone)) with a molecular mass (M_n) of 60,000 from Aldrich. The active compounds used were Ibuprofen in powder with a molecular mass (M_r) of 206.28, supplied by Sigma-Aldrich; Caffeine anhydrous in powder with (M_r) 194.20 from Fluka; Gallic acid in powder with (M_n) 170.12 from Sigma-Aldrich. As dispersant material, PVA (Poly(vinyl alcohol)), 87-89% hydrolyzed was used, with a (M_w) range of 31,000-50,000 from Aldrich and finally, the solvent dichloromethane stabilized with 20 ppm of amylene, supplied by Panreac.

2.4.2 TEXTILE SUBSTRATES

The standard textile substrates woven fabrics used were: Cotton fabric (CO) (Style 400, ISO 105 - F02) Polyamide fabric (PA) (Style 361, ISO 105-F03), Polyester fabric (PET) (Style 777, ISO 105-F04), and Acrylic fabric (PAC) (Style 864, ISO 105-F05) from Test Fabrics Inc (USA).

2.4.3 SKIN PERMEATION

The type of skin used to obtain a mass transport model through the skin by *in vitro* technique was pig skin. It was obtained from the unboiled back of domestic pigs (Landrace Large White race). The treated and dermatomed pigskin discs were supplied by a research group (Biophysics of Lipids and Interphases group) of IQAC-CSIC. The OECD Guidelines and the opinion of the Scientific Committee on Cosmetic Products and Non-Food Products (SCCNFP) were closely a considerable reference in the present study. phosphate-buffered saline at pH 7.4 supplied by Sigma in distilled water (containing 0.9% NaCl, 0.02% KCl and 0.8% phosphate buffer) was used as receptor fluid.,.

All chemicals used were of analytical grade.

2.5 EXPERIMENTAL METHODS AND TECHNIQUES

The methods or techniques used in the present work follow the structure according to its experimental steps.

2.5.1 PREPARATION OF MICROSPHERES

All the microspheres were performed by a double emulsion ($w_1/o/w_2$ type in the case of caffeine encapsulation, but of $o_1/o_2/w$ type for ibuprofen and gallic acid encapsulation) using the conventional solvent evaporation method.

Briefly, the polymer (PLGA or PCL) and the active principle (caffeine or ibuprofen or gallic acid) were separately dissolved in methylene chloride and either in water (in the case of caffeine) or in isopropyl alcohol (for ibuprofen) or in monalcol (for gallic acid), respectively.

The simple emulsion (w_1/o or o_1/o_2) was generated by mechanical agitation (Ultra-turrax T25, Figure 13; Table 6) for several minutes. Afterwards, this simple emulsion was added to a continuous phase, constituted of 150 ml aqueous solution of PVA (dispersant) (2% w/w) and emulsified for several minutes resulting in a double emulsion ($w_1/o/w_2$ or $o_1/o_2/w$). The mixture was maintained under constant agitation until the total evaporation of the solvent and the

consequent microsphere formation. The method used was carried out at 4°C in the case of caffeine, but for ibuprofen and gallic acid it was carried out at room temperature. [16,17,22,75-81]

ULTRATURRAX T25 (Figure 13; Table 6) as a homogenizer is ideal to stir volumes from 1-2000mL (H₂O) in such applications as homogenizing wastewater samples, dispersion tasks under vacuum, or sample preparation in medical diagnostics. Stainless steel or plastic homogenizing tools can be used. Stirrer features a digital display, step less speed adjustment, and overload protection. Meets IP 20 protection class according to DIN EN 60529.



Figure 13. T-25 Digital Ultraturrax IKA ©

Table 6. Specifications of ULTRATURRAX T25

MANUFACTURER	IKA
MODEL	T25
POWER	500 W
SPEED RANGE	3500-24000 rpm
SAMPLE VOLUME	1-2000 mL

2.5.2 CHARACTERIZATION OF MICROSPHERES

For the characterization of the obtained microspheres, 4 tests were done: Scanning Electron Microscopy (SEM), Encapsulation Efficiency, Fourier Transform Infrared Spectroscopy (FTIR) and Particle Size Distribution [7].

2.5.2.1 SCANNING ELECTRON MICROSCOPY (SEM)

The treated fabrics were analyzed by SEM (model JSM-5610, JEOL, Tokyo, Japan; Figure 14; Table 7). The SEM analysis was performed on cotton fabric with microspheres and void microspheres for each substance.

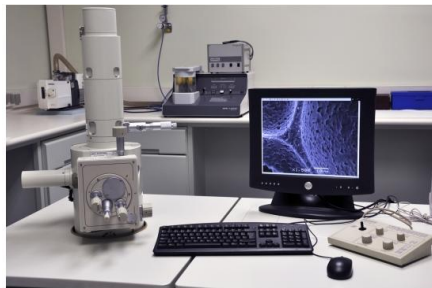


Figure 14. Scanning Electron Microscope (JEOL, JSM-5610)

Table 7. Specifications of Scanning Electron Microscope

MANUFACTURER	JEOL
MODEL	JSM-5610
RESOLUTIONS (SEI)	3.0 nm guaranteed
MAGNIFICATION	x 18
IMAGE MODE	SEI*, BEI*
PROBE CURRENT	1 pA to 1 μ A
MODE	High Vacuum

(*SEI: Secondary electron image; *BEI: Backscattered electron image)

The scanning electron microscope is based on the interaction between an electron beam and the surface of a given solid material. The result is a high-resolution image of the surface topography of the material that can be analyzed using image analysis tools. To handle non-conductive samples, as in this case, there is sputtering equipment (Figure 15) to lay thin layers of gold on the surface of the samples, making them electrically conductive and enabling their visualization using the microscope.

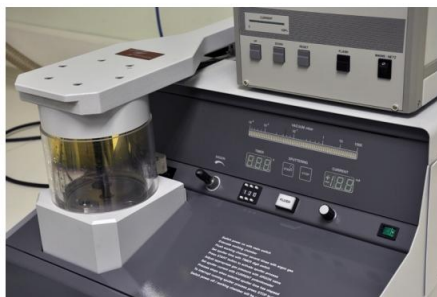


Figure 15. Sputtering equipment

2.5.2.2 ENCAPSULATION EFFICIENCY

Encapsulation efficiency of active compounds in microspheres was detected indirectly in the liquid phase by UV/Vis Spectrophotometer (Shimadzu UV-2401 PC) after centrifugation (Figure 16; Table 8) of dissolution for several minutes [82,83]. The ratio of amount of active agent entrapped in the dispersion was calculated by the following equation:

$$EE (\%) = \frac{C_t - C_d}{C_t} \cdot 100 \quad (46)$$

where C_t is the theoretical concentration of microencapsulated drug, C_d is the drug concentration that remains in the bath solution, therefore the amount of drug that has not been microencapsulated.



Figure 16. Centrifuge and UV/Vis Spectrophotometer

Table 8. Specifications of UV/Vis Spectrophotometer

MANUFACTURER	Shimadzu
WAVELENGTH RANGE	190 to 900 nm
MONOCHROMATOR SYSTEM	Single monochromator with a high-performance blazed holographic grating in the aberration corrected Czerny-Turner mounting
RESOLUTION	0.1 nm
LIGHT SOURCE	50 W halogen lamp (2,000 hours life) and D2 lamp (500 hours life)
SOFTWARE	Personal Spectroscopy Software (standard) Spectrum, Quantitative, Time Course
SPECIFICATIONS	

2.5.2.3 FOURIER TRANSFORM INFRARED SPECTROSCOPY (FTIR)

A Fourier-transform infrared spectrometer FTIR (Avatar System 320; Figure 17; Table 9) was used to identify the chemical structure of the formulation of microspheres which were prepared by grinding the powder sample with KBr (wave-numbers 500-4000 cm⁻¹, at a resolution of 4 cm⁻¹ and collected for 20 scans). Moreover, it allows the detection of interactions between active agents and polymers, as well as, the determination of the changes on original polymers and the settlement of microspheres as matrix.



Figure 17. FTIR Spectrometer Avatar System 320.

Table 9. Specifications of FTIR spectrometer

MANUFACTURER	Nicolet
SPECTROMETER	Avatar System 320
SOURCE	IR
DETECTOR	DTGS KBr
BEAMSPLITTER	KBr
SAMPLE SPACING	2.0000
DIGITIZER BITS	20
MIRROR VELOCITY	0.6329
APERTURE	100.00

2.5.2.4 PARTICLE SIZE DISTRIBUTION

Particle size distribution of microspheres was carried out at Malvern Nanosizer (Model Nano-ZS Series, Malvern; Figure 18; Table 10). Microspheres samples were introduced into a DTS1060C – Clear disposable zeta cell and water was used as a dispersant at 25°C. The results were reported as an intensity size distribution.



Figure 18. Zetasizer Nano ZS.

Table 10. Specifications of Nanosizer (Size range and Zeta Potential analysis)

MANUFACTURER	Malvern
MODEL	Zetasizer Nano-ZS
SIZE RANGE (NANO S AND NANO ZS)	
SIZE RANGE MAXIMUM (Diameter)	0.3 mm-10 microns
MINIMUM SAMPLE VOLUME	12 μ L
CONCENTRATION-MINIMUM	0.1 mg/ mL 15 KDa protein, 0.1 ppm of 60 nm polystyrene latex
CONCENTRATION-MAXIMUM	40% w/v
MEASUREMENT ANGLES	12.8° and 175° (Nano ZS)
ZETA POTENTIAL (NANO Z, ZS AND NANO ZS90)	
SIZE RANGE SUITABLE FOR MEASUREMENT (Diameter)	Minimum 3.8 μ m, maximum 100 microns
ZETA POTENTIAL RANGE	No effective limitations
MAXIMUM SAMPLE CONCENTRATION	40% w/v
MAXIMUM SAMPLE CONDUCTIVITY	300 mS/cm
CONDUCTIVITY ACCURACY	\pm 10%

2.5.3 IMPREGNATION OF MICROSPHERES ON TEXTILE SUBSTRATE

The application of microcapsules onto the fabrics was carried out by impregnation process using a Pad-Dry (Figure 19) technique of 30 cm width (ERNST BENZ AG KLD-HT and KTF/m250) and followed by a process of drying at room temperature, with the padding pressure, to obtain a *pick-up* of $80\pm 5\%$, from the microencapsulation formulations. The treated fabric samples were finally conditioned at $20\pm 2^\circ\text{C}$ and $65\pm 5\%$ relative humidity for 24 hours before weighting and proceeding to other experiments [9-12].

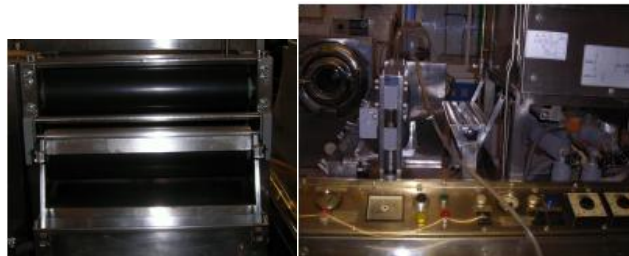


Figure 19. Pad-Dry technique.

2.5.4 ANALYSIS OF DRUG RELEASE

To analyze kinetic release of active compounds, samples of 1 g of the treated fabric were submerged into the thermostated vessels which were filled with deionized water and physiological saline at infinite bath conditions at a temperature of 37°C (Figure 20). This analysis aims to study the environmental effects on the drug release systems, for instance the effect of saline medium (physiological saline), simulating the skin's sweat. The amount of active principle realised to the bath was determined by UV/Vis Spectrophotometer at different periods of time. The results will show the degree of fixation and retention capabilities of the microencapsulated compounds when they are in contact with water and sweat.



Figure 20. Analysis of Drug Release in a thermostated water bath.

2.5.5 OBTAINING A MASS TRANSPORT MODEL THROUGH THE SKIN

The *in vitro* technique used was an experimental apparatus (Franz Diffusion Cells) aimed to measure skin permeability [32]. The *in vitro* studies are carried out with pig skin on Franz static diffusion cells (3 mL, 1.86 cm²) (Figure 21 and 22) in order to know the evolution of the amount of the principle present in each of the different skin compartments (SC, epidermis and dermis) as well as in the receptor fluid, as a function of time (percutaneous absorption essay) [14,15,48,70,84].

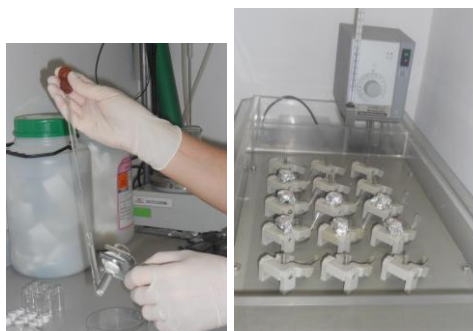


Figure 21. Franz Cells (3 mL, 1.86 cm², Lara-Spiral, Courtenon, France).
Franz Cells in a thermostated water bath.

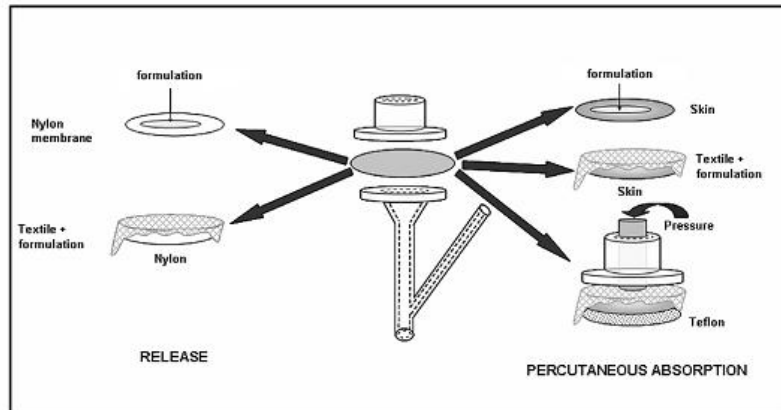


Figure 22. Schematic diagram indicating the different permeation experiments performed on release and skin penetration of ibuprofen.

The skin is dermatomed to a thickness of $700 \mu\text{m} \pm 50 \mu\text{m}$ (Dermatome GA630, Aesculap, Germany). A punch is used to obtain skin discs¹ (2.5 cm inner diameter) which fit into the cell.

A magnetic stirring bar is introduced in the lower part of the cell and it is filled with a receptor fluid through the lateral inlet of the cell. The receptor fluid is usually phosphate-buffered saline at pH 7.4 in distilled water. The penetration cells are placed in a thermostated water bath assuring a skin surface temperature at 32°C while being subjected to magnetic stirring.

The integrity of the skin samples is evaluated by measuring the transepidermal water loss (TEWL) with a Tewameter TM210 (Courage & Khazaka; Figure 23; Table 11). A minimum of 6 diffusion cells with the corresponding skin samples of at least three donors are used for each experimental assay. Each sample of treated fabric is applied on the skin.



Figure 23. Tewameter TM 210.

¹ The treated and dermatomed pig skin discs were supplied by research group of IQAC-CSIC.

Table 11. Specifications of Tewameter.

MANUFACTURER	Courage & Khazaka
MODEL	TM 210
DIMENSIONS	Hollow cylinder 2 cm, ϕ 1 cm Probe 15.3 cm
RESOLUTION	Humidity ± 0.01 % RH Temperature ± 0.01 °C
WATERLOSS	± 0.5 g/hm ² for RH ≥ 30 %; ± 1.0 g/hm ² for RH ≤ 30 %
TEMPERATURE	± 0.5 ° C

At the end of the period of exposure, the skin surface is washed by a specific procedure: first with water or sodium lauryl ether sulfate solution and then twice with water; a cotton swab is used to dry the skin. Moreover, 8 stripping are carried out on the surface horny layers of stratum corneum with adhesive tapes (D-Squame, Cuderm Corporation, Dallas, USA) applied under controlled pressure. The epidermis is pulled apart from the dermis after heating the skin at 80°C for a few seconds (Figure 24). From the dermis, the skin which has been in contact with textile and the Franz cell has been separated and has considered as a surplus sample to be analyzed.



Figure 24. Separation of skin layers.

The active principles present in the different samples analyzed (receptor fluids, washing solutions, SC on tapes, epidermis and dermis) were extracted and diluted with an appropriate solvent. After one night of contact with the solvent, all samples were stirred during 30 min at room temperature and the dermis, epidermis and stratum corneum samples were sonicated for 15 min. After sonication the samples were filtrated on Nylon filter (0.45 μ m, Cameo N, Scharlab, Spain), and then the concentration of the solutions were determined by HPLC (Figure 25; Table 12).



Figure 25. HPLC (VWR-Hitachi equipment (L-2400 UV/Vis detector)).

Table 12. Specifications of HPLC (VWR-Hitachi equipment (L-2400 UV/Vis detector)).

MANUFACTURER	VWR-Hitachi Elite LaChrom
DETECTOR	L-2400 UV/Vis
PUMPING SYSTEM	L-2130
INJECTION SYSTEM	L-2200 Autosampler
SOFTWARE	D-6000 Interfase
COLUMN	LiChrocart 250-4/LiChrosorb RP-18 (5µm)

The kinetic study through cotton fabric samples with PCL-microspheres (ibuprofen) applied onto the skin was obtained and was analyzed with corresponding kinetic models (Chapter 1. (1.6.3)).

CHAPTER 3: PREPARATION OF MICROSPHERES AND THEIR CHARACTERIZATION

3.1 PREPARATION OF MICROSPHERES

The conditions of each of the processes corresponding to preparation of PLGA-microspheres with caffeine, PCL-microspheres with ibuprofen and PCL-microspheres with gallic acid, are shown in the following tables [16-18,22,53,75-81].

3.1.1 PLGA-MICROSPHERES WITH CAFFEINE

The preparation of caffeine microspheres were obtained by solvent evaporation method resulting a double emulsion $w_1/o/w_2$. PLGA-microspheres without active compound were obtained by the same procedure and with the same experimental conditions the PLGA-microspheres with the active compound [78].

The types of materials and their amounts are shown in Table 13. And the experimental conditions to obtain these are shown in Table 14.

Table 13. Type of materials and their amounts.

POLYMER	PLGA (Poly(lactide-co-glycolide))	250 mg
ACTIVE COMPOUND	CAFFEINE	83,2 mg
DISPERSANT	PVA (Poly(vinyl alcohol))	3.06 g
SOLVENT OF POLYMER (o)	DCM (Dichloromethane)	10 mL
SOLVENT OF ACTIVE COMPOUND (w₁)	Distilled water	10 mL
SOLVENT OF DISPERSANT (w₂)	Distilled water	150 mL

PREPARATION OF MICROSPHERES AND THEIR CHARACTERIZATION

Table 14. Experimental conditions of preparation of caffeine PLGA-microspheres.

TYPE OF EMULSION	$w_1/o/w_2$				
RATIO (PLGA:CAFFEINE)	3:1				
PARAMETERS	T (°C)	STIRRER	SPEED (rpm)	Addition time	Stirring Time
ACTIVE COMPOUND (w_1)	4	Magnetic	700	-	15 min
POLYMER (o)	4	Magnetic	370	-	10 min
DISPERSANT (w_2)	Room	Magnetic	1,100	-	2 h
W_1/O emulsion	4	Ultra-turrax T25	24,000	7 min	15 min
$W_1/O/ W_2$ emulsion	4	Ultra-turrax T25	24,000	8 min	10 min
(Solvent evaporation)	Room	Magnetic	400	-	8 h

3.1.2 PCL-MICROSPHERES WITH IBUPROFEN

Ibuprofen PCL-microspheres were prepared by solvent evaporation method resulting a double emulsion $o_1/o_2/w$. PCL-microspheres without active compound were also obtained by the same procedure. The differences respect to PLGA-microspheres with caffeine, apart from using a different polymer (PCL), another solvent was also used to dissolve the active compound. The reason of such changes is basically that the ibuprofen is partially soluble in water and therefore, an organic solvent (2-propanol) had to be used [81].

The types of materials and their amounts are shown in Table 15. And conditions followed to obtain these microspheres are shown in Table 16.

Table 15. Type of materials and their amounts.

POLYMER	PCL (poly(ϵ -caprolactone))	250 mg
ACTIVE COMPOUND	IBUPROFEN	250 mg
DISPERSANT	PVA (Poly(vinyl alcohol))	3.06 g
SOLVENT OF POLYMER (o)	DCM (Dichloromethane)	10 mL
SOLVENT OF ACTIVE COMPOUND (w_1)	2-PROPANOL	10 mL
SOLVENT OF DISPERSANT (w_2)	Distilled water	150 mL

PREPARATION OF MICROSPHERES AND THEIR CHARACTERIZATION

Table 16. Experimental conditions of preparation of ibuprofen PCL-microspheres.

TYPE OF EMULSION	$o_1/o_2/w$				
RATIO (PCL:IBUPROFEN)	1:1				
PARAMETERS	T (°C)	STIRRER	SPEED (rpm)	Addition time	Stirring Time
ACTIVE COMPOUND (w_1)	4	Magnetic	300	-	15 min
POLYMER (o)	4	Magnetic	370	-	1h 30min
DISPERSANT (w_2)	Room	Magnetic	1,100	-	2 h
W_1/O emulsion	Room	Ultra-turrax T25	24,000	11 min	5 min
$W_1/O/ W_2$ emulsion	Room	Ultra-turrax T25	24,000	14 min	11 min
(Solvent evaporation)	Room	Magnetic	500	-	20 h

3.1.3 PCL-MICROSPHERES WITH GALLIC ACID

The preparation of gallic acid PCL-microspheres was made by the solvent evaporation method resulting a double emulsion $o_1/o_2/w$ as in the case of PCL-microspheres with ibuprofen. Therefore, the void PCL-microspheres were obtained by the same procedure. However, in this case, the solvent of agent compound used, was another one since the solubility of gallic acid in water was not as good as in monalcol.

The types of materials and their amounts are shown in Table 17. And the experimental conditions to obtain them are shown in Table 18.

Table 17. Materials and their amounts.

POLYMER	PCL (poly(ϵ -caprolactone))	250 mg
ACTIVE COMPOUND	GALLIC ACID	250 mg
DISPERSANT	PVA (Poly(vinyl alcohol))	3.06 g
SOLVENT OF POLYMER (o)	DCM (Dichloromethane)	10 mL
SOLVENT OF ACTIVE COMPOUND (w_1)	Monalcol	25 mL
SOLVENT OF DISPERSANT (w_2)	Distilled water	150 mL

PREPARATION OF MICROSPHERES AND THEIR CHARACTERIZATION

Table 18. Experimental conditions of preparation of gallic acid PCL-microspheres.

TYPE OF EMULSION	$o_1/o_2/w$				
RATIO (PCL:GALLIC ACID)	1:1				
PARAMETERS	T (°C)	STIRRER	SPEED (rpm)	Addition time	Stirring Time
SOLUTIONS					
ACTIVE COMPOUND (w_1)	4	Magnetic	300	-	15 min
POLYMER (o)	4	Magnetic	370	-	1h 30min
DISPERSANT (W_2)	Room	Magnetic	1,100	-	2 h
W_1/O emulsion	Room	Ultra-turrax T25	24,000	30 min	10 min
$W_1/O/ W_2$ emulsion	Room	Ultra-turrax T25	24,000	10 min	10 min
(Solvent evaporation)	Room	Magnetic	400	-	20 h

3.2 CHARACTERIZATION OF MICROSPHERES

The conditions of each process corresponding to characterization of microspheres are shown below. These conditions were the same for all types of microspheres.

3.2.1 SCANNING ELECTRON MICROSCOPY (SEM)

The morphology of microspheres was investigated using a SEM and the conditions of Scanning Electron Microscopy are shown in the following Table 19.

Table 19. Conditions of the Scanning Electron Microscopy.

SAMPLE DIMENSIONS	2 x 1 cm ²
COATING	Gold
INTENSITY	30 Ma
WORKING DISTANCE	60 mm
PRESSURE	0.005 mbar
TIME	130 s

3.2.2 ENCAPSULATION EFFICIENCY

Encapsulation efficiency was studied to know the ratio of amount of active compound entrapped in the dispersion. The experimental conditions of encapsulation efficiency determination of microspheres are shown in the following tables. Table 20 shows the conditions of the centrifugation process and Table 21 shows the conditions of UV/Vis Spectrophotometer.

Table 20. Conditions of centrifugation process.

SAMPLE VOLUME (mL)	2
SPEED (rpm)	1,000
CENTRIFUGATION TIME (min)	30

PREPARATION OF MICROSPHERES AND THEIR CHARACTERIZATION

Table 21. Conditions of UV/Vis Spectrophotometer.

ACTIVE COMPOUNDS \ PARAMETERS	CAFFEINE	IBUPROFEN	GALLIC ACID
CELL	QUARTZ	QUARTZ	QUARTZ
LIGHTPATH (mm)	10	10	10
λ WAVELENGTH (nm)	273	263	269

3.2.3 FOURIER TRANSFORM INFRARED SPECTROSCOPY (FTIR)

FTIR was used to identify the chemical structure of the formulation of microspheres and to detect interactions between active agents and polymers and also, to determinate the changes on original polymers and forming microspheres as matrix. The conditions of Fourier Transform Infrared Spectroscopy are shown in the following Table 23.

Table 23. Conditions of the Fourier Transform Infrared Spectroscopy.

TABLET	KBr
SAMPLE CONCENTRATION (ACTIVE COMPOUND/KBr)	1 % (w/w)
WAVENUMBERS	500 - 4,000 cm^{-1}
RESOLUTION	4 cm^{-1}
CO-ADDING	20 scans

3.2.4 PARTICLE SIZE DISTRIBUTION

The conditions of Nanosizer to determine the particle size distribution are shown in the following Table 24.

Table 24. Conditions of Nanosizer.

MATERIAL MANAGER	LIPOSOME
DISPERSANT	WATER
CELL	DTS 1060C – Clear disposable zeta cell
T ($^{\circ}\text{C}$)	25

3.3 RESULTS AND DISCUSSION

The results corresponding to each of the types of microspheres (caffeine, ibuprofen and gallic acid) are shown below.

3.3.1 SEM – PLGA-MICROSPHERES WITH CAFFEINE

The fabrics with caffeine PLGA-microspheres have been analyzed by SEM and the SEM micrographs are shown below.

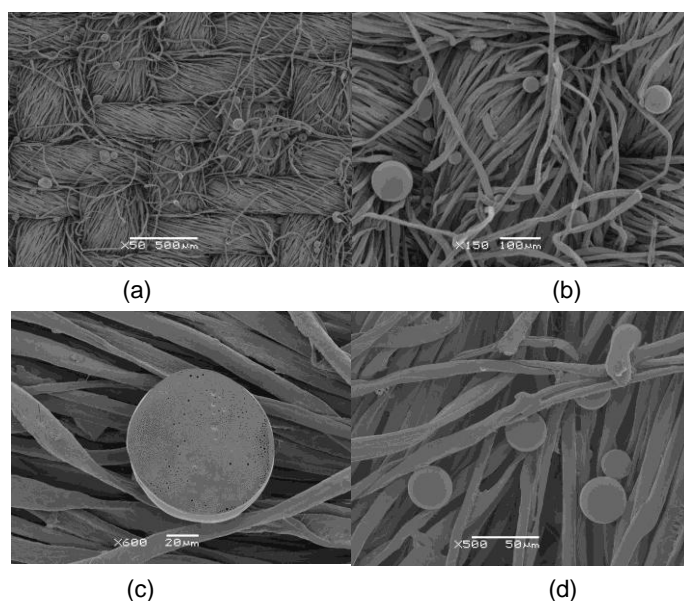


Figure 26. Scanning electron micrographs of PLGA-microspheres on cotton fabric. (a) PLGA-microspheres with caffeine (x50) (b) PLGA-microspheres with caffeine (x150). (c) cross-sectional picture of caffeine PLGA-microsphere (x600). (d) PLGA-microspheres without caffeine (x500).

SEM micrographs of PLGA-microspheres with caffeine and void PLGA-microspheres confirmed what has been obtained. The adhesion between fabrics and PLGA-microspheres is given, since polyvinyl alcohol (PVA) acts as binder [84] between fabrics and PLGA-microspheres. Both of them have a spherical shape with a smooth surface due to PVA. Cross-sectional picture of caffeine (c) is a good result to demonstrate that internally the PLGA-microspheres are all highly porous.

3.3.2 SEM – PCL-MICROSPHERES WITH IBUPROFEN

Fabrics with ibuprofen PCL-microspheres have been analyzed by SEM and the SEM micrographs are shown below.

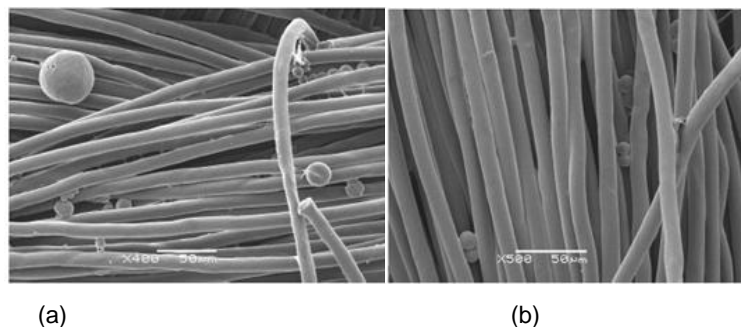


Figure 27. Scanning electron micrographs of PCL-microspheres on cotton fabric. (a) PCL-microspheres with ibuprofen (x400). (b) PCL-microspheres without ibuprofen (x500).

It can be observed that the PCL-microspheres have been obtained and both maintain the same characteristics. These two micrographs (Figure 27) show that PCL-microspheres with a spherical shape smooth surface have been formed, composed of PVA, but internally are porous (although it is not appreciated in these micrographs). The surfaces layer of PVA acts as a binder [85] between PCL-microspheres and fabric. The way they are bonded as can be seen in the pictures.

3.3.3 SEM-PCL MICROSPHERES WITH GALLIC ACID

Cotton fabrics with gallic acid PCL-microspheres have been analyzed by SEM and the SEM micrographs are shown below.

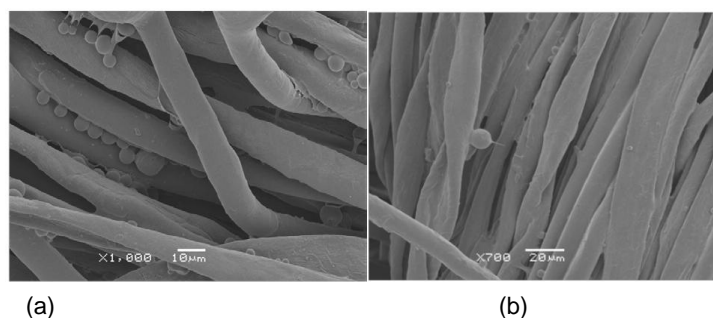


Figure 28. Scanning electron micrographs of PCL-microspheres on cotton fabric. (a) microspheres with gallic acid (x400). (b) PCL-microspheres without gallic acid (x500).

Both micrographs (Figure 28) show that PCL-microspheres have been formed with a spherical shape and smooth surface, composed of a PVA layer, but they are probably internally porous. PVA also acts as a binder [85] between PCL-microspheres and fabric and is clearly appreciated

in the picture (a).

3.3.4 ENCAPSULATION EFFICIENCY – PLGA-MICROSPHERES WITH CAFFEINE

Table 25 shows the caffeine encapsulation efficiencies. Three repetitions were carried out and the overall average was about 28% [86].

Table 25. Encapsulation efficiency of the caffeine PLGA-microspheres.

Sample	Encapsulation efficiency (%)
1	27.97
2	27.89
3	27.97

Encapsulation efficiencies achieved are remarkably low, and there is no literature to compare them with other encapsulation efficiencies and to establish whether the methodology followed is optimal or not. Therefore, further studies are needed to achieve stabilization of the caffeine in the polymer matrix, because of the greater affinity of this with the medium than with the polymer.

3.3.5 ENCAPSULATION – PCL-MICROSPHERES WITH IBUPROFEN

Table 26 shows ibuprofen encapsulation efficiencies, three repetitions were carried out and the overall average was about 84%.

Table 26. Encapsulation efficiency of the ibuprofen PCL-microspheres.

Sample	Encapsulation efficiency (%)
1	88.02
2	82.32
3	82.17

According to the literature [87], the efficiency obtained is too high as shown in the results. Thus, it might ensure us that the designed method for preparation of ibuprofen PCL-microspheres is very efficient.

3.3.6 ENCAPSULATION EFFICIENCY – PCL-MICROSPHERES WITH GALLIC ACID

Table 27 shows the gallic acid encapsulation efficiencies, three repetitions were carried out and the overall average was about 31% [86].

Table 27. Encapsulation efficiency of the gallic acid PCL-microspheres.

Sample	Encapsulation efficiency (%)
1	31.79
2	33.83
3	27.50

The results show low efficiencies of encapsulation, but there are no references of similar studies on active compounds. Therefore, it not possible to assure whether the results are good or not.

3.3.7 FTIR – PLGA-MICROSPHERES WITH CAFFEINE

The results corresponding to FTIR analysis are shown below. Discussion will be based on two types of FTIR spectrum, the first one (Figure 29) is the comparison between polymer and void PLGA-microspheres, and the second one (Figure 30) is the comparison between PLGA-microspheres with caffeine and caffeine.

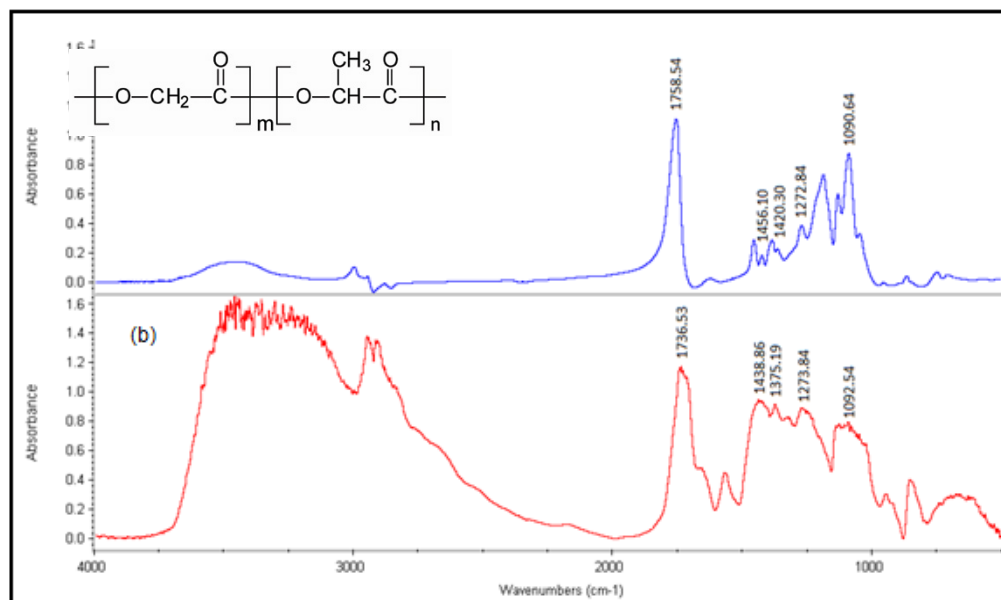


Figure 29. FTIR spectrum of (a) PLGA polymer and (b) PLGA-microspheres without caffeine.

Figure 29 shows the FTIR spectrum of (a) PLGA polymer and (b) PLGA-microspheres without caffeine. Several structural differences are obvious both characteristic frequencies movements of the components as defined in the characteristic peaks [88-90]. The frequencies between 3550 and 3200 cm^{-1} are linked to the stretching O-H from the intermolecular and intramolecular

PREPARATION OF MICROSPHERES AND THEIR CHARACTERIZATION

hydrogen bonds of PVA (dispersant of the microspheres) [91]. The vibrational band observed between 2840 and 3000 cm^{-1} refers to the stretching C-H from alkyl groups. The frequency of 1758.54 cm^{-1} belonging to the strain carbonyl group (C=O stretching) is part of PLGA. It has suffered a displacement and an increase in the bandwidth of the frequency (1736.53 cm^{-1}) in the spectrum of PLGA-microspheres without caffeine. This movement is due to the presence of PVA in the PLGA-microspheres. Polymeric chain has also been modified. Similarly, the frequencies of the methyl group (1456.10 cm^{-1}) of PLGA moves and increases the bandwidth in the frequency of 1438.86 cm^{-1} for PLGA-microspheres without caffeine. Also, it is shown the minimum frequency shift of 1090.64 cm^{-1} (C-O-C asymmetric stretching) and 1272.84 cm^{-1} (C-H) belonging to the PLGA regarding frequencies of 1092.54 cm^{-1} (C-O-C asymmetric stretching) and 1273.84 cm^{-1} (C-H) PLGA-microspheres without caffeine. Finally, the frequency of 1420.30 cm^{-1} (C-H deformation caused by the link -O-CH₂) of PLGA in the spectrum of the PLGA-microspheres without caffeine has disappeared.

These structural changes suggest that the PLGA polymer, which comes from a linear chain turns to a polymeric matrix form.

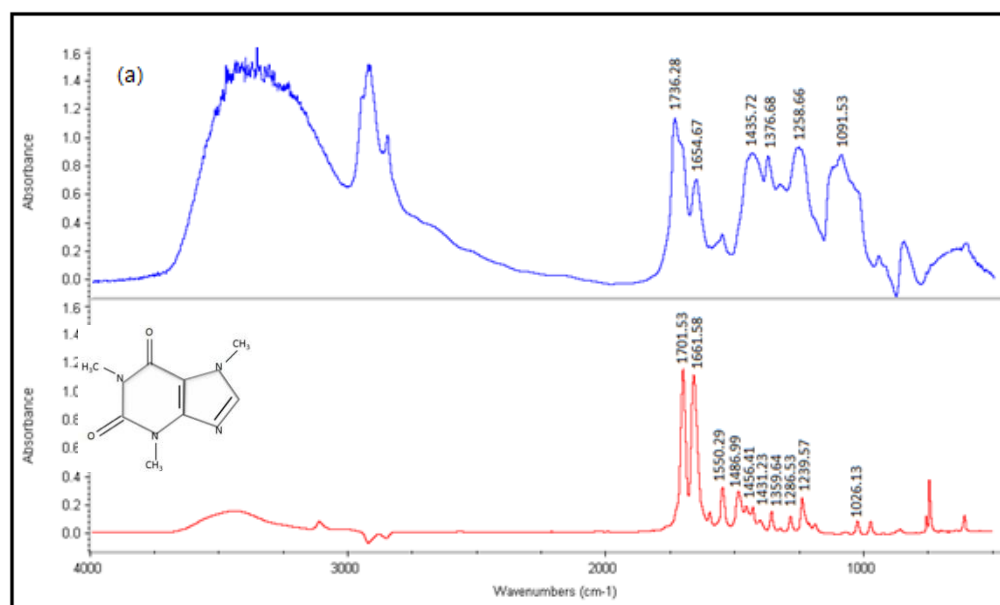


Figure 30. FTIR spectrum of (a) caffeine PLGA-microspheres and (b) caffeine.

Figure 30 shows the FTIR spectrum of (a) caffeine PLGA-microspheres and (b) caffeine [92,93]. Comparing the spectrum of caffeine to caffeine PLGA-microspheres encapsulated in PLGA, many structural differences represented by the displacements of the characteristic frequencies of the components can be seen. In the frequencies between 3550 and 3200 cm^{-1} , the signal produced by stretching O-H of PVA is again observed [91]. And also vibrational band between 2840 and 3000 cm^{-1} is linked to the stretching C-H of PVA [91]. In the frequency of 1701.53 cm^{-1} , belonging to the tension of the carbonyl group (C=O stretching) as part of caffeine, there is a movement and an increased bandwidth of the frequency (1736.28 cm^{-1}) in the spectrum PLGA-microspheres containing caffeine. This influence is due to the presence of the polymer and PVA

[91], because both have this bond in their structures. Another peak to note is 1661.58 cm^{-1} (C=N stretching) in the spectrum of caffeine. This is very significant on the PLGA-microspheres with caffeine when there is no signal in the polymer or void PLGA-microspheres in this frequency (Figure 24). Moreover, the latter suffers a slight shift to a frequency of 1654.67 cm^{-1} . These changes could be possibly assigned to an interaction between the oxygen atoms of carbonyl groups of the polymer and/or PVA and nitrogen atom from the caffeine molecule. Other important frequencies that are part from the structure of caffeine and, as in previous case, are identified the peaks corresponding to displacements, such as: CH_3 asymmetric stretching (1456.4 cm^{-1} , 1431.23 cm^{-1} and 1359.64 cm^{-1}), the C-N stretching (1286.53 cm^{-1}) and cyclic C=N tension (1550.29 cm^{-1}).

3.3.8 FTIR – PCL-MICROSPHERES WITH IBUPROFEN

Results corresponding to FTIR analysis are shown. There are two types of spectrum. The first one (Figure 31) shows the comparison between polymer and void PCL-microspheres, and the second one (Figure 32) corresponds to the comparison between ibuprofen and the PCL-microspheres with ibuprofen.

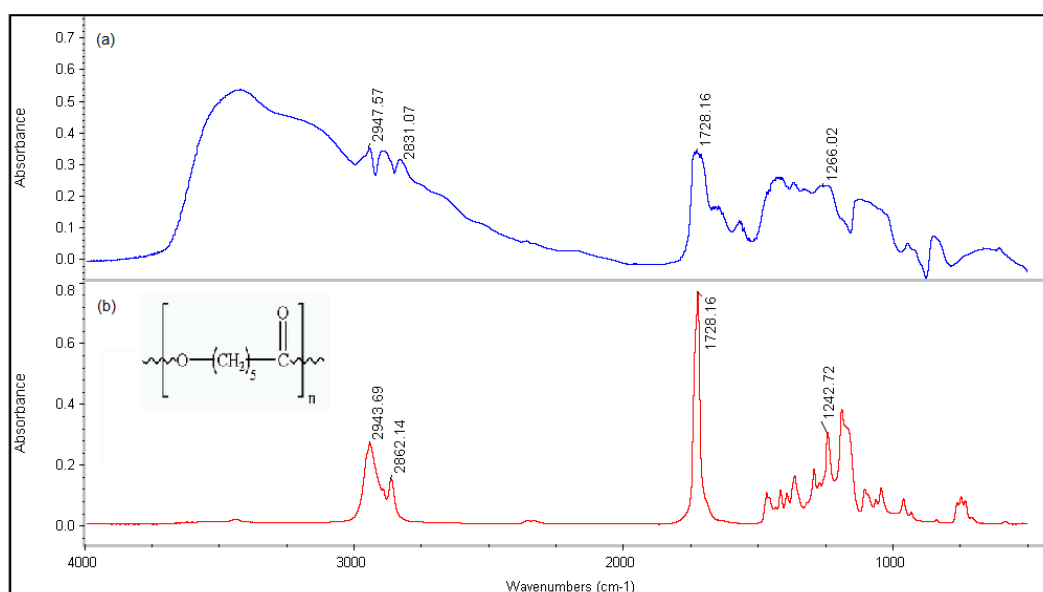


Figure 31. FTIR spectrum of (a) PCL-microspheres without ibuprofen and (b) PCL polymer.

Figure 31 shows the FTIR spectrum of (a) PCL-microspheres without ibuprofen and (b) PCL polymer [94-95]. When comparing both spectrums, many structural differences can be seen in frequencies of the vibrational/rotational movements. The frequencies between 3550 and 3200 cm^{-1} are belonging to the stretching O-H from the intermolecular and intramolecular hydrogen bonds of PVA (dispersant of the microspheres) [91]. The vibrational band observed between 2840 and 3000 cm^{-1} refers to the stretching C-H from PVA alkyl groups. These peaks are also in the polymer PCL. Frequency of $1728,16\text{ cm}^{-1}$, belongs to the tension of the carbonyl group (C=O stretching) as a part of the polymer and PVA. There is also a displacement corresponding

PREPARATION OF MICROSPHERES AND THEIR CHARACTERIZATION

to an asymmetric movement, COC stretching, in the frequency of $1266,02\text{ cm}^{-1}$. These movements that occur during the process, are crucial to justify optimal formation of the PCL-microspheres. PCL polymer has changed from a linear chain to a polymeric matrix form.

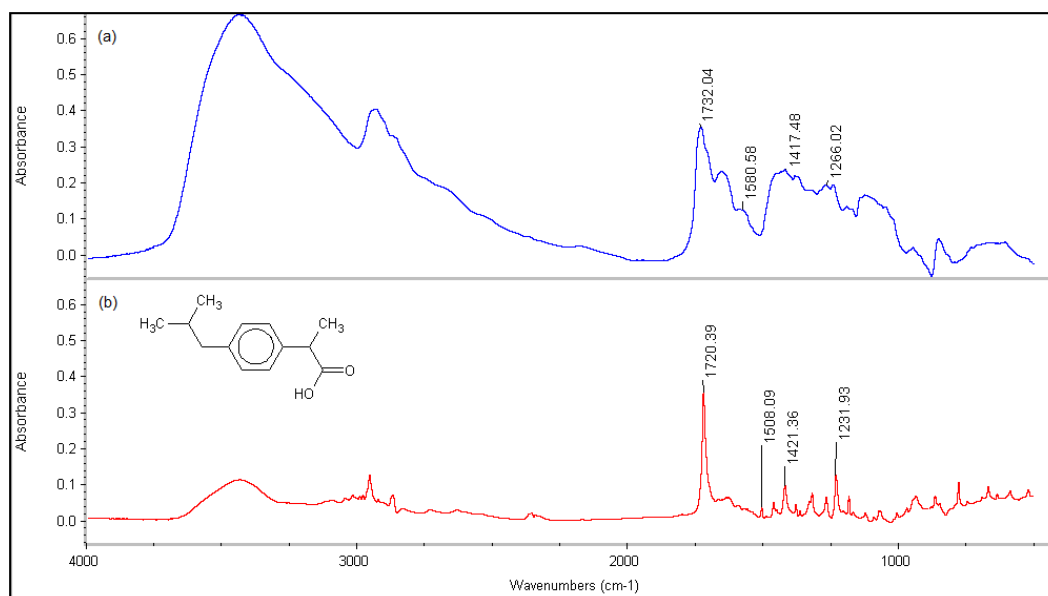


Figure 32. FTIR spectrum of (a) PCL-microspheres with ibuprofen and (b) ibuprofen.

Figure 32 shows the FTIR spectrum of (a) PCL-microspheres with ibuprofen and (b) ibuprofen [96-97]. As shown in the image of the different spectra, several characteristic frequencies that conform the spectral identify of the active compound disappear. The most important bonds in the ibuprofen molecule are the following ones: COOH (C=O stretching in the frequency of $1231,19\text{ cm}^{-1}$ corresponding to C=O stretching (COOH) and O-H bending) and CH₃ and the aromatic group in frequency of $1421,36\text{ cm}^{-1}$ (CH₃ asymmetric bend). The spectrum of PCL-microspheres with the active agent show the presence of PVA like in the previous Figure 31. Frequencies between 3550 and 3200 cm^{-1} , show once again the signal produced by stretching O-H of PVA [91]. Moreover, the vibrational band between 2840 and 3000 cm^{-1} belongs to the stretching C-H of PVA [91]. In the frequency of 1720.39 cm^{-1} , which belongs to the tension of the carbonyl group (C=O stretching) as part of ibuprofen, there is a movement and an increased bandwidth of the frequency (1736.28 cm^{-1}) in the spectrum PCL-microspheres containing caffeine. This influence is due to the polymer and PVA [91], because both have this bond in their structures. This means that the PCL-microspheres spectrum is the addition between the active compound and the polymer, and, as a result, it is shown that ibuprofen is encapsulated in the polymer cores. It is important to consider that the ibuprofen has steric hindrance, as it belongs to an aromatic group (range from 950 to 1006 cm^{-1}). This can affect in the absorption signals of the molecule. For that reason, the signals corresponding to CH₃ movements are not much representative in the spectrum, with a frequency of $1421,36\text{ cm}^{-1}$ (CH₃ asymmetric bend). These specific peaks observed in the spectrum of PCL-microspheres characterize the ibuprofen being encapsulated. Therefore, the possible interaction between polymer (C=O stretching, $1732,04\text{ cm}^{-1}$) and active compound (COOH, $1231,19\text{ cm}^{-1}$) could be by hydrogen bonds.

3.3.9 FTIR – PCL-MICROSPHERES WITH GALLIC ACID

The results corresponding to FTIR analysis are shown below. There are two types of FTIR spectrum, the first one (Figure 33) is the comparison between polymer and void PCL-microspheres, and the second one (Figure 34) is the comparison between gallic acid, void PCL-microspheres and PCL-microspheres with gallic acid.

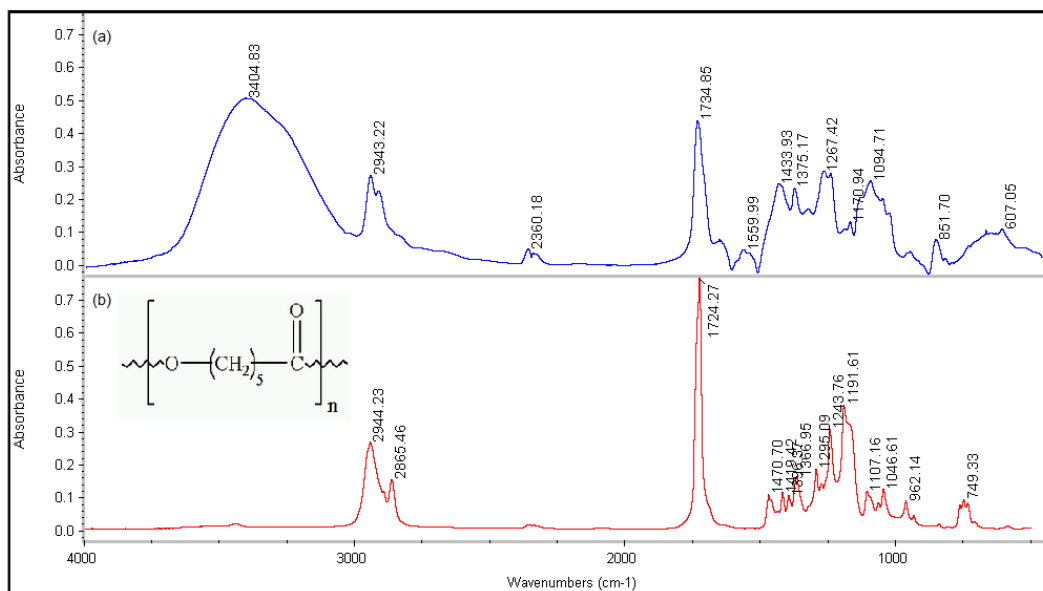


Figure 33. FTIR spectrum of (a) PCL-microspheres without gallic acid and (b) PCL polymer.

Figure 33 shows the FTIR spectrum of (a) PCL-microspheres without gallic acid and (b) PCL polymer [94-95]. It can be observed that the structure between both is almost the same, but there are some differences to be considered. It should be specially noted the movement of the groups C=O stretching ($1728,37\text{ cm}^{-1}$), CH_2 stretching ($2865,46\text{ cm}^{-1}$), symmetric CH_3 stretching ($1366,95\text{ cm}^{-1}$) and COC stretching (1243.76 cm^{-1} , 1191.61 cm^{-1} , $1107,16\text{ cm}^{-1}$) of PCL in regard to void PCL-microspheres. In the case of C=O stretching appears the same as the previous cases, because the presence of PVA is demonstrated. The characteristic frequencies of PVA are between 3550 and 3200 cm^{-1} belonging to the stretching O-H from the intermolecular and intramolecular hydrogen bonds and the vibrational band observed between 2840 and 3000 cm^{-1} belonging to the stretching C-H from alkyl groups of PVA, these peaks also belong to the polymer PCL [91]. These movements show that the polymer changes from a linear structure to a closed spherical structure.

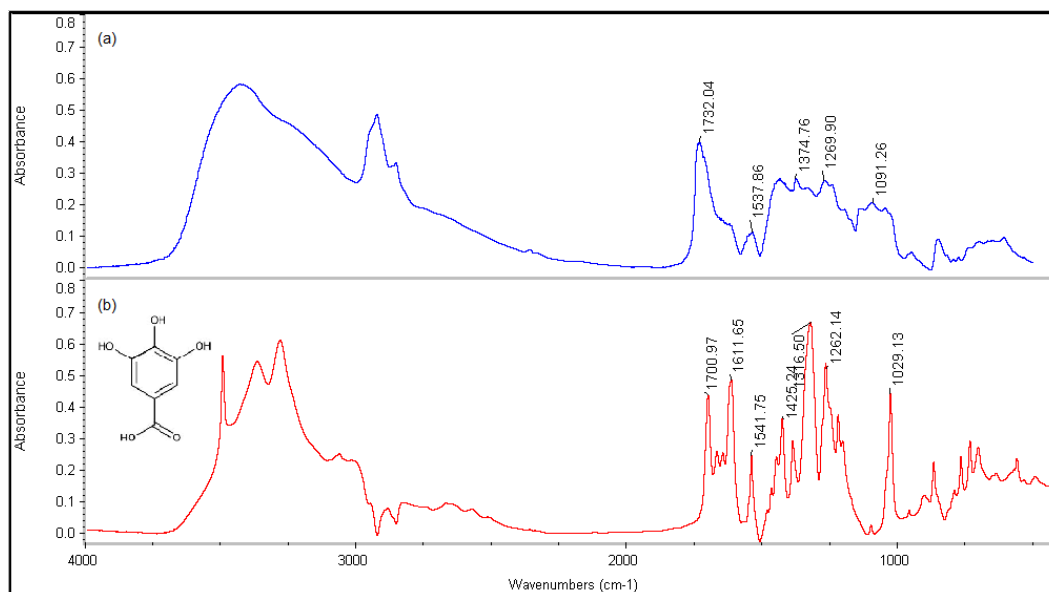


Figure 34. FTIR spectrum of (a) PCL-microspheres with gallic acid, (b) gallic acid.

Figure 34 shows the FTIR spectrum of (a) gallic acid PCL-microspheres and (b) gallic acid [98-99]. As shown in the spectra, there are some differences between the PCL-microspheres and the active compound. The most important bonds in the molecule of gallic acid are OH, COOH and the aromatic compound. The movements corresponding to these bonds are shown in the spectrum of PCL-microspheres. To be precise, in the frequency of $1700,97\text{ cm}^{-1}$ corresponding to carbonyl stretching (C=O), the C=C stretching ($1611,65\text{ cm}^{-1}$) and the CH₂ stretching ($1541,75\text{ cm}^{-1}$). Moreover, there is another important frequency corresponding to the ring vibration ($1029,13\text{ cm}^{-1}$) which is hidden in the case of PCL-microspheres. The frequency belonging to C=O stretching is also from PVA [91], therefore, the presence of PVA is shown again in the spectrum of PCL-microspheres with gallic acid. In the OH range of frequencies between 3550 and 3200 cm^{-1} (corresponding to PVA [91]), there are some modifications in the spectrum of PCL-microspheres with gallic acid in regard to void system. That modification suggests that the incorporation of gallic acid into the system add different –OH groups linked to aromatic ring (that fact can be seen in b)) to the general spectrum of the void PCL-microspheres.

These spectral changes demonstrate that the gallic acid may be inside of PCL-microspheres (as a consequence of these movements). Therefore it can be confirmed that there is a possible interaction between gallic acid and the polymeric matrix. Regarding to the molecular structure of these components, the interaction could be between OH bonds of gallic acid and C=O bonds of the polymer.

3.3.10 PARTICLE SIZE DISTRIBUTION – PLGA-MICROSPHERES WITH CAFFEINE

The particle size distribution by intensity of PLGA-microspheres is shown in the following Figure 35.

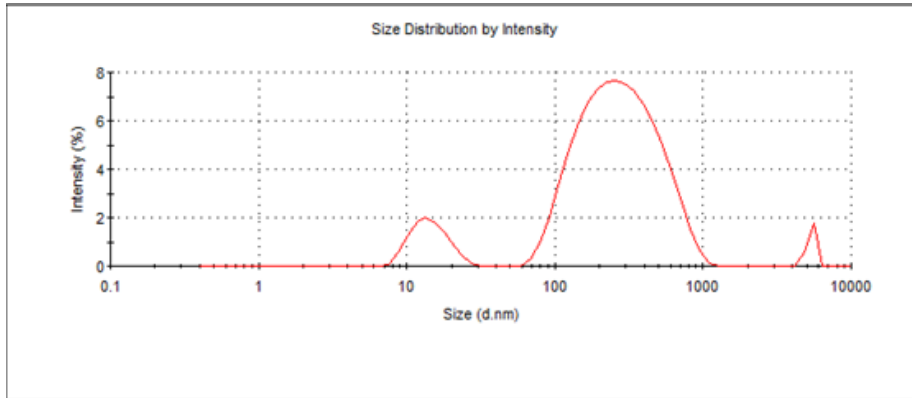


Figure 35. Size distribution by intensity of caffeine PLGA-microspheres.

Figure 35, shows three different intensities belonging to caffeine PLGA-microspheres. The most important of them is about 87.5% intensity and the average particle diameter is 159.1 nm. These results show that the PLGA-microspheres are less than 1 μm, which implies that PLGA-nanospheres are not achieved, instead of microspheres.

The polydispersity value (0.925) is almost 1, stating that there are many PLGA-microspheres with similar sizes. The PDI values range from 0 to 1 and higher values, indicates a less homogeneous particles size distribution. Therefore, the results indicate that microparticles which have been generated have homogeneity in size distribution.

3.3.11 PARTICLE SIZE DISTRIBUTION – PCL-MICROSPHERES WITH IBUPROFEN

The particle size distribution by intensity of PCL-microspheres is shown in the following Figure 36.

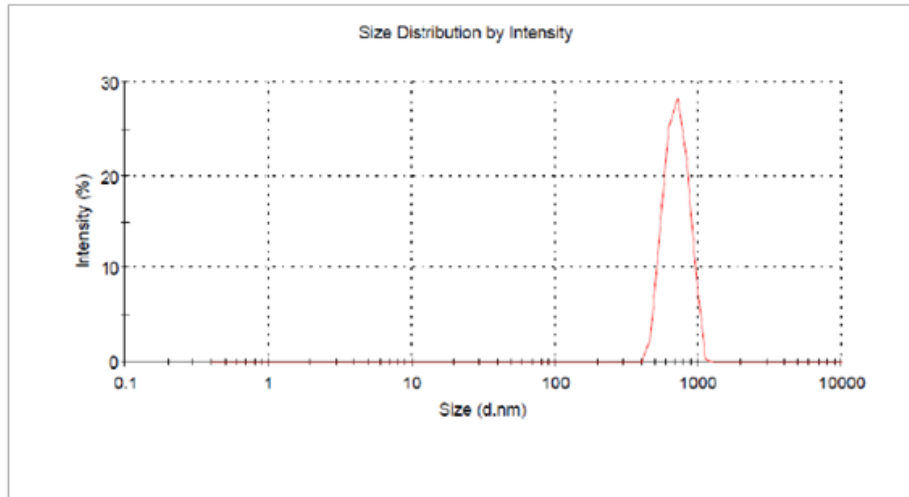


Figure 36. Size distribution by intensity of ibuprofen PCL-microspheres.

The average particle diameter is 846.9 nm and so, the microparticles can be considered as PCL-microspheres, since they are about 1 μm .

The polydispersity value is about 1.000 that means there are many PCL-microspheres with similar sizes, but with lower homogeneity than PLGA-microspheres with caffeine.

3.3.12 PARTICLE SIZE DISTRIBUTION – PCL-MICROSPHERES WITH GALLIC ACID

The particle size distribution by intensity of PCL-microspheres is shown in the following Figure 37.

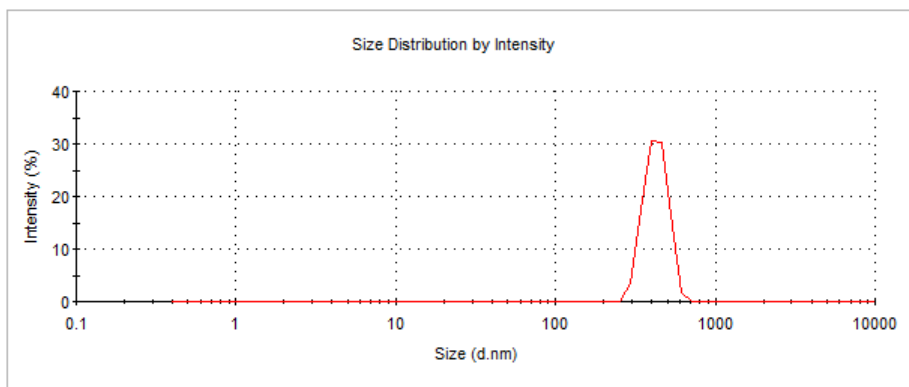


Figure 37. Size distribution by intensity of gallic acid PCL-microspheres.

The average particle diameter is 851.9 nm and so, the microparticles can be considered as PCL-microspheres, because are about 1 μm . The polydispersity value is about 0.815, The results in this case indicate higher homogeneity in particle size distribution than in the other cases.

3.4 CONCLUSIONS

It has been shown that the microencapsulation of caffeine, ibuprofen and gallic acid is possible. Furthermore, in the case of ibuprofen encapsulation high level of efficiency has been achieved compared to the literature [86]. Good results of efficiency corresponding to the encapsulation of caffeine and gallic acid have been obtained. Taking into account that there is no much literature on this subject it might be a great progress in terms of technology.

Frequencies movements from FTIR spectroscopy could give an idea of the possible interaction between PLGA - microspheres and caffeine (nitrogen bond), PCL – microspheres and ibuprofen (hydrogen bond), PCL – microspheres and gallic acid (hydrogen bond).

SEM results show that all microspheres have a spherical shape and there are internally porous with external PVA layer, and this, moreover acts as a binder between fabric and the microspheres.

The particle size distribution results show that all dispersions are homogeneous solutions with particle size average of 159.1 nm (PLGA-microspheres with caffeine), 846.9 nm (PCL-

microspheres with ibuprofen) and 851.9 nm (PCL-microspheres with gallic acid). Therefore, these results show that ones are nanoparticles and the other are microparticles.

CHAPTER 4: IMPREGNATION OF MICROSPHERES ON TEXTILE SUBSTRATE

4.1 PAD-DRY TECHNIQUE

Microspheres were applied using Pad-Dry technique. The conditions required for this procedure are shown in the table below. These are the same for all types of microspheres.

Table 28. Conditions of textile impregnation process.

FINISHING CONDITIONS	
SUBSTRATE	Fabric Cotton/Polyamide/Acrylic/Polyester
FABRIC DIMENSIONS	25 x 40 cm ²
LIQUOR RATIO	3 – 5 L/Kg
PICK-UP	80-90%
DRYING CONDITIONS	Room temperature

4.2 RESULTS AND DISCUSSION

The results belonging to % by weight (dry) of various treated fabrics significantly differ to the ones with the % permeation in the different solutions of microspheres. Results are shown below.

4.2.1 PAD-DRY TECHNIQUE – PLGA-MICROSPHERES WITH CAFFEINE

The results of the finishing process (pad-dry) corresponding to the application of the solution of caffeine PLGA-microspheres are shown in the following Table 29.

Table 29. Results of the finishing process of several textile fabrics.

Textile	% Pick-up*	% o.w.f.*
Dry product applied		
CO	83.37	2.37
PA	80.94	1.75
PAC	82.49	1.98
PET	81.21	1.26

* %pick-up, the theoretical percentage of product after impregnation; and % o.w.f. (over weight of fibres) of product applied, calculated by weight difference between dry non-treated textile and dry textile after Pad-Dry process.

These results show that the fabrics absorb the solution of PLGA-microspheres, but the o.w.f values are very low, which means that the amount of PLGA-microspheres on the fabrics is not really high. There might be two main reasons explaining this behavior: either the low efficiency in the preparation process of PLGA-microspheres or the affinity of the system.

The most important characteristic parameters controlling the affinity of the fabrics with other components is zeta potential. Zeta potential is not a constant value for textiles, but it gives information about the nature and dissociation of functional groups, hydrophilicity or hydrophobicity of the fibre surface, as well as the ions or water sorption. Zeta potential plays an important role in the electrical characterization of textiles in wet processing. In general, specific adsorption of ions or dissociation of surface groups in aqueous solution results in a surface charge. Fibre surface charge depends on the molecular and supramolecular structure and swelling capacity, as well as on ionogenicity, structure and concentration of adsorbate. Wet treatments change the fibre surface charge as well as zeta potential and adsorption ability [100].

According to the existing literature on this subject [99] (Table 30), zeta potentials for the standard fabrics at pH 10 are all different and due to the different chemical and structural composition of the textile materials. In Table 30, it different values of zeta potential according to standard fabrics, taken from the literature available [100] and also the zeta potential value of PLGA-microspheres (measured values from nanosizer) are shown.

Table 30. Zeta potential values of the standard fabrics [100] and measured zeta potential value of PLGA-microspheres with caffeine.

Textile	ξ - potential (mV)
CO	-24.50
PA	-42.00
PAC	-55.50
PET	-69.00
PLGA-microspheres with caffeine	-17.30

Polyester fabric displayed the most negative zeta potential (-69.00 mV). Zeta potential is higher in hydrophobic fabrics than hydrophilic fabrics, due to the hydration capacity. Cotton fabric has the lowest zeta potential (-24.50 mV). These fibres are negatively charged due to the presence of hydroxy and carboxy groups. The functional groups influence the zeta potential, but fibre's swelling has also an important role. Interfibrillar swelling enlarges the surface area, and causes the shift of the shear plane into the liquid phase lowering the zeta potential. Polyamide has numerous carboxylate groups and also a large number of other chargeable groups, including nitrogen-containing groups; all these groups result in a high zeta potential (-42.00 mV). The zeta potential of acrylic lies between the values for polyester and polyamide at -55.50 mV. As hydrophobic acrylic fabric has a high zeta potential, the presence of sulphonate groups in this fabric influences on the absorbability of polyelectrolyte [100].

Results show that the PLGA-microspheres have a low zeta potential if they are compared to fabrics. Thus, the affinity between them according to this parameter should decrease when zeta potential value of the fabrics is high. Therefore, the measured values of o.w.f are the ones expected: the value of o.w.f in cotton fabrics is the highest value obtained respect to other sort

of fabrics. For this reason, it is important to consider another important parameter: the chemical structure of polymer. Although, the behavior of the PLGA-microspheres containing PVA on its surface with the fabrics will be more affected by the chemical structure than the polymer matrix. The PLGA polymer has an amorphous structure and less hydrophobic than the PCL, therefore, results show that the affinity with the fabrics increases when their hydrophilicity is higher [20-23].

4.2.2 PAD-DRY TECHNIQUE – PCL-MICROSPHERES WITH IBUPROFEN

The results of the finishing process (pad-dry) corresponding to the application of the solution of ibuprofen PCL-microspheres are shown in the following Table 31.

Table 31. Results of the finishing process of several textile fabrics.

Textile	% <i>Pick-up</i> *	% o.w.f.*
		Dry product applied
CO	76.13	4.30
PA	80.20	4.36
PAC	81.79	4.64
PET	77.65	5.65

* %*pick-up*, the theoretical percentage of product after impregnation; and % o.w.f. (over weight of fibres) of product applied, calculated by weight difference between dry non-treated textile and dry textile after Pad-Dry process.

Results differ depending on the fabric being treated, due to fabric affinity with the PCL-microspheres, like in the previous case. However, the tendency is the opposite respect to the previous case, since the polyester has given the highest value. For this reason, in the following table (Table 32) the zeta potential values of the standard fabrics, as previously observed, and the zeta potential of ibuprofen PCL-microspheres are shown.

Table 32. Zeta potential values of the standard fabrics [100] and measured zeta potential value of PCL-microspheres with ibuprofen.

Textile	ξ - potential (mV)
CO	-24.50
PA	-42.00
PAC	-55.50
PET	-69.00
PCL-microspheres with ibuprofen	-3.380

Results show, that PCL-microspheres with ibuprofen have a really low zeta potential respect to the fabrics. Thus, the affinity between them, according to this parameter should be similar in all cases, because the zeta potential differences are relevant. the value of o.w.f in polyester fabric is the highest, therefore, respect to previous studies with PLGA-microspheres with caffeine, the

same effects can be shown in this case. Since, the PCL polymer has a crystalline structure and it is highly hydrophobic, the affinity with polyester fabric is higher than with the rest of fabrics [20-23].

4.2.3 PAD-DRY TECHNIQUE – PCL-MICROSPHERES WITH GALLIC ACID

The results of the finishing process (pad-dry) corresponding to the application of the solution of gallic acid PCL-microspheres are shown in the following Table 33.

Table 33. Results of the finishing process of several textile fabrics.

Textile	% <i>Pick-up</i> *	% o.w.f.*
Dry product applied		
CO	82.52	1.51
PA	79.84	1.55
PAC	83.52	1.72
PET	83.19	2.51

* %*pick-up*, the theoretical percentage of product after impregnation; and % o.w.f. (over weight of fibres) of product applied, calculated by weight difference between dry non-treated textile and dry textile after Pad-Dry process.

It can be observed that the impregnation (dry) value of the cotton fabric is the lowest of while polyester fabric has the highest value. The most important factors (such as the efficiencies and the affinities of the fabric with the PCL-microspheres) are the same as in previous cases,

The tendency of o.w.f is really similar to the previous case (PCL-microspheres with ibuprofen). The different values of zeta potential belonging to standard fabrics again [100] and PCL-microspheres with gallic acid are shown in Table 34.

Table 34. Zeta potential values of the standard fabrics [100] and measured zeta potential value of PCL-microspheres with gallic acid.

Textile	ξ - potential (mV)
CO	-24.50
PA	-42.00
PAC	-55.50
PET	-69.00
PCL-microspheres with gallic acid	-7.450

Results show that the PCL-microspheres with gallic acid have a really low zeta potential respect to the fabrics, but in this case, they are a little bit higher than the PCL-microspheres with ibuprofen. Thus, the same conclusion as in the previous case can be reached, namely, the affinity between them according to this parameter should be similar in all cases since the differences of zeta potential are high. And, for the same reason, as in the case of PCL-microspheres with ibuprofen, the effect of the chemical structure is important, since the

tendency is really similar between each other. For this reason, the PCL-microspheres in both cases have higher affinity with polyester fabric than the rest [20-23].

It can be seen that due to they are complex systems, it cannot be demonstrated that the zeta potential is the most important effect in these systems.

4.3 CONCLUSIONS

The results in the case of the PLGA-microspheres with caffeine are opposite to the results from the test on gallic acid and ibuprofen, therefore it can be demonstrated that the most important factor is the affinity between fabrics and microspheres, Both PLGA and PCL are polyesters, but they have different chemical structures [20-23]. Besides that, the zeta potential [100] which depends also on the chemical structure is one important parameter to consider regarding to the affinity of the system. PCL is a crystalline polymer and highly hydrophobic, however the PLGA polymer is amorphous and less hydrophobic than PCL. According to that, zeta potential values in the case of PCL-microspheres are smaller than PLGA-microspheres. For this reason, PLGA-microspheres have higher affinity with cotton fabric than with the rest, and on the contrary, PCL-microspheres have more affinity with polyester, since PCL is more hydrophobic than PLGA.

There are small differences between PCL-microspheres with ibuprofen and the ones of gallic acid. However, zeta potential values for both are quite different. Affinity in the case of PCL-microspheres with ibuprofen is higher than the PCL-microspheres with gallic acid due to the difference of the zeta potential values between fabrics and microspheres.

CHAPTER 5: ANALYSIS OF DRUG RELEASE

5.1 DRUG RELEASE ESSAY

Drug release essay consists on submerging the treated fabrics into thermostated vessels filled with deionized water or physiological saline at semi-infinite bath conditions at a temperature of 37°C. (Described in Chapter 2. (2.5.4.)).

The experimental conditions of Drug Release are shown below. These are the same for all type of microspheres.

Table 35. Conditions of Drug Release essay.

WEIGHT SAMPLE (g)	1
VOLUME OF MEDIUM (mL)	100
MEDIUM TYPES	DEIONIZED WATER OR PHYSIOLOGICAL SALINE
T (°C)	37
BATH CONDITIONS	SEMI-INFINITE

5.2 RESULTS AND DISCUSSION

Experimental results are treated following two different types of modification approaches: phenomenological models based on Theoretical Mechanisms of Drug Release and quantitative following Semi-empirical Equations, in order to know the mechanism of drug release for each kind of system (Tables 36, 37 and 38).

5.3 THEORETICAL MECHANISMS OF DRUG RELEASE

Results corresponding to the mechanisms of Drug Release for different systems according to Figure 8 are shown below.

5.3.1 THEORETICAL MECHANISMS – PLGA-MICROSPHERES WITH CAFFEINE

From the results shown in the following graphics (Figures 38 - 41), the caffeine release from PLGA-microspheres of all treated fabric samples (CO, PA, PAC and PET) seems to be characterized by a bimodal behavior [101-102]. Because, there are two clear stages in the rate of delivering. The first one is very quick and afterwards, there is a very slow increase on bath

concentration.

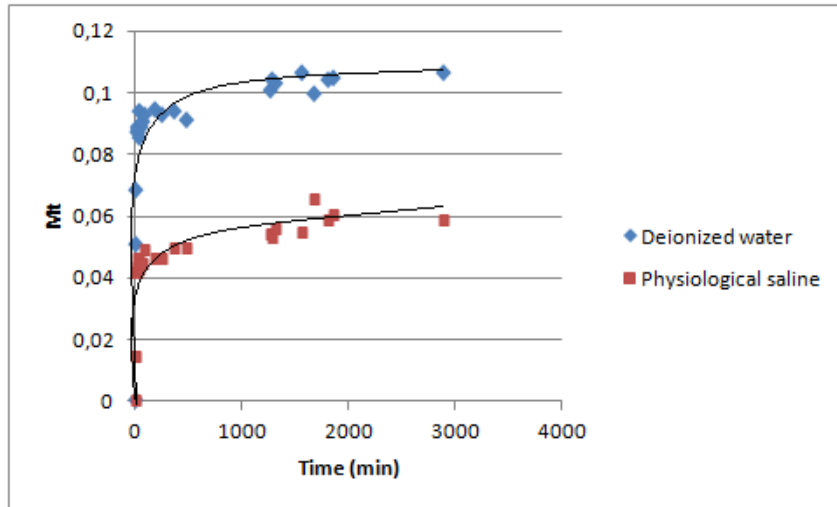


Figure 38. Kinetic release of PLGA-microspheres with caffeine applied onto cotton fabric at 37°C according the experimental medium. M_t (g caffeine/ g fabric).

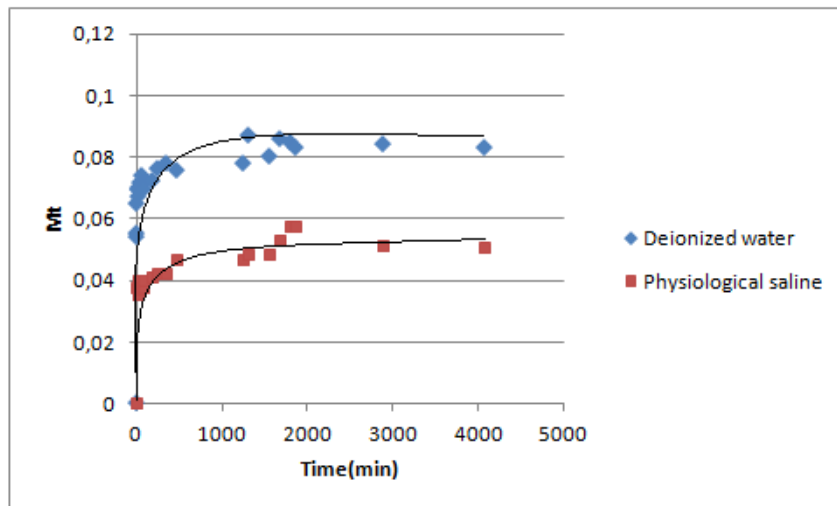


Figure 39. Kinetic release of PLGA-microspheres with caffeine applied onto polyamide fabric at 37°C according the experimental medium. M_t (g caffeine/ g fabric).

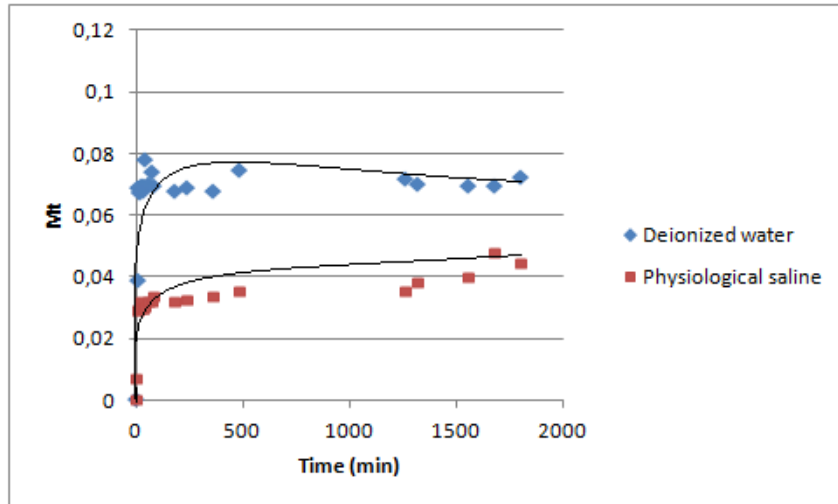


Figure 40. Kinetic release of PLGA-microspheres with caffeine applied onto acrylic fabric at 37°C according the experimental medium. M_t (g caffeine/ g fabric).

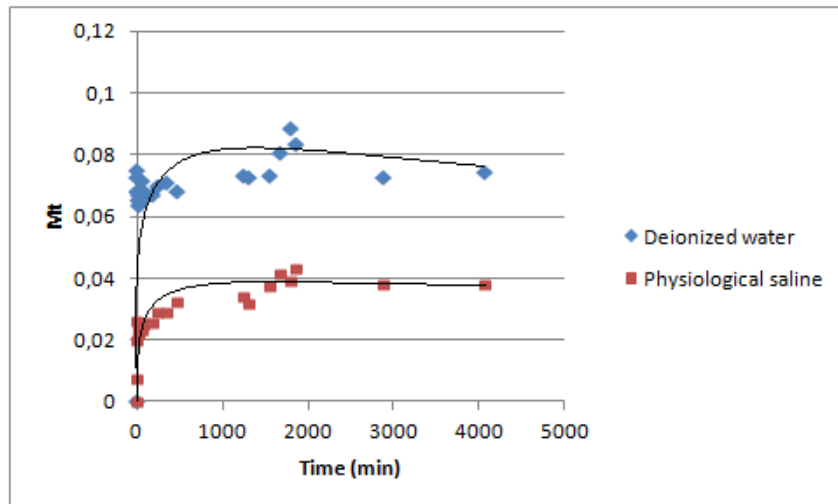


Figure 41. Kinetic release of PLGA-microspheres with caffeine applied onto polyester fabric at 37°C according the experimental medium. M_t (g caffeine/ g fabric).

Comparison of different kinetic profiles from the theoretical curves (A, B, C and D) is illustrated in Figure 8. The behavior of the different fabrics, regardless the media is similar to the theoretical curve B/D. This bimodal kinetic profile could be explained by a burst effect and a part of the drug entrapped in the polymeric matrix, which requires a longer time for degradation.

It can be seen that the amount of caffeine released is lower in physiological saline solution than in deionized water for all fabrics. Therefore, the influence of the medium is really important. In the case of physiological saline medium, saline ions can interact with the system showing different behaviors [20]. The release of caffeine may be inhibited due to interactions between the system (caffeine, PLGA-microspheres and fabrics) and ions of physiological saline, as a result, the percentage of caffeine released is lower than in the deionized water medium. Moreover, the solubility of caffeine is 16 mg/mL, and therefore, this active agent will be more

stable in water than in saline medium.

According to the polymer, PLGA degrades fast and in saline medium its degradation increases. For this reason, the burst effect is big and the amount of caffeine released is low over time in all cases [20, 23].

5.3.2 THEORETICAL MECHANISMS – PCL-MICROSPHERES WITH IBUPROFEN

The ibuprofen release from PCL-microspheres of all treated fabric samples (CO, PA, PAC and PET) is also characterized by a bimodal behavior depending on the type of fabric as shown in following figures.

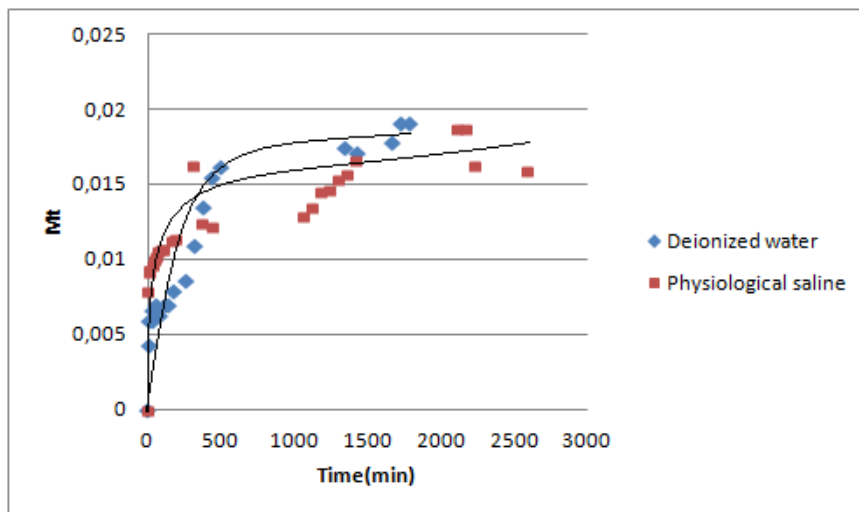


Figure 42. Kinetic release of PCL-microspheres with ibuprofen applied onto cotton fabric at 37°C according the experimental medium. M_t (g ibuprofen/ g fabric).

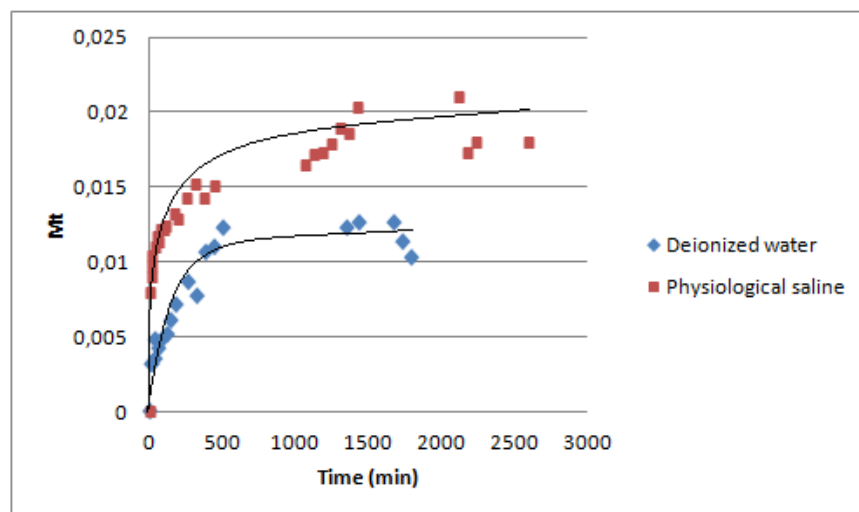


Figure 43. Kinetic release of PCL-microspheres with ibuprofen applied onto polyamide fabric at 37°C according the experimental medium. M_t (g ibuprofen/ g fabric).

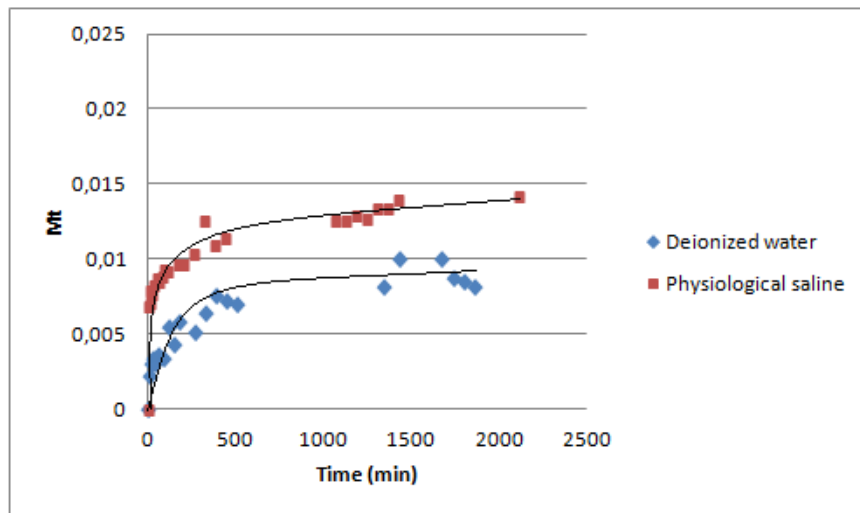


Figure 44. Kinetic release of PCL-microspheres with ibuprofen applied onto acrylic fabric at 37°C according to the experimental medium. M_t (g ibuprofen/ g fabric).

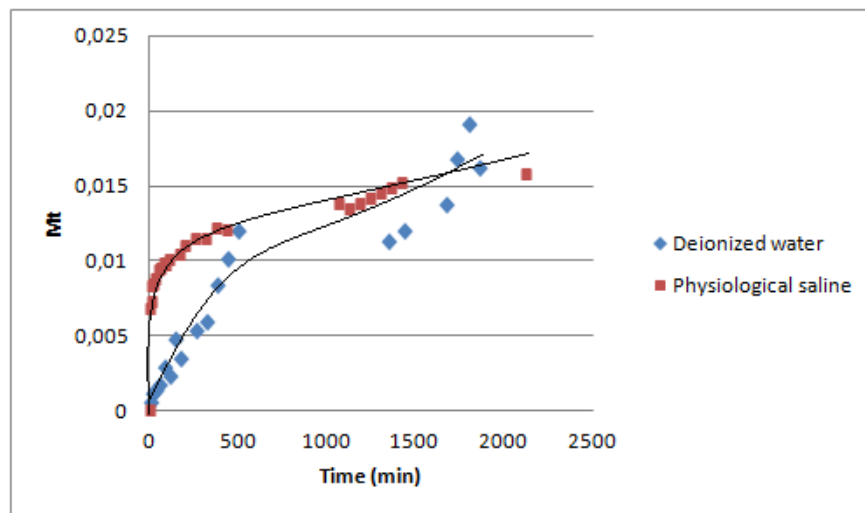


Figure 45. Kinetic release of PCL-microspheres with ibuprofen applied onto polyester fabric at 37°C according to the experimental medium. M_t (g ibuprofen / g fabric).

When comparing these results to the caffeine results, there is an inverse effect. In the case of Ibuprofen, the amount of active compound released is higher in physiological saline solution than in deionized water for all the fabrics except for cotton. The behaviour of the fabrics in water medium is similar to the theoretical curve D and in saline medium is like theoretical curve between B/C. Although in general terms there is always a burst effect, but is even more evident in the case of the physiological saline medium, since the saline medium accelerates the polymer degradation [20].

Polyamide and cotton have a behaviour that suggest two curves on the same curve in the physiological medium and in cotton. Such phenomena is also observed in the deionized water. Probably it is due to changes on surface potential because cotton and polyamide have different

superficial characteristics and liquid absorption percentages. In the case of cotton, the absorption of water is higher compared to other fabrics, moreover its zeta potential is about -24.50 mV, the lowest one. For these reasons, the behaviour of the caffeine released from cotton in both media is similar. However, in the physiological saline medium the ibuprofen released is slower than in water. This can be for the affinity of the ibuprofen, because both the zeta potential of PCL-microspheres with ibuprofen (-3.38 mV) and the zeta potential of the cotton and polyamide, -24.50 mV and -42.00 mV respectively have high differences between each other. Therefore, it seems that the ions from saline medium can interact with the system and inhibit the release of ibuprofen [20], which leads to a release system in two steps.

In the case of polyamide, it does not happen the same phenomena in deionized water. This is due to the different fabric features. The surface of polyamide fabric is more chargeable the cotton fabric's one, thus it seems that the physiological saline medium interacts [20] more than the one with deionized water due to the saline ions. Water can produce the solvation phenomena to the chargeable surface, which, at the same time, can avoid ibuprofen release. Moreover, since this active agent is partially soluble in water, it can behave with further stability inside the system than in water medium.

In the cases of acrylic and polyester fabrics, the amount of active agent released is lower than the other ones. The influence of the different characteristics of fabrics and PCL-microspheres with ibuprofen are obvious: when the value of zeta potential increases, the amount of released ibuprofen goes down. The zeta potential of both fabrics is higher, therefore the inhibition effect of saline ions increases. In the case of polyester fabric, the behaviour is similar in both media, because this sort of fabric has a high zeta potential and consequently it is the most hydrophobic and thus less absorbed. There is a difference between the media in this case: the burst effect is slower in water than in saline medium. This effect is observed in all type of fabrics. As previously noted, ibuprofen is partially soluble in water, and this implies a bigger delay of ibuprofen release in water.

5.3.3 THEORETICAL MECHANISMS – PCL-MICROSPHERES WITH GALLIC ACID

The results of gallic acid release from PCL-microspheres of all treated fabric samples (CO, PA, PAC and PET) are shown in the following figures.

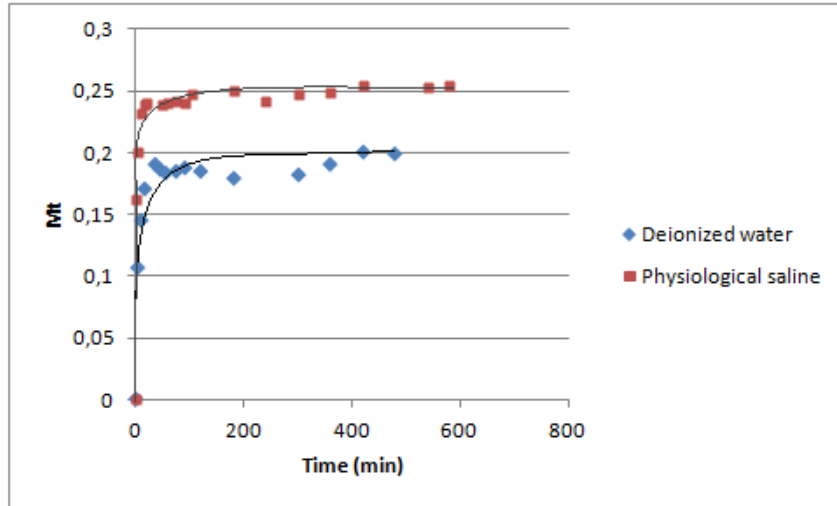


Figure 46. Kinetic release of PCL-microspheres with gallic acid applied onto cotton fabric at 37°C according the experimental medium. M_t (g gallic acid/ g fabric).

According to Figure 8, cotton fabric behaviours in water or saline medium are similar to the theoretical curve B due to an important burst effect. Respect to caffeine case, it can be seen the same tendency but with a contrary effect. Since, the gallic acid release is higher in physiological saline than in water. The solubility of gallic acid in water is really lower (11.50 mg/mL) than caffeine, but higher than ibuprofen. And also, this active agent has 3 hydroxil groups and 1 carboxyl group that can interact more with water (solvation phenomena). For those reasons, release is higher in saline medium than in water.

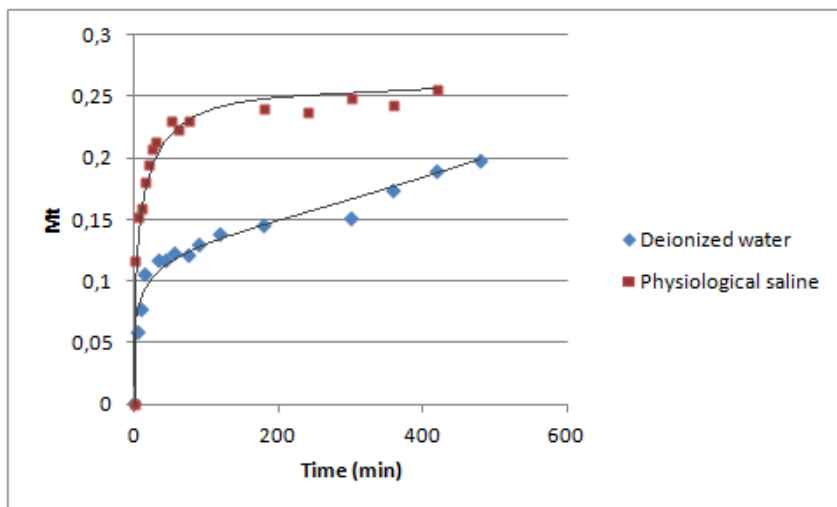


Figure 47. Kinetic release of PCL-microspheres with gallic acid applied onto polyamide fabric at 37°C according the experimental medium. M_t (g gallic acid/ g fabric).

The results in this case show that gallic acid behavior is really different in each medium. The release in water is close to theoretical curve B, but in physiological saline it is close to curve D. The influence of saline medium is evident, since due to the low solubility of gallic acid, it is more stable in a medium saline. Moreover, the type of the fabric is important, because polyamide has a chargeable surface allowing a solvation phenomena of water and giving a gradual increase of the gallic acid released over time.

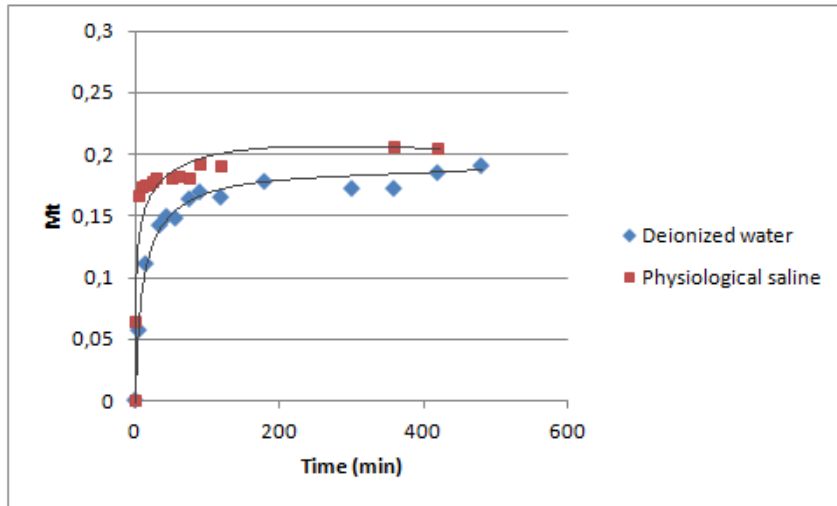


Figure 48. Kinetic release of gallic acid microspheres applied onto acrylic fabric at 37°C according the experimental medium. M_t (g gallic acid/ g fabric).

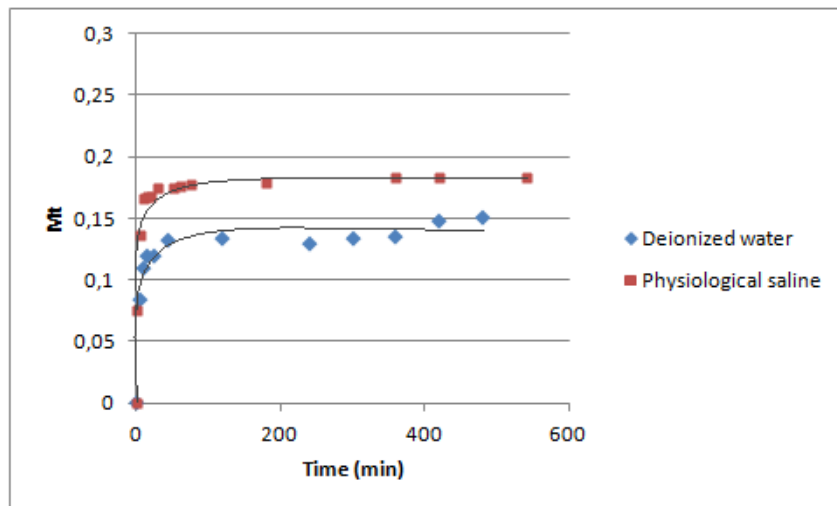


Figure 49. Kinetic release of PCL-microspheres with gallic acid applied onto polyester fabric at 37°C according the experimental medium. M_t (g gallic acid/ g fabric).

These fabrics (acrylic and polyester) show similar behaviours, because both have similar features. In both media, the theoretical model is between the types B and D. Burst effect can be observed again and it is more evident in the physiological saline than in water. As previously developed, the solubility of gallic acid in water is low and also its chemical structure, and therefore the release will be slower in water than in physiological saline. The amount of gallic

acid released in the physiological saline, from acrylic and polyester fabrics, is lower than in the rest of fabrics. Therefore, the influence of the medium [19] in the system can be shown : both fabrics have a high zeta potential value and the saline ions can have easily interacted with them or with PCL-microspheres. As a result, the release of the active compound can be inhibited over time.

5.4 POWER LAW

The results corresponding to Power Law Equation (1) for different systems are shown below.

5.4.1 POWER LAW – PLGA-MICROSPHERES WITH CAFFEINE

It has been taken under consideration the two steps described in the discussion of graphics, just for that reason, it would be assumed that the fabrics have two behaviors and were treated in two steps, short times (K_1) (Table 36) and long times (K_2) (Table 37). Using Eq. (1), the value of the exponent n , indicative of kind of mass transport mechanism was calculated.

Table 36. Estimated parameters, short times (K_1) and n values obtained from fitting drug release experimental data to Power Law (Eq. (1)).

Fabric type	T (°C)	Classification (Figure 5)	Experimental medium	K_1	n_1	R^2	Drug Delivery System
CO	37	B/D	Deionized water	0.4676	0.2273	0.9741	Fickian diffusion
	37	B/D	Physiological saline	0.2371	0.4909	0.9139	Fickian diffusion
PA	37	B/D	Deionized water	0.5981	0.0881	0.8912	Fickian diffusion
	37	B/D	Physiological saline	0.4826	0.0913	0.9848	Fickian diffusion
PAC	37	B/D	Deionized water	0.5064	0.2588	0.8934	Fickian diffusion
	37	B/D	Physiological saline	0.1467	0.6825	0.9439	Anomalous diffusion
PET	37	B/D	Deionized water	0.6786	0.0265	0.9220	Fickian diffusion
	37	B/D	Physiological saline	0.3929	0.1070	0.9398	Fickian diffusion

From experimental results, K_1 values are, higher in deionized water than in physiological saline solution for all samples checked, except for polyamide fabric (similar values in both media). It happens the same with n , although in the opposite direction happens. Nevertheless, most of the samples prepared, except for PAC, show Fickian diffusion mechanism, as it was expected (Table 36) [28,31-41].

It can also be demonstrated the influence of saline solution [20], since this can interact and change the release behaviour in all cases.

Table 37. Estimated parameters, long times (K_2) and n values obtained from fitting drug release experimental data to Power Law (Eq. (1)).

Fabric type	T (°C)	Classification (Figure 8)	Experimental medium	K_2	n_2	R^2	Drug Delivery System
CO	37	B/D	Deionized water	0,7276	0,0382	0.9255	Fickian diffusion
	37	B/D	Physiological saline	0,5487	0,0620	0.9356	Fickian diffusion
PA	37	B/D	Deionized water	0,6979	0,0390	0.9118	Fickian diffusion
	37	B/D	Physiological saline	-	-	0.8901	-
PAC	37	B/D	Deionized water	0,8270	0,0142	0.8949	Fickian diffusion
	37	B/D	Physiological saline	0,4953	0,0642	0.9201	Anomalous diffusion
PET	37	B/D	Deionized water	-	-	0.9303	-
	37	B/D	Physiological saline	0,1902	0,4714	0.9290	Fickian diffusion

Some of the systems checked don't allow finding these second constants, as PA in physiological saline solution and PET in deionized water. In cotton and acrylic, the results show the same tendency observed in K_1 , while constants obtained in deionized water are higher than the ones in physiological saline solution. The values of n also follow the same tendency observed in early stages of delivery process and they are higher in physiological saline solution than in deionized water.

In the two stages of the delivery process, the values of K and n follow a similar behaviour when treated with of PLGA-microspheres with caffeine.

5.4.2 POWER LAW – PCL-MICROSPHERES WITH IBUPROFEN

The value of the exponent n (indicative of mass transport mechanism) was calculated using Eq. (1), and the results are shown below (Table 38).

Table 38. Estimated parameters, (K) and n values obtained from fitting drug release experimental data to Power Law (Eq. (1)).

Fabric type	T (°C)	Classification (Figure 8)	Experimental medium	K	n	R ²	Drug Delivery System
CO	37	D	Deionized water	0,0860	0,2948	0.9077	Fickian diffusion
	37	B	Physiological saline	0,3313	0,1288	0.9272	Fickian diffusion
PA	37	D	Deionized water	0,0567	0,3805	0.9568	Fickian diffusion
	37	B/C	Physiological saline	0,3159	0,1368	0.9619	Fickian diffusion
PAC	37	D	Deionized water	2,9424	0,3109	0.9272	Fickian diffusion
	37	B/C	Physiological saline	0,3734	0,1258	0.9614	Fickian diffusion
PET	37	D	Deionized water	2,8987	0,3034	0.9299	Fickian diffusion
	37	B/C	Physiological saline	0,3474	0,1335	0.9862	Fickian diffusion

According to correlation coefficients obtained for all fabrics, it can be deduced that ibuprofen release from PCL-microspheres could be explained using power law models in only one stage.

The results from cotton and polyamide show that K values are higher in physiological saline than in water. However, in the case of polyester and acrylic fabrics, the values are the contrary: higher in water than in saline medium. That fact could be attributed to a possible surface potential equilibrium, because cotton and polyamide have better absorption than acrylic and polyester fabrics. It can be shown that burst effect is more important when the surface is charged by electrolytes from the saline medium than when water molecules are the only ones being absorbed. Therefore, this means that the influence of the chemical structure of ibuprofen is also important, since ibuprofen shows better stability in physiological saline than in water due to its low solubility in water (0.14 mg/mL).

5.4.3 POWER LAW – PCL-MICROSPHERES WITH GALLIC ACID

The analyzed fabrics have two different behaviors and were treated in two steps, like in the caffeine case, short times (K_1) (Table 39) and long times (K_2) (Table 40). Using Eq. (1), the value of the exponent n , indicative of mass transport mechanism was calculated.

Table 39. Estimated parameters, short times (K_1) and n values obtained from fitting drug release experimental data to Power Law (Eq. (1)).

Fabric type	T (°C)	Classification (Figure 8)	Experimental medium	K_1	n_1	R^2	Drug Delivery System
CO	37	B	Deionized water	0.3186	0.3017	0.9182	Fickian diffusion
	37	B	Physiological saline	0.6394	0.1392	0.9788	Fickian diffusion
PA	37	B	Deionized water	0.1378	0.4431	0.9629	Fickian diffusion
	37	D	Physiological saline	0.4453	0.1771	0.9726	Fickian diffusion
PAC	37	B/D	Deionized water	0.1368	0.5100	0.9778	Fickian diffusion
	37	B/D	Physiological saline	0.3428	0.3877	0.9033	Fickian diffusion
PET	37	B/D	Deionized water	0.4141	0.2220	0.8511	Fickian diffusion
	37	B/D	Physiological saline	0.4068	0.3126	0.9691	Fickian diffusion

Release mechanisms of gallic acid from PCL-microspheres in all samples was governed by Fickian diffusion, as shown in Table 39.

As it happens in with caffeine trial, when fitting this mathematical model to the experimental results obtained, delivery data must be spread into two different stages: short times (more linear) and long times (different tendencies). The high values of regression coefficients obtained, confirm the rightness of the hypothesis.

Table 40. Estimated parameters, long times (K_2) and n values obtained from fitting drug release experimental data to Power Law (Eq. (1)).

Fabric type	T (°C)	Classification (Figure 8)	Experimental medium	K_2	n_2	R^2	Drug Delivery System
CO	37	B	Deionized water	0.4729	0.1052	0.9321	Fickian diffusion
	37	B	Physiological saline	0.7323	0.0490	0.9370	Fickian diffusion
PA	37	B	Deionized water	0.2313	0.2351	0.9877	Fickian diffusion
	37	D	Physiological saline	0.6990	0.0568	0.9036	Fickian diffusion
PAC	37	B/D	Deionized water	0.2468	0.2256	0.9041	Fickian diffusion
	37	B/D	Physiological saline	0.6877	0.0623	0.9274	Fickian diffusion
PET	37	B/D	Deionized water	0.2443	0.2273	0.9077	Fickian diffusion
	37	B/D	Physiological saline	0.8553	0.0194	0.9528	Fickian diffusion

In long times, the mechanism of gallic acid delivery is governed by Fickian diffusion in all samples as shown table 40.

At early stages, K values are higher in saline solution. CO and PA show significant differences that become smaller in the case of PAC and close to zero for PET. However, when long periods of time are taken, behavior converges to only one tendency. There are significant differences between K values in the two media of delivery and higher values for physiological saline solution. The important reason is the chemical structure of gallic acid, since the presence of the polar groups (3 hydroxyl and one carboxylic) can make it be more stable in a saline medium.

5.5 KORSEMEYER-PEPPAS EQUATION APPROXIMATION AND HIGUCHI MODEL

Since the release mechanism of active compound follows a Fickian diffusion, both the Higuchi (Eq. (2)) governed by this mechanism and the approach of Korsenmeyer-Peppas (Eq. (3)) for plane surfaces, have been assumed. Parameters corresponding to these equations for different systems and according to the experimental medium are shown in the same table, due to the mathematical relation that exists between them.

5.5.1 KORSEMEYER-PEPPAS EQUATION APPROXIMATION AND HIGUCHI MODEL – PLGA-MICROSPHERES WITH CAFFEINE

Using Eq. (2) and Eq. (3), K_H and D/δ^2 parameters, respectively, (as apparent diffusion coefficients), are shown in Table 41.

Table 41. Estimated parameters applying Higuchi Equation (2) and Korsenmeyer-Peppas equation approximation (3).

Fabric type	T (°C)	Experimental medium	D/δ^2	K_H	R^2
CO	37	Deionized water	0.0116	0.2429	0.9193
	37	Physiological saline	0.0162	0.2875	0.9877
PA	37	Deionized water	0.0084	0.2072	0.9052
	37	Physiological saline	0.0070	0.1893	0.9848
PAC	37	Deionized water	0.0289	0.3836	0.9817
	37	Physiological saline	0.0137	0.2639	0.9439
PET	37	Deionized water	0.0264	0.3663	0.9072
	37	Physiological saline	0.0079	0.2004	0.9947

From the results of Table 41, regression coefficients almost 1, which assures that the model is right for these experimental results.

In the case of acrylic and polyester fabrics, the most conducive medium to the mass transport of caffeine is deionized water. Acrylic and polyester samples have bigger mass transfer coefficients than cotton and polyamide. That fact could probably be attributed to the differences on hydrophilicity of fabrics and/or zeta potential values. Mass transfer coefficient of polyamide in the deionized water medium, is greater than in saline solution, and although values are much lower than in acrylic and polyester, cotton almost behaves in quite the opposite way.

The effect of media is important because kinetic parameters are different. The mass transfer coefficient is lower in deionized water than in physiological saline. The release of caffeine may be inhibited, due to some interactions between system carboxyl groups and ions of physiological saline [20]. Both PA and PET have this group in their structure, as well as the PLGA-microspheres and the active agent. However, CO and PAC have higher values than the others, since they do not have carbonyl groups in their chemical structures.

5.5.2 KORSEMEYER-PEPPAS EQUATION APPROXIMATION AND HIGUCHI MODEL – PCL-MICROSPHERES WITH IBUPROFEN

Using Eq. (2) and Eq. (3), K_H and D/δ^2 parameters, respectively, (as apparent diffusion coefficients), are shown in Table 42.

Table 42. Estimated parameters applying Higuchi Equation (2) and Korsenmeyer-Peppas equation approximation (Eq. (3)).

Fabric type	T (°C)	Experimental medium	D/δ^2	K_H	R^2
CO	37	Deionized water	0.0002	0.0355	0.9053
	37	Physiological saline	0.0036	0.1346	0.9128
PA	37	Deionized water	0.0003	0.0383	0.8642
	37	Physiological saline	0.0030	0.1240	0.9392
PAC	37	Deionized water	0.1158	0.7678	0.8872
	37	Physiological saline	0.0042	0.1460	0.9082
PET	37	Deionized water	0.1031	0.7246	0.9384
	37	Physiological saline	0.0037	0.1373	0.9319

Regression coefficients are good enough to consider that the model fits experimental results.

It can be observed that in the case of cotton and polyamide the tendency is similar: they both have almost the same apparent diffusion coefficient in two media. On the contrary, in the case of acrylic and polyester the results observed are quite far from cotton and polyamide but they are quite close one to each other. For this reason, it is important to take into account the properties of the fabrics, the hydrophilic fabrics (cotton and polyamide) retain more microspheres than hydrophobic fabrics (acrylic and polyester). Besides that, in saline medium [20], mass transfer coefficients are lower than in water in all cases. And, as above mentioned, the saline medium can interact with the system and inhibit the release of the active compound and hence, the values are low and release is slower than in water.

However, it is not only a matter of microcapsules affinity in the different media, but an equilibrium between desorption of active compound, re-absorption by fabrics and the final release to corresponding medium.

5.5.3 KORSEMEYER-PEPPAS EQUATION APPROXIMATION AND HIGUCHI MODEL – PCL-MICROSPHERES WITH GALLIC ACID

Using Eq. (2) and Eq. (3), K_H and D/δ^2 parameters, respectively, (as apparent diffusion coefficients), are shown in Table 43.

Table 43. Estimated parameters applying Higuchi Equation (2) and Korsenmeyer-Peppas equation approximation (Eq. (3)).

Fabric type	T (°C)	Experimental medium	D/δ^2	K_H	R^2
CO	37	Deionized water	0.0004	0.0446	0.9976
	37	Physiological saline	0.0024	0.1101	0.9762
PA	37	Deionized water	0.0026	0.1143	0.9833
	37	Physiological saline	0.0014	0.0846	0.9741
PAC	37	Deionized water	0.0045	0.1507	0.9974
	37	Physiological saline	0.0160	0.2855	0.9435
PET	37	Deionized water	0.0088	0.2123	0.9774
	37	Physiological saline	0.0149	0.2754	0.9737

Regression coefficients obtained show that Higuchi model is an accurate approach to fit the experimental results.

In the case of gallic acid, the mass transfer coefficient shows the differences between saline medium and deionized water medium, stating that the value obtained for physiological saline solution is higher, except for the case of polyamide fabric. This shows that the saline medium can be considered an important factor in these systems, since it allows interaction.

In water deionized medium, the release of gallic acid is faster in polyester fabrics than in other sort of fabrics, where release is lower (depending on hydrophilicity/hydrophobicity). In physiological saline, the behaviour is totally different, because the lowest values correspond to acrylic and polyester while the highest correspond to cotton and polyamide.

5.6 CONCLUSIONS

The kinetic study was determined assuming the release of active compound in two steps in the case of caffeine system and gallic acid system (short and long times) due to their different behaviours. However, Higuchi equation can be assumed for all systems in short times, because the release mechanism is governed by Fickian Diffusion in all cases ($n < 0.5$). It can also be demonstrated that the saline medium is an important factor, since it accelerates the degradation of the polymer, allowing ions to interact with the system and therefore, inhibit or accelerate the active compounds release.

The main influence in these drug release systems is the affinity of active compound with the system. Different behaviours are shown, depending on the kind of fabrics. In the case of water medium, mass transport coefficients increase when hydrophobicity is higher. In saline medium, the tendency is different, because the saline ions can modify the of active compound release.

Another important influence to be considered is the polymer one, according to the behaviour of caffeine encapsulated with PLGA in comparison to the others (PCL-microspheres). The PCL as a crystalline polyester is degraded more slowly than PLGA, which is an amorphous and less hydrophobic polymer. Therefore, degradation will be faster in the case of the PLGA-microspheres than the PCL-microspheres. Moreover, this factor increases in saline medium, therefore PLGA-microspheres release less amount of active compound in saline medium than in water. On the contrary, PCL-microspheres release more active compound in water than in saline solution [19,20,23].

To sum up, there are several factors influencing this sort of systems, both the affinity of microspheres with fabrics and the equilibrium between desorption of active agent, re-absorption by fabrics and final release to different media. Such processes are different depending on the type of active compound, the polymeric matrix and the substrate used, and as consequence, the results obtained will be different as per the trials carried out.

CHAPTER 6: MASS TRANSPORT MODEL THROUGH THE SKIN

6.1 PERCUTANEOUS ABSORPTION ESSAY

The skin permeability is measured by percutaneous absorption assay using Franz Diffusion Cells (*in vitro* technique).

This study has only been carried out for ibuprofen system (applied on cotton fabric), because the experimental results from checked samples were good enough to discuss the percutaneous absorption essay. And also, because there is no literature for this type of study and it is of great interest to achieve improvements in the biotechnology field. The *in vitro* studies were carried out with pig skin on Franz static diffusion cells in order to know the evolution of the amount of the principle present in each of the different skin compartments (SC, epidermis and dermis) as well as in the receptor fluid, as a function of time by HPLC analysis. To determine the pig skin feasibility to use in absorption percutaneous experiments TEWL (transepidermal water loss) and skin thickness were measured, also the environmental conditions (T and HR) (Table 44).

Table 44. Conditions of TEWL (TM210). All parameters are an average value.

NUMBER OF CELLS	SKIN THICKNESS (µm)	TEWL ± SD	T (°C)	% HR
6	687.3 ± 20	8.77 ± 0.18	32.50 ± 0.5	50.77 ± 0.5
LABORATORY CONDITIONS				
INITIAL PARAMETERS		FINAL PARAMETERS		
T (°C)	% HR	T (°C)	% HR	
27 ± 1.0	37 ± 1.0	27 ± 1.0	36 ± 1.0	

The experimental conditions of *in vitro* experiments are detailed in Table 45.

Table 45. Experimental conditions of Franz Cell apparatus.

PENETRATION CELLS	Area = 1.86 cm ²	Volume = 3 mL	-
SKIN DISCS	Thickness = 700 μm ± 50 μm	Inner diameter = 2.5 cm	Stored Temperature = -20 °C
RECEPTOR FLUID	Phosphate – buffered saline	pH = 7.4	In Milli Q water (0.9% NaCl, 0.02% KCl and 0.8% phosphate buffer)
WATER BATH	Temperature = 32 °C	Stirring 700 rpm	-
TREATED FABRICS	Area = 7.07 cm ²	Applied product = 74.34 μg ± 5.77	-

Once finished the percutaneous absorption experiment for a given exposure time, the conditions to separate the different skin layers are detailed in Table 46.

Table 46. Experimental for skin layers separation.

SOLVENT OF EXTRACTION	Methanol			
SEPARATION STRATUM CORNEUM	8 strips		Pressure = 80 g/cm ²	
SEPARATION EPIDERMIS – DERMIS	T = 80 °C			
VOLUME EXTRACTION	V _{TEXTILE} 10 mL	V _{SC} 2 mL	V _E = V _D 1 mL	V _{RECEPTOR FLUID} 5 mL
STIRRING	700 rpm	30 min	Room Temperature	
SONICATION	15 min		Room Temperature	
FILTRATION	Nylon Filter Ø = 0.45 μm			

After skin layers separation and the corresponding Ibuprofen extraction (Table 46), HPLC analysis was performed, following the experimental conditions showed at Table 47.

Table 47. Conditions of HPLC analysis.

ELUENT	33 % A (H ₂ O + 1.2 % H ₃ PO ₄) 67 % B Methanol
FLOW	1 mL/min
INJECTION VOLUME	40 μL
RETENTION TIME	12 min
WAVELENGTH (λ)	264 nm
CALIBRATION CURVE	y = 1124.1x + 416.38

6.2 RESULTS AND DISCUSSION - MASS TRANSPORT MODEL THROUGH THE SKIN

Mass transport model through the skin was determined from the kinetic study of skin layers. For this study, the percutaneous absorption essay was carried out repeatedly (3 repetitions) for several samples of treated cotton with ibuprofen PCL-microspheres at different times.

The results of ibuprofen diffusion for PCL-microspheres system applied on cotton fabric are expressed as $\mu\text{g}/\text{cm}^2$, at different times. They are indicated in Table 48.

Table 48. The amount of drug released in each part of the skin versus time. Exposure times: from 0 to 37 h. Values represent mean \pm S.D (n = 3).

TIME (h)	Tex* ($\mu\text{g}/\text{cm}^2$)	SC* ($\mu\text{g}/\text{cm}^2$)	E* ($\mu\text{g}/\text{cm}^2$)	D* ($\mu\text{g}/\text{cm}^2$)	S* ($\mu\text{g}/\text{cm}^2$)	RF* ($\mu\text{g}/\text{cm}^2$)	Total ($\mu\text{g}/\text{cm}^2$)
0	15.07 \pm 3.94	nd**	nd**	nd**	nd**	nd**	15.07 \pm 3.94
1	9.08 \pm 0.36	1.34 \pm 0.52	0.32 \pm 0.10	0	1.70 \pm 0.87	0	12.44 \pm 0.48
3	8.97 \pm 0.78	1.62 \pm 0.22	0.91 \pm 0.38	0.94 \pm 0.12	2.40 \pm 2.05	0	14.84 \pm 1.21
6	9.59 \pm 0.35	2.45 \pm 0.31	1.79 \pm 0.14	1.53 \pm 0.29	0.97 \pm 0.22	0	16.32 \pm 2.47
24	8.36 \pm 1.90	2.94 \pm 0.46	2.89 \pm 0.09	1.55 \pm 0.15	2.15 \pm 0.87	0.64 \pm 0.65	17.88 \pm 2.31
37	8.10 \pm 0.52	1.07 \pm 0.42	0.58 \pm 0.15	1.26 \pm 0.45	3.35 \pm 0.16	5.11 \pm 0.86	19.47 \pm 0.58

*Abbreviations: Tex: Textile; SC: Stratum Corneum; E: Epidermis; D: Dermis; S: Surplus; RF: Receptor fluid;

**nd: not detected

The kinetic evolution of ibuprofen penetrated in each skin layer is shown in Figure 50. As it can be seen, the kinetic study shows that ibuprofen has penetrated through every layer of the skin, even it reaches the receptor fluid for a time longer than 24 hours.

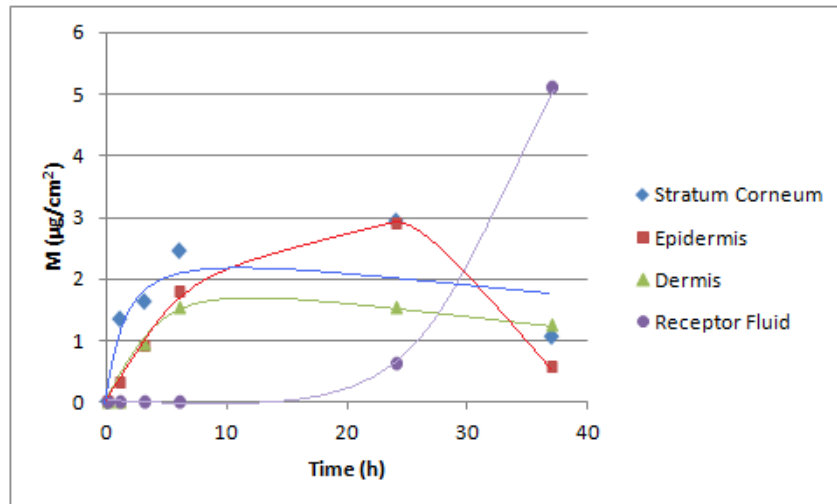


Figure 50. Kinetic release of PCL-microspheres with ibuprofen applied on to cotton fabric through the skin layers.

From the results obtained, it can be seen that at early times, the ibuprofen delivery to Stratum Corneum increases up to 6 hours approximately and then, it gradually decreases over time. But, This is a normal tendency, since in the second layer of skin (epidermis), the release of ibuprofen is slower. However, taking the same time (6 hours) the amount of ibuprofen released increases more in this layer than in the dermis. This fact could be due to a saturation of the ibuprofen between the two first layers of the skin. Therefore, the close contact with the skin and the occlusion of the skin could be the main reasons for the active compound can cross the skin barrier located in the stratum corneum [14]. For this reason, in 24 hours, the release of ibuprofen has increased in the epidermis, but instead, has decreased in the stratum corneum and in the dermis. In contrast, in the receptor fluid is when it begins to increase. Therefore, one can observe that there is an equilibrium between one layer and another, up to 37 hours, when the ibuprofen release decreases in the epidermis and therefore, there is a considerable increase of ibuprofen release in the receptor fluid. It should also be taken into account the amount of hours for the study, as the degradation of the system can increase, either PCL-microspheres or the experimental devices itself, in this case the pigskin.

The model developed by Guy and Hadgraft has been used with the aim of investigating the ibuprofen released through the skin. In the equation (24), the relationship between the diffusion coefficient of the drug through the different skin layers (D_s) and the formulation thickness during a given period t (L_0), is considered the apparent diffusion coefficient.

When $D_{ap} = \frac{D_s}{L_0}$, the equation (24) is transformed in the following expression (47):

$$\frac{M_t}{M_\infty} = \left(1 - \exp\left(-D_{ap} \frac{t}{KL}\right) \right) \quad (47)$$

Which has been used in our work taken into account the experimental parameters obtained for each skin layer. As regards to the partition coefficient (K) of ibuprofen, Herkenne et al [104] determined that parameter in SC using propylene glycol as a solvent. The individual partition coefficients obtained as a function of ibuprofen concentration in the cosolvent are graphically plotted in Figure 51. Although the solvent used in our work has been methanol, the solubility of ibuprofen in both solvents is quite similar (ibuprofen solubility in propylenglycol: 140.00 mg/mL [105] whereas in methanol is: 144.50 mg/mL). Therefore, as it can be deduced from the values shown in Figure 51, the partition coefficient (K) of ibuprofen is about 1.

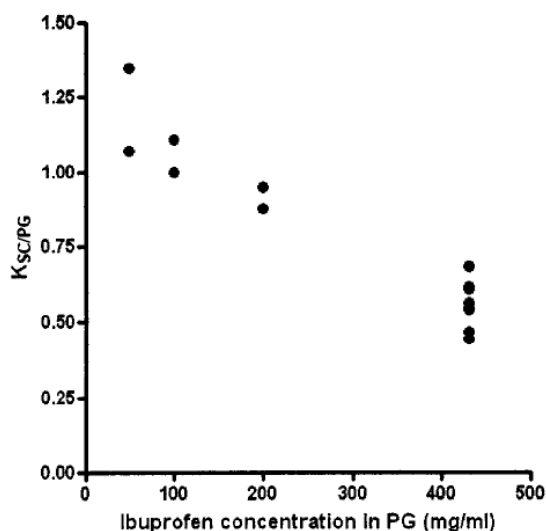


Figure 51. Individual SC/PG partition coefficients measured *in vivo* as a function of ibuprofen concentration in the cosolvent [104]

For the calculation of the apparent diffusion coefficients of ibuprofen, it must be considered the hydrophilic or lipophilic character of each skin compartment. The stratum corneum (SC) is a lipophilic layer whereas the epidermis and, in particular, dermis are the hydrophilic areas of the skin (viable skin). The results on apparent diffusion coefficients obtained for each layer are shown in Table 49.

Table 49. Apparent diffusion coefficients for Stratum Corneum and Epidermis-Dermis.

LAYERS	THICKNESS (μm)	D_{ap} (cm/s)
STRATUM CORNEUM	20	$1.20 \cdot 10^{-7}$
VIALE SKIN (EPIDERMIS-DERMIS)	667.3	$6.673 \cdot 10^{-6}$

It can be seen that in the lipophilic area of skin (stratum corneum), the release of the active compound is the slowest, this is due to the properties of its barrier function. The diffusion through the SC is mainly a lipidic intercellular pathway, therefore it can be considered the rate-limiting step for most compounds. However, once the active compound crosses through the epidermis and dermis (hydrophylic area of skin) the release rate increases significantly, even reaching to the receptor fluid.

As the ibuprofen penetrates into the skin, its solubility increases. According to the literature [104,106-108], the solubility of ibuprofen in a phosphate buffer solution (receptor fluid) at a temperature of 37 °C and pH = 7.4 is 6.02 mg/mL. However, ibuprofen has a very low water solubility (0.14 mg/mL), and in the lipophylic layer (SC) the ibuprofen release is slower than in the hydrophilic domain (epidermis-dermis).

PCL-microspheres can reduce the diffusivity of active compound in the first layer of the skin due to a surface skin saturation and thus, driving to a slower delivery of ibuprofen versus time. Therefore, the phenomenas observed are either the drug release fully determined by the affinity of the active compound with the different layers of the skin, collapse on the surface of the skin together with a slower drug release.

Once ibuprofen enters to the hydrophilic part of the skin, its solubility increases, release to the receptor fluid is faster, while the solubility of the ibuprofen is very high (6.02 mg/mL). Moreover, in previous studies about the variation of solubility of the ibuprofen versus time [107] , it is demonstrated that its solubility increases exponentially in the time. Due to the hydrophobic nature of ibuprofen, the aggregation of ibuprofen powders is obtained during the dissolution testing [107]. And, in this study, there is a good dispersion of the ibuprofen, because, basically, this takes part of a microencapsulation system, thus avoiding the aggregation of the active agent.

As a conclusion, the model of mass transport of ibuprofen through the skin used in this study is illustrated in the scheme of Figure 52. As it can be seen, an specific equation is used for each skin layer considering the percutaneous absorption kinetics of ibuprofen. This simple and practical model allows the control of a drug delivery system consisting of PCL-microspheres applied on textile substrate as a method of controlled release of ibuprofen.

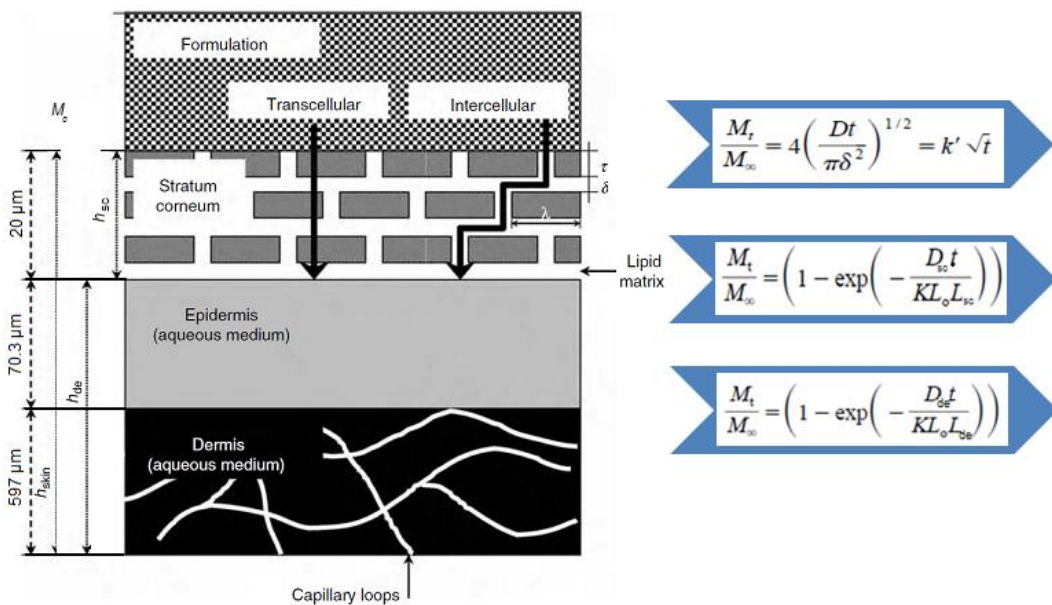


Figure 52. Model of mass transport of ibuprofen through the skin.

6.3 CONCLUSIONS

This study shows that the bioavailability of a model of ibuprofen microencapsulated in the skin can be evaluated by Franz-cells *in vitro* technique. This technique, combined with the appropriate analysis of the experimental data, provides kinetic parameters needed to design rationally a topical patch. Moreover, the role of PCL-microspheres, as a mass transport carrier in topical formulations of moderately lipophilic drugs as ibuprofen, has been examined carefully. The ibuprofen get in the SC slowly and seems to alter ibuprofen's solubility in the barrier. However, the diffusivity of the drug across the epidermis-dermis (aqueous area) increases significantly, and the drug delivery is directly affected by the solubility of active compound. Quantitative characterization of the uptake of ibuprofen itself into the different layers of the skin from PCL-microspheres represents a logical research effort for future investigations.

CHAPTER 7: CONCLUSIONS AND FUTURE OUTLOOK

7.1 FINAL CONCLUSIONS

The present study has shown that the main objective has been successfully achieved. According to that, microencapsulation applied on fabrics can be considered as a good controlled release system. As a result, the project reached to a general kinetic model using smart textiles as a mass transport system through the skin.

For this main aim, each of the objectives has been satisfactorily completed.

The microencapsulation of caffeine, ibuprofen and gallic acid has been achieved with success. Moreover, the encapsulation of ibuprofen has been carried out with great efficiency, as never before according to the available literature. Besides that, encapsulation of caffeine and gallic acid have been also showed good results.

Results from FTIR spectroscopy could give an idea of the possible interaction between PLGA - microspheres and caffeine (nitrogen bond), PCL – microspheres and ibuprofen (hydrogen bond), PCL – microspheres and gallic acid (hydrogen bond).

The case of the application of microspheres on textiles, shows that PLGA-microspheres with caffeine are the opposite of gallic acid and ibuprofen PCL-microspheres, probably due to the factor clearly of affinity, since the first one are made of PLGA and the others are made of PCL. Therefore, it is demonstrated that the chemical structure of the polymers is one of the most important effects in the affinity of the system.

The kinetic study shows a bimodal determined behaviour in the case of gallic acid and caffeine systems (short and long times). However, Higuchi equation can be assumed for all systems in short times, since the release mechanism governed by Fickian diffusion is applicable in all cases. The main influence in these drug release systems is the affinity of active agent with the system. It can be shown that the behaviours are different depending on the kind of fabrics. In the case of water medium, the mass transport coefficients increase when the hydrophobicity is higher. In the saline medium, the tendency is different, because the ions saline can modify the release of active compound.

Therefore, it can be deduced that the release mechanism will depend directly on the affinity between the different system components, textile-microspheres, microspheres-active principle and system (microspheres on textiles)-medium.

To sum up, it has been demonstrated that the microencapsulation applied on textiles is a good

system of controlled drug release. As a result, the project has been completed with a general kinetic model by smart textiles as a transport system through the skin.

7.2 FUTURE OUTLOOK

Mainly, the future impact of the present study is the obtaining of a controlled drug delivery system to release an active compound at the right time and on the right place.

One of the first problems that should be solved in the future is the distribution of the particle size and therefore, to get a better homogeneity in order to have better control in the drug release. To that purpose, it would be necessary to modify the conditions of the preparation process of microspheres.

A general kinetic model by smart textiles as a mass transport system through the skin has been obtained. However, the "burst" problem persists, and so it suggests further studies to improve the stability and efficiency in this sort of systems.

Furthermore, another important issue is the affinity between the microspheres and fabrics that affects the previous problem. Therefore, it would be recommended to study zeta potential of each fabric in different conditions and also, it could be possible using sandwich systems or some systems that keeps better the applied microspheres on the fabrics with the aim of decreasing the initial loss of the active agent.

Besides that, one of the most relevant advantage of the present study is its potential application in different fields, such as the pharmaceutical one. In this particular field, the present work could provide a way to avoid pharmaceutical side effects, thanks to the polymeric base, which is biodegradable and therefore, respectful to both the human being and the environment.

CHAPTER 8: STAY ABROAD (GHENT UNIVERSITY)

8 STAY ABROAD (GHENT UNIVERSITY)

Collaboration in NO BUG Project. *Novel release system and Bio-based Utilities for mosquito repellent textiles and Garments*. Seventh Framework Programme; Theme 4; Ghent University. Faculty of Engineering. Department of Textiles. Technologic Park. 19/09/2011- 06/02/2012 Ghent (Belgium).

8.1 BACTERIAS INCORPORATED IN FIBERS BY ELECTROSPINNING TECHNIQUE

The main aim of this work is to incorporate bioactive materials in textile fibers. The project aims to obtain an effective and long lasting mosquito repellent personal protective equipment (PPE) using bio-repellents. My work consisted on preparing bioactive systems by microencapsulation methods and then, the incorporating of these substances on nanofibers through electrospinning technique.

Therefore, my work could be divided by four steps:

1. The spores were tested to prove that they could survive the physical process parameters in the extruder, those are: , high temperature, high pressure and residence time.
2. Incorporation of the spores in the nanofibers by electrospinning technique.
3. Study of the microspheres preparation with spores by sonication technique.
4. Obtaining of the nanofibres with incorporated microspheres by electrospinning technique.

Due to the short time of the stay, that work was finished until third step, and the results obtained were not totally satisfactory. The basic problem was the optimization of the electrospinning process, since the compatibility between spores and nanofibers was not good and neither the stability of the system due to the existence of spores (partially soluble) [109-131].

REFERENCES

-
- [1] B. Boh, B. Sumiga, Microencapsulation technology and its applications in building construction materials, *Materials and Geoenvironment*, 55 n 3 (2008) 329-344.
- [2] H. Yoshizawa, Trends in microencapsulation research, *KONA Powder and Particle*, n 22 (2004) 23-31.
- [3] S. Benita, Microencapsulation. Methods and Industrial Applications, *Drugs and pharmaceutical sciences*, 73 (1996) 424.
- [4] N. Venkata Naga Jyothi, P. Muthu Prasanna, Suhas Narayan Sakarkar, K. Surya Prabha, P. Seetha Ramaiah and G. Y Srawan, Microencapsulation techniques, factors influencing encapsulation efficiency, *Journal of Microencapsulation*, 27 (2010) 187–197.
- [5] A. Voigt, H. Lichtenfeld, G.B. Sukhorukov, H. Zastrow, E. Donath, H. Bäumlner and H. Möhwald, Membrane filtration for microencapsulation and microcapsules fabrication by layer-by-layer polyelectrolyte adsorption, *Industrial & Engineering Chemistry Research*, 38 (1999) 4037-4043.
- [6] I. M. Martins, S. N. Rodrigues, F. Barreiro and A. E. Rodrigues, Microencapsulation of thyme oil by coacervation, *Journal of Microencapsulation*, 26 (2009) 667–675.
- [7] P. Monllor, M.A. Bonet; F. Cases. Characterization of the behaviour of flavour microcapsules in cotton fabrics, *European Polymer Journal*, 43 (2007) 2481-2490.
- [8] G. Nelson, Application of microencapsulation in textiles, *International Journal of Pharmaceutics*, 242 (2002) 55-62.
- [9] J.R. Sánchez Martín, Los tejidos inteligentes y el desarrollo tecnológico de la industria textil, *Técnica Industrial*, 268 (2007) 39-45.
- [10] J. Hu, Adaptive and functional polymers, textiles and their applications. Imperial College Press (2011) 127, 146-148.
- [11] N. Garti, Nanotechnologies for solubilization and delivery in foods and cosmetics pharmaceuticals. DEStech Publications (2012) 343-346.
- [12] F. Salaün, E. Devaux, S. Bourbigot, P. Rumeau, Application of contact angle measurement to the manufacture of textiles containing microcapsules, *Textile Research Journal*, 79 (2009) 1202-1212.

- [13] I. F. Uchegbu, Drug Delivery, Polymers in Drug Delivery, Taylor & Francis Group, LLC (2006) 1-5.
- [14] L. Rubio, C. Alonso, L. Coderch, J. L. Parra, M. Martí, J. Cebrián, J. A. Navarro, M. Lis and J. Valldeperas, Skin delivery of caffeine contained in biofunctional textiles, Textile Research Journal, (2010) 1215-1221.
- [15] M. Martí, R. Rodríguez, N. Carreras, M. Lis, J. Valldeperas, L. Coderch, and J.L. Parra, Monitoring of the microcapsule/liposome application on textile fabrics, Journal of the Textile Institute, 103 N1 (2012) 19-27.
- [16] V. Sáez, E. Hernáez, L.S. Angulo, Mecanismos de liberación de fármacos desde materiales polímeros, Revista Iberoamericana de Polímeros, 5 (2004) 55-69.
- [17] V. Sáez, E. Hernáez, L.S. Angulo, Sistemas de liberación controlada de medicamentos, Revista Iberoamericana de Polímeros, 3 (2002) 1-17.
- [18] S. Freiberg, X.X. Zhu, Polymer microspheres for controlled drug release, International Journal of Pharmaceutics, 282 (2004) 1-18.
- [19] K.E. Uhrich, S. M. Cannizzaro, R.S. Langer and K.M. Shakesheff, Polymeric systems for controlled drug release, Chemical Reviews, 99 (1999) 3181-3198.
- [20] T.G. Park, W. Lu, G. Crotts, Importance of in vitro experimental conditions on protein release kinetics, stability and polymer degradation in protein encapsulated poly(D, L-lactic acid-co-glycolic acid) microspheres, Journal of Controlled Release 33 (1995) 211-222.
- [21] S. Li, M. Vert, Biodegradable polymers: polyesters. Encyclopedia of Controlled Drug Delivery, E. Mathiowitz (Ed.), Wiley (1999) 71– 93.
- [22] M. Vert, J. Feijen, A. Albertsson, G. Scott, E. Chiellini, Biodegradable polymers and plastics, Royal Society of Chemistry, (1992).
- [23] A. Goepferich, J. Tessmar, Polyanhydride degradation and erosion, Adv. Drug Deliv. 54 (2002) 911– 931.
- [24] A.V. Rawlings, Cellulite and its treatment, International Journal of Cosmetic Science, 28 (2006), 175–190.
- [25] R. Pardo Lozano, Y. Alvarez García, D. Barral Tafalla, M. Farré Albaladejo, Cafeína: un nutriente, un fármaco, o una droga de abuso, Adicciones, 19 (2007) 225-238.

- [26] T.G.Kantor, Ibuprofen. *Annals of Internal Medicine*, 91 (1979) 877–882.
- [27] O.I. Aruoma, A. Murcia, J. Butler and B. Halliwell, Evaluation of the antioxidant and prooxidant actions of gallic acid and its derivatives, *Journal of Agricultural and Food Chemistry*, 41 N 11 (1993) 1880-1885.
- [28] J. Siepmann, N.A. Peppas, Modeling of drug release from delivery systems based on hydroxypropyl methylcellulose (HPMC), *Advanced Drug Delivery Reviews*, 48 (2001) 139-157.
- [29] M. Vallet, A.L. Doadrio, Liberación de fármacos en matrices biocerámicas: Avances y perspectivas, *Fundación José Casares Gil (Instituto de España, Real Academia Nacional de Farmacia)*, Monografía XIX, (2009), 76-77.
- [30] Pharmacy - Encyclopedia of controlled drug delivery, 1&2 (1999) 495-497.
- [31] J. Siepmann, H. Kranz, R. Bodmeier, N. A. Peppas, HPMC – Matrices for controlled drug delivery: a new model combining diffusion, swelling, and dissolution mechanisms and predicting the release kinetics, *Pharmaceutical Research*, 16, n 11, (1999), 1748- 1756.
- [32] M. J. Abdekhodaie, Y. – L. Cheng, Diffusional release of a dispersed solute from planar and spherical matrices into finite external volume, *Journal of Controlled Release*, 43, (1997) 175-182.
- [33] J. Siepmann, F. Lecomte, R. Bodmeier, Diffusion- controlled drug delivery systems: calculation of the required composition to achieve desired release profiles, *Journal of Controlled Release*, 60, (1999) 379-389.
- [34] K. Kumari, P.P. Kundu, Studies on in vitro release of CPM from semi-interpenetrating polymer network (IPN) composed of chitosan and glutamic acid, *Indian Academy of Sciences*, 31, n 2, (2007) 159-167.
- [35] N.A. Peppas, Analysis of fickian and non-fickian drug release from polymers, *Pharm. Acta Helv*, 60 (1985) 110–111.
- [36] N.A. Peppas, R.W. Korsmeyer, Dynamically swelling hydrogels in controlled release applications, *Hydrogels in Medicine and Pharmacy*, 3, CRC Press, Boca Raton, (1986) 109–136.
- [37] T.T. Wang, T.K. Kwei, H.L. Frisch, Diffusion in glassy polymers III, *Journal of Polymer Science*, 7 (1968) 2019–2028.

- [38] G.S. Park, Transport principles — solution, diffusion and permeation in polymer membranes, *Synthetic Membranes: Science, Engineering and Applications*, D. Reidel Publishing Company, Dordrecht, (1986) 57–108.
- [39] H.L. Frisch, Sorption and transport in glassy polymers, *Polymer Engineering and Science*, 20 (1980) 2–13.
- [40] P.L. Ritger, N.A. Peppas, A simple equation for description of solute release I. Fickian and non-fickian release from non-swellable devices in the form of slabs, spheres, cylinders or discs, *Journal of Controlled Release*, 5 (1987) 23–36.
- [41] P.L. Ritger, N.A. Peppas, A simple equation for description of solute release II. Fickian and anomalous release from swellable devices, *Journal of Controlled Release*, 5 (1987) 37–42.
- [42] N. A. Peppas, K. B. Keys, M. Torres – Lugo, Anthony M. Lowman. Poly (ethylene glycol) – containing hydrogels in drug delivery, *Journal of Controlled Release*, 62, (1999) 81-87.
- [43] C.S. Brazel, N. A. Peppas, Modeling of drug release from swellable polymers, *European Journal of pharmaceutics and biopharmaceutics*, 49, (2000) 47-58.
- [44] J. Crank (Ed.), *The mathematics of diffusion*, Clarendon Press, Oxford, (1975).
- [45] H. Lapidus, N.G. Lordi, Drug release from compressed hydrophilic matrices, *Journal Pharmaceutical Science*, 57 (1968) 1292–1301.
- [46] H.S. Carslaw, J.C. Jaeger (Eds.), *Conduction of heat in solids*, Clarendon Press, Oxford, 1959.
- [47] R.W. Baker, H.K. Lonsdale, *Controlled release: mechanisms and rates*, *Controlled Release of Biologically Active Agents*, Plenum Press, New York (1974) 15–72.
- [48] M. Grassi, G. Grassi, R. Lapasin, I. Colombo, *Understanding drug release and absorption mechanisms*, Taylor and Francis Group, (2007) Chapter 9, 583-584.
- [49] R.S. Harland, N.A. Peppas, On the accurate experimental determination of drug diffusion coefficients in polymers, *S.T.P. Pharm. Sci.*, 3 (1993) 357.
- [50] K. Tojo, et al., Characterization of a membrane permeation system for controlled delivery studies, *AIChE J.*, 31 (1985) 741.
- [51] N. Laghoueg, et al., Oral polymer–drug devices with a core and an erodible shell for constant drug delivery, *Int. J. Pharm.*, 50 (1998) 133.

- [52] A. Lavasanifar, et al., Microencapsulation of theophylline using ethylcellulose: in vitro drug release and kinetic modeling, *J. Microencapsul.*, 14 (1997) 91.
- [53] M.L. Lorenzo-Lamosa, et al., Design of microencapsulated chitosan microspheres for colonic drug delivery, *J. Contr. Rel.*, 52 (1998) 109.
- [54] E.M. Ouriemchi, J.M. Vergnaud, Processes of drug transfer with three different polymeric systems with transdermal drug delivery, *Comput. Theor. Polym. Sci.*, 10 (2000) 391.
- [55] Y. N. Kalia, R. H. Guy, Modeling transdermal drug release, *Advanced Drug Delivery Reviews*, 48 (2001) 159-172.
- [56] M. Grassi, G. Grassi, R. Lapasin, I. Colombo, Understanding drug release and absorption mechanisms, Taylor and Francis Group, (2007) Chapter 2, 53-59, 65-66.
- [57] N. He, et al., Model analysis of flux enhancement across hairless mouse skin induced by chemical permeation enhancers, *Int. J. Pharm.*, 9 (2005) 297.
- [58] M. Grassi, G. Grassi, R. Lapasin, I. Colombo, Understanding drug release and absorption mechanisms, Taylor and Francis Group, (2007) Chapter 9, 585-586.
- [59] T.J. Franz, Percutaneous absorption on the relevance of in vitro data, *J. Invest. Dermatol.*, 64 (1975) 190.
- [60] T.J. Franz, The finite dose technique as a valid in vitro model for the study of percutaneous absorption in man, *Curr. Probl. Dermatol.*, 7 (1978) 58.
- [61] T. Higuchi, Rate of release of medicaments from ointment bases containing drugs in suspension, *J. Pharm. Sci.*, 50 (1961) 874.
- [62] B. Illel, et al., Follicles play an important role in percutaneous absorption, *J. Pharm. Sci.*, 80 (1991) 424.
- [63] F. Yamashita, M. Hashida, Mechanistic and empirical modeling of skin permeation of drugs, *Advanced Drug Delivery Reviews*, 55 (2003) 1185-1199.
- [64] G.L. Flynn, S.H. Yalkowsky, T.J. Roseman, Mass transport phenomena and models: theoretical concepts, *J. Pharm. Sci.*, 63 (1974) 479.
- [65] M. Grassi, Membranes in drug delivery, in *Handbook of membrane separations: chemical, pharmaceutical, and biotechnological applications*, Sastre, A.M., Pabby, A.K., Rizvi, S.S.H., Eds., Marcell Dekker, (2007).

- [66] M. Grassi, G. Grassi, Mathematical modelling and controlled drug delivery: matrix systems, *Curr. Drug Deliv.*, 2 (2005) 97.
- [67] S.K. Inoue, R.B. Guenther, S.W. Hoag, Algorithm to determine diffusion and mass transfer coefficients, in *Proceedings of the Conference on Advances in Controlled Delivery*, 145 (1996).
- [68] I. Colombo, et al., Determination of the drug diffusion coefficient in swollen hydrogel polymeric matrices by means of the inverse sectioning method, *J. Contr. Rel.*, 47 (1997) 305.
- [69] M. Grassi, et al., Effect of milling time on release kinetics from co-ground drug polymer systems, in *Proceedings of the 2003 AAPS Annual Meeting and Exposition*, # M1201, Grassi, M., Magarotto, N.L., Ceschia, D., Eds., (2003).
- [70] N. Coceani, I. Colombo, M. Grassi, Acyclovir permeation through rat skin: mathematical modelling and in vitro experiments, *International Journal of Pharmaceutics*, 254 (2003) 197-210.
- [71] A.S. Michaels, S.K. Chandrasekaran, J.E. Shaw, Drug permeation through human skin, theory and in vitro experimental measurement, *AIChE. J.*, 21 (1975) 985.
- [72] U.V. Banakar, *Pharmaceutical dissolution testing*, Marcel Dekker, (1992).
- [73] M. Grassi, G. Grassi, R. Lapasin, I. Colombo, *Understanding drug release and absorption mechanisms*, Taylor and Francis Group, (2007) Chapter 9, 590-592.
- [74] M. Grassi, G. Grassi, R. Lapasin, I. Colombo, *Understanding drug release and absorption mechanisms*, Taylor and Francis Group, (2007) Chapter 9, 592-595.
- [75] M. Fernandes, L. Simon, N.W. Loney, Mathematical modeling of transdermal drug-delivery systems: analysis and applications, *J. Membr. Sci.*, 256 (2005) 184.
- [76] M. Grassi, G. Grassi, R. Lapasin, I. Colombo, *Understanding drug release and absorption mechanisms*, Taylor and Francis Group, (2007) Chapter 9, 595-596.
- [77] Manitz, R., et al., On mathematical modeling of dermal and transdermal drug delivery, *J. Pharm. Sci.*, 87 (1998) 873.
- [78] S. Bourgeois, M. A. Bolzinger, J. Pelletier, J. P. Valour, S. Briançon, Caffeine microspheres – An attractive carrier for optimum skin penetration, *IFSCC Magazine*, 12 n 4, (2009) 359-363.
- [79] A. M. Le Ray, S. Chiffolleau, P. Looss, G. Grimandi, A. Gouyette, G. Daculsi and C. Merle, Vancomycin encapsulation in biodegradable poly(ϵ -caprolactone) microparticles for bone implantation. Influence of the formulation process on size, drug loading, in vitro release and cytocompatibility, *Biomaterials*, 24 n 3, (2003) 443-449.

- [80] A. Daneshfar, H. S. Ghaziaskar and N. Homayoun, Solubility of gallic acid in methanol, ethanol, water, and ethyl acetate, *Journal of Chemical Engineering Data*, 53 n 3, (2008) 776-778.
- [81] Y. Kawashima, T. Niwa, T. Handa, H. Takeuchi, T. Iwamoto, K. Itoh, Preparation of controlled-release microspheres of ibuprofen with acrylic polymers by a novel quasi-emulsion solvent diffusion method, *Journal of Pharmaceutical Sciences*, 78 n 1, (1989) 68–72.
- [82] S. Galindo-Rodríguez, E. Allemann, E. Doelker and H. Fessi, Versatility of three techniques for preparing ibuprofen-loaded methacrylic acid copolymer nanoparticles of controlled sizes, *Journal of Drug Delivery Science and Technology*, 15 n 5, (2005) 347-354.
- [83] Z. Ma, D. Yu, C. J. Branford-White, H. Nie, Z. Fan, L. Zhu, Microencapsulation of tamoxifen: Application to cotton fabric, *Colloids and Surfaces B: Biointerfaces*, 69 (2009) 85–90.
- [84] F. P. Schmook, J. G. Meingassner, A. Billich, Comparison of human skin or epidermis models with human and animal skin in in vitro percutaneous absorption, *International Journal of Pharmaceutics*, 215 (2001) 51-56.
- [85] T.E. Rolando, Solvent-free adhesives, *RAPRA Technology LTD.*, 9 n5, (1998) 4-5.
- [86] X. Fu, Q. Ping, Y. Gao, Effects of formulation factors on encapsulation efficiency and release behavior in vitro of huperzine A-PLGA microspheres, *Journal of Microencapsulation*, 22 (2005) 705-714.
- [87] E. Leo, F. Forni, M. T. Bernabei, Surface drug removal from ibuprofen-loaded PLA microspheres, *International Journal of Pharmaceutics*, 196 (2000) 1–9.
- [88] M. van de Weerta, R. van 't Hofb, J. van der Weerd, R.M.A. Heeren, G. Posthuma, W.E. Hennink, D.J.A. Crommelin, Lysozyme distribution and conformation in a biodegradable polymer matrix as determined by FTIR techniques, *Journal of Controlled Release*, 68 (2000) 31–40.
- [89] L. Shi, M.J. Caulfield, R.T. Chern, R.A. Wilson, G. Sanyal, D.B. Volkin, Pharmaceutical and Immunological evaluation of a single-shot of hepatitis B vaccine formulated with PLGA microspheres, *Journal of Pharmaceutical Sciences*, 91 N4 (2002) 1019-1035.
- [90] W. Tong, L. Wang and M.J. D'Souza, Evaluation of PLGA microspheres as delivery system for antitumor agent-camptothecin, *Drug Development and Industrial Pharmacy*, 29, N7 (2003) 745–756.

- [91] H. S. Mansur, C. M. Sadahira, A. N. Souza, A. P. Mansur, FTIR spectroscopy characterization of poly(vinyl alcohol) hydrogel with different hydrolysis degree and chemically crosslinked with glutaraldehyde, *Materials Science and Engineering*, 28 (2008) 539-548.
- [92] M.M. Paradkar, J. Irudayaraj, A rapid FTIR spectroscopic method for estimation of caffeine in soft drinks and total methylxanthines in tea and coffee, *Journal of Food Science*, 67 n7 (2002) 2507-2511.
- [93] Y. Daghbouche, S. Garrigues, M. Teresa Vidal and M. de la Guardia, Flow injection fourier transform infrared determination of caffeine in soft drinks, *Anal. Chem.*, 69 n6 (1997) 1086–1091.
- [94] V.R. Sinha, K. Bansal, R. Kaushik, R. Kumria, A. Trehan, Poly- ϵ -caprolactone microspheres and nanospheres: an overview, *International Journal of Pharmaceutics*, 278 (2004) 1–23.
- [95] V. Natarajan, N. Krithica, B. Madhan, P.K. Sehgal, Formulation and evaluation of quercetin polycaprolactone microspheres for the treatment of rheumatoid arthritis, *Journal of Pharmaceutical Sciences*, 100 (2011) 195–205.
- [96] S. R. Matkovic, G. M. Valle and L. E. Briand, Quantitative analysis of ibuprofen in pharmaceutical formulations through FTIR spectroscopy, *Latine American Applied Research*, 35 n3 (2005) 189-195.
- [97] K. L. Andrew Chan and Sergei G. Kazarian, High-throughput study of poly(ethylene glycol)/ibuprofen formulations under controlled environment using FTIR imaging, *J. Comb. Chem.*, 8 (2006) 26-31.
- [98] P.Z. Araujo, P.J. Morando and M.A. Blesa, Interaction of catechol and gallic acid with titanium dioxide in aqueous suspensions. 1.Equilibrium Studies, *Langmuir*, 21 (2005) 3470-3474.
- [99] I. Mohammed-Ziegler, F. Billes, Vibrational spectroscopic calculations on pyrogallol and gallic acid, *Journal of Molecular Structure: THEOCHEM*, 618 n3 (2002) 259–265.
- [100] A. M. Grancaric, A. Tarbuk and T. Pusic, Electrokinetic properties of textile fabrics, *Coloration Technology*, 121 (2005) 221-227.
- [101] R.M. Ribeiro-Costa, A.J. Alves, N.P. Santos, S.C. Nascimento, E.C.P. Gonçalves, N.H. Silva, N.K. Honda, N.S. Santos-Magalhaes, In vitro and in vivo properties of using acid encapsulated into PLGA-microspheres, *Journal of Microencapsulation*, 21, (2004) 371-384.
- [102] C. Wang, W. Ye, Y. Zheng, X. Liu, Z. Tong, Fabrication of drug-loaded biodegradable

microcapsules for controlled release by combination of solvent evaporation and layer-by-layer self-assembly, *International Journal of Pharmaceutics*, 338, (2007) 165-173.

[103] B.S. Zolnik, P.E. Leary, D.J. Burgess, Elevated temperature accelerated release testing of PLGA microspheres, *Journal of Controlled Release*, 112, (2006) 293-300.

[104] C. Herkenne, A. Naik, Y. N. Kalia, J. Hadgraft, R. H. Guy, Effect of propylene glycol on ibuprofen absorption into human skin in vivo, *Journal of Pharmaceutical Sciences*, 97 N 1 (2008) 185-197.

[105] E.I. Guisado, M.E. Gil, M.A. Camacho, A.I. Torres, Estudio de solubilidad de ibuprofeno en medio acuoso: Elaboración de una formulación líquida de uso pediátrico, 164 VI Congreso SEFIG y 3^{as} Jornadas de Tecnología Farmacéutica (2003) 161-164.

[106] K. A. Levis, M. E. Lane, O. I. Corrigan, Effect of buffer medium composition on the solubility and effective permeability coefficient of ibuprofen, *International Journal of Pharmaceutics*, 253 (2003) 49–59.

[107] M. Charoenchaitrakool, F. Dehghani, and N. R. Foster, Micronization by rapid expansion of supercritical solutions to enhance the dissolution rates of poorly water-soluble pharmaceuticals, *Ind. Eng. Chem. Res.*, 39 (2000) 4794-4802.

[108] A. Ducret, M. Trani, and R. Lortie, Lipase-catalyzed enantioselective esterification of ibuprofen in organic solvents under controlled water activity, *Enzyme and Microbial Technology*, 22 (1998) 212-216.

[109] S. De Vrieze, T. Van Camp, A. Nelvig, B. Hagström, P. Westbroek, K. De Clerck, The effect of temperature and humidity on electrospinning, *Proceedings Autex Conference (2008)*, proceedings cd-rom.

[110] S. De Vrieze, T. Van Camp, P. Westbroek, K. De Clerck, Characterization of nanofibrous material, *Proceedings Autex Conference (2008)*, proceedings cd-rom.

[111] S. De Vrieze, T. Van Camp, P. Westbroek, K. De Clerck, Electrospinning: The road to a new class of materials; *Proceedings Textiles of the Future (2008)*, proceedings Cd-Rom.

[112] S. De Vrieze, K. De Clerck, 80 Years of electrospinning; *International conference: Latest advancements in high tech textiles and textile-based materials*, (2009) 5 pages on CD-Rom.

[113] V. Nierstrasz, L. Ciera, K. De Clerck, L. Van Langenhove, Novel release system and biobased utilities for insect repellent textiles, *11th World Textile Conference (2011)* 846-847.

[114] N. Ashammakhi, I. Wimpenny, L. Nikkola, Y. Yang, *Electrospinning: methods and*

development of biodegradable nanofibres for drug release, American Scientific Publishers, 5 n1 (2009) 1-19.

[115] N. Naveen, R. Kumar, S. Balaji, T.S. Uma, T.S. Natrajan and P.K. Sehgal, Synthesis of nonwoven nanofibers by electrospinning - A promising biomaterial for tissue engineering and drug delivery, *Advanced Biomaterials*, 12 n8 (2010) 380-387.

[116] K.E. Knockenhauer, K.M. Sawicka, S.R. Simon, Encapsulation within nanofibers confers stability to the protective antigen protein, bioengineering conference, Proceedings of the 2010 IEEE 36th Annual Northeast (2010) 1-2.

[117] A. Shteyman, K.M. Sawicka, S.R. Simon, Engineering nanofibers for a novel intradermal vaccination method for whooping cough, bioengineering conference, Proceedings of the 2010 IEEE 36th Annual Northeast (2010) 1-2.

[118] J.T. McCann, M. Marquez and Y. Xia, Melt Coaxial Electrospinning: A versatile method for the encapsulation of solid materials and fabrication of phase change nanofibers, *Nano Letters*, 6, n12 (2006) 2868-2872.

[119] V. Kalra, J.H. Lee, J.H. Park, M. Marquez, and Y.L. Joo, Confined assembly of asymmetric block-copolymer nanofibers via multiaxial jet electrospinning, *Nano Small Micro*, 5, n20 (2009) 2323-2332.

[120] B. De Schoenmaker, L. Van der Schueren, S. De Vrieze, P. Westbroek, K. De Clerck, Wicking properties of various polyamide nanofibrous structures with an optimized method, *Journal of Applied Polymer Science*, 120 (2011) 305-310.

[121] L. Van der Schueren, B. De Schoenmaker, Ö. Kalaoglu, K. De Clerck, An alternative solvent system for the steady state electrospinning of polycaprolactone, *European Polymer Journal*, 47 (2011) 1256–1263.

[122] S. De Vrieze, N. Daels, K. Lambert, B. Decostere, S. Van Hulle, K. De Clerck, Filtration performance of electrospun polyamide nanofibres loaded with bactericides,, *Textile Research Journal*, 82 (2012) 37-44.

[123] N. Daels, S. De Vrieze, I. Sampers, B. Decostere, P. Westbroek, A. Dumoulin, P. Dejans, K. De Clerck, S. Van Hulle; Potential of a functionalised nanofibre microfiltration membrane as an antibacterial water filter, *Desalination*, 275 (2011) 285-290.

[124] S. Schulz and J. S. Dickschat, Bacterial volatiles: the smell of small organisms, *Natural Product Reports*, 24 (2007) 814–842.

[125] Sarah Moore, Annick Lenglet, and Nigel Hill, *Insect repellents principles, methods and*

uses, Taylor & Francis Group LLC, Chapter 14 (2006) 1-67.

[126] E. Schwartz, L. H. Weld, A. Wilder-Smith, F. von Sonnenburg, J. S. Keystone, K. C Kain, J. Torresi and D. O. Freedman, Seasonality, annual trends, and characteristics of dengue among Ill returned travelers, 1997–2006, *Emerging Infectious Diseases*, 14, n7 (2008) 1081-1088.

[127] D. O. Freedman, L. H. Weld, P. E. Kozarsky, T. Fisk, R. Robins, F. von Sonnenburg, J. S. Keystone, P. Pandey and M. S. Cetron, Spectrum of disease and relation to place of exposure among Ill returned Travelers, *The New England Journal of Medicine*, 354 n2 (2006) 119-130.

[128] L. H. Chen, M. E. Wilson, P. Schlagenhauf, Prevention of malaria in long-term travelers, *JAMA*, 296 n18 (2006) 2234-2244.

[129] M. K. Faulde, W. M. Uedelhoven and R. G. Robbins, Contact toxicity and residual activity of different permethrin-based fabric impregnation methods for *aedes aegypti* (Diptera: Culicidae), *Ixodes ricinus* (Acari: Ixodidae), and *Lepisma saccharina* (Thysanura: Lepismatidae), *Journal of Medical Entomology*, 40 n6 (2003) 935-941.

[130] K. E. Appel, U. Gundert-Remy, H. Fischer, M. Faulde, K. G. Mross, S. Letzel, B. Rossbach, Risk assessment of Bundeswehr (German Federal Armed Forces) permethrin-impregnated battle dress uniforms (BDU), *International Journal of Hygiene and Environmental Health*, 211 (2008) 88–104.

[131] J. S. Dickschat, H. B. Bode, S. C. Wenzel, R. Müller and S. Schulz, Biosynthesis and identification of volatiles released by the myxobacterium *stigmatella auriantaca*, *ChemBioChem*, 6 (2005) 2023-2033.

This article was downloaded by: [Centro de Investigacion y Desarrollo]

On: 27 December 2011, At: 03:43

Publisher: Taylor & Francis

Informa Ltd Registered in England and Wales Registered Number: 1072954 Registered office: Mortimer House, 37-41 Mortimer Street, London W1T 3JH, UK



Journal of the Textile Institute

Publication details, including instructions for authors and subscription information:

<http://www.tandfonline.com/loi/tjt20>

Monitoring of the microcapsule/liposome application on textile fabrics

Meritxell Martí ^a, Raquel Rodríguez ^a, Núria Carreras ^b, Manel Lis ^b, Josep Valldeperas ^b,
Luisa Coderch ^a & José Luís Parra ^a

^a IQAC-CSIC, Jordi Girona 18-26, Barcelona 08034, Spain

^b INTEXTER (UPC), Colom 15, Terrassa 08222, Spain

Available online: 24 Jun 2011

To cite this article: Meritxell Martí, Raquel Rodríguez, Núria Carreras, Manel Lis, Josep Valldeperas, Luisa Coderch & José Luís Parra (2012): Monitoring of the microcapsule/liposome application on textile fabrics, *Journal of the Textile Institute*, 103:1, 19-27

To link to this article: <http://dx.doi.org/10.1080/00405000.2010.542011>

PLEASE SCROLL DOWN FOR ARTICLE

Full terms and conditions of use: <http://www.tandfonline.com/page/terms-and-conditions>

This article may be used for research, teaching, and private study purposes. Any substantial or systematic reproduction, redistribution, reselling, loan, sub-licensing, systematic supply, or distribution in any form to anyone is expressly forbidden.

The publisher does not give any warranty express or implied or make any representation that the contents will be complete or accurate or up to date. The accuracy of any instructions, formulae, and drug doses should be independently verified with primary sources. The publisher shall not be liable for any loss, actions, claims, proceedings, demand, or costs or damages whatsoever or howsoever caused arising directly or indirectly in connection with or arising out of the use of this material.

Monitoring of the microcapsule/liposome application on textile fabrics

Meritxell Martí^{a*}, Raquel Rodríguez^a, Núria Carreras^b, Manel Lis^b, Josep Valldeperas^b, Luisa Coderch^a and José Luís Parra^a

^a*IQAC-CSIC, Jordi Girona 18-26, Barcelona 08034, Spain;* ^b*INTEXTER (UPC), Colom 15, Terrassa 08222, Spain*

(Received 9 January 2010; final version received 17 November 2010)

In recent years, new technologies have led to the production of biofunctional textiles. These biofunctional textiles contain microscopic capsules of ingredients that break as the fabric rubs the skin, releasing the active agents. Absorption and desorption behaviour of active agents embedded into the different biofunctional textiles should be taken into account when determining the amount of active agents incorporated into these textiles and when following the delivery mechanism as the fabric comes in contact with the skin. In this work, an encapsulated active agent (a sun filter, ethyl hexyl methoxycinnamate [EHMC] into microcapsules or liposomes) was applied by foulard onto different fabrics. The amount of capsules and active agents embedded into the fibres were quantified by (1) weight difference between untreated and treated fabrics, (2) extraction with isopropanol in an ultrasound bath, or (3) extraction with isopropanol/water 50/50 in a Soxhlet device. Sun filter detection of the extraction baths was followed by HPLC and by UV spectrophotometry. The results show that the real amount of the EHMC present in different textile substrates depends on the way that the active agent is trapped, the ionic character of the fibres and on the vehicles used.

Keywords: biofunctional textiles; microcapsules; liposomes; EHMC; absorption/desorption behaviour

Introduction

In recent years, the textile industry has initiated the production of functional textiles. One such textile constitutes the basis for the delivery system of cosmetic or pharmaceutical substances when the textile gets in contact with the skin. As most of the body is covered with some sort of textile, the potential of biofunctional textiles is considerable. Textiles that have functional properties for the skin have been studied and patented (Guarducci, 2006; Wachter, Weuthen, Panzer, & Paff, 2005).

Encapsulation is one of the techniques used to apply the substances onto the textiles (Nelson, 2002). Microcapsules have a diameter between 1 and 1000 µm (Aggarwal, Dayal, & Kumar, 1998). The capsule is a kind of box that provides both a space for storing an active agent and a protective shield from external agents such as sunlight, heat and moisture; this shield may be obtained by a natural or synthetic polymeric substance. The encapsulated compound can be released by mechanical means, temperature, diffusion, pH, biodegradation and dissolution means.

Liposomes have been used as models for complex biological membranes in biophysical and medical research owing to their lipid bilayer structural similarity. Moreover, liposomes have been the subject of

numerous studies because of their importance as microencapsulation devices for drug delivery and their applications in cosmetics (Betz, Aeppli, Menshutina, & Leuenberger, 2005; Lian & Ho, 2001; Teschke & Souza, 2002).

In recent years, liposomes have been used in the textile industry as dyeing auxiliaries, mainly for wool dyeing (Montazer, Validi, & Toliyat, 2006).

The sun filters applied on the skin are usually lipophilic molecules incorporated into oil/water (O/W) emulsions containing surfactants. It is well known that a large number of topical formulations contain emulsifiers that can modify both the skin lipids and their barrier function. One way to avoid the harmful effects of emulsifiers could be the use of biomolecules with similar characteristics to those of the lipids in the stratum corneum, i.e. liposomes prepared from internal wool lipids and incorporated ethyl hexyl methoxycinnamate (EHMC) as a sun filter (Ramón et al., 2005). When such liposomes were used, the skin penetration was retarded, suggesting a certain reinforcement of the stratum corneum barrier. In this work the same sun filter was used as a reference probe to study the preparation of biofunctional textiles with liposomes or microcapsules.

Most studies on the incorporation of active agents into textile substrates place more emphasis on the

*Corresponding author. Email: meritxell.marti@iqac.csic.es

characterization of the entrapping system (Badulescu, Vivod, Jausovec, & Voncina, 2008; Li, Boyter, & Qian, 2005), the type and amount of resin needed to improve the microcapsule adhesion to fabrics (Monllor, Capablanca, et al., 2009), and on their use in standard textile machinery (Rodrigues et al., 2009). The release of active agents from the microcapsule or from the textile entails complicated mechanisms that include mass transport through different media and layers in order to reach the surface of the skin. This release depends on the exact amount of active agents incorporated into the fabric. The number of active molecules is responsible for the concentration gradient that governs transport to the inner layers of the skin.

This study seeks to establish a methodology to quantify the amount of active agent, i.e. a sun filter, incorporated into the fabric to develop a biofunctional textile by a Pad-Dry process, using a well known foulard machine. Attention should be focused on the encapsulation process in which the active agent has been trapped and on the chemical characteristics of the textile substrates in which the sun filter is applied. The sun filter encapsulated into microcapsules or liposomes was applied onto different fabrics, cotton, polyamide, acrylic and polyester. The amount of capsules and active agent embedded into the fibres was assessed by different methodologies to determine the most convenient application procedure to be used by textile manufacturers.

No resin was used to promote the adhesion of microcapsules to the fabrics because one of the main factors in the preparation of a biofunctional textile is the active agent delivery mechanism given that the use of resins could interfere in this release. The results from the extraction and detection have optimised methodologies and demonstrated the different affinity of microcapsules or liposomes with the different textiles assayed.

Materials and methods

Materials

The following standard fabrics were used: plain cotton fabric (bleached desized cotton print cloth, Style 400 ISO 105-F02), spun polyamide fabric (PAM) (Style 361, ISO 105-F03), polyester fabric (PES) (Style 777, ISO 105-F04), acrylic fabric (PAC) (Style 864, ISO 105-F05). All chemicals used were of analytical grade. For high-performance liquid chromatography (HPLC) analysis, methanol (HPLC grade) and distilled water were used.

Microcapsules (38% EHMC, 56.8% water) were supplied by the Lipotec Group (Gavà, Spain) and were constituted by an O/W emulsion with a shield of silica

acid and xanthan gum as an external wall. Formulations of lecithin liposomes containing sun filter (1% EHMC, 3% lecithin, 25% cationic compound, Dehyquart L 80 from Henkel) were also prepared by the Lipotec Group.

Application process

All fabric samples were conditioned under standard atmospheric pressure at $20\pm 2^\circ\text{C}$ and $60\pm 5\%$ relative humidity for 24 hours prior to future application. The application of the microcapsules or liposomes onto the fabrics was performed by foulard process using a Pad-Steam-Rame pilot plant of 30 cm width (ERNST BENZ AG KLD-HT and KTF/m250), with the corresponding pressure to obtain a pick-up of $80\pm 5\%$ [(mass of bath solution taken by the textile/mass of dry textile) $\times 100$] from the microencapsulation or liposome formulations. Microcapsules were applied with a 20% of solution (7.6% EHMC) at pH 4.1 onto fabrics samples ($25 \times 40 \text{ cm}^2$); liposomes were applied at 100% (1% EHMC) at pH 3.9 onto pieces of fabric $25 \times 35 \text{ cm}^2$. Due to their little size, the impregnation was carried on in a beaker, where the fabric samples were completely submerged into the treatment bath before passing through pad cylinders. Thereafter, the impregnated fabrics were put into a curing and heat-setting chamber and maintained at 47°C for 10 minutes. The treated fabric samples were finally conditioned at $20\pm 2^\circ\text{C}$ and $60\pm 5\%$ relative humidity for 24 hours before weighing to determine the amount of product incorporated into the fabrics. All treatments were made in duplicate and the results were a medium of two values.

Biofunctional textile extraction

Textile samples, about 1 g of each fabric, were extracted using two different methodologies: (1) with 100 ml isopropanol/water (50/50), 1/100 bath ratio for one hour at its boiling point 82.3°C by a Soxhlet extractor, and (2) with isopropanol 100% twice with a 1/30 bath ratio at 35°C followed by a 15-minute sonication in a vial by an ultrasound bath (100 W Labsonic 1510, B. Braun, Melsungen, Germany). After extraction, the samples were dried for 48 hours under the same room conditions ($20\pm 2^\circ\text{C}$ and $60\pm 5\%$ relative humidity) before weighing.

EHMC detection

EHMC from the different extraction bath samples was determined by HPLC equipped with an UV-Vis detector or by UV-Vis spectrophotometer.

The HPLC instrument used was a Hitachi-Merk Elite LaChrom (Darmstadt, Germany). The apparatus is

equipped with L-6000 Intelligent Pump, AS-4000 Auto sampler and L-4250 UV-Vis detector working at 307 nm. The system was operated from the software Merck EZChrom Elite v3.1.3. The column used was a LiChrocart 125-4/Lichrosorb RP-18 (5 μm) (Darmstadt, Germany). The mobile phase was 12% water (0.5 ml H_3PO_4 85%/L)/88% methanol at 1 ml/min flow rate. The EHMC retention time was about 5.5 minutes. The area under the peak was used to calculate the concentration of EHMC using external standards that showed linearity over the concentration range of 0.05 to 140 $\mu\text{g}/\text{ml}$. The intraday and interday variations of the method were less than 5%.

A Cary 300 Bio spectrophotometer UV-Visible (Varian, USA) was used to detect the EHMC in isopropanol/water (50/50 v/v) solution at a wavelength of 310 nm. Calibration curves were used, employing liposomes or microcapsules as standards, and the curves showed linearity over the concentration range of 0.05 g/l to 0.5 g/l in both cases.

Results and discussion

The amount of the active principle (EHMC) incorporated into textiles was based on the weight of the fabrics processed or on the extracts. It is therefore necessary to determine the real amount of EHMC in the formulations (microcapsules and liposomes) supplied by the Lipotec Group. To this end, dried extracts were obtained by prior water evaporation. The EHMC amount present in these products was analysed by HPLC and the results are indicated in Table 1.

As shown in Table 1, small differences were found between the percentage of dry weight and EHMC analysed and the values indicated in the technical product file provided by the company: liposomes, 29% of dry product and 1% EHMC; and microcapsules, 43.2% of dry product and 38% EHMC.

The performance of the release systems could be affected by a number of factors such as biocompatibility, biostability, biodegradability, the amount of efficient drug delivery, and controllability (dosage control, rate control and time control) in the development and design of textile drug delivery systems (Nierstrasz, 2007).

For these reasons it is very important to know the precise amount of active agents to be applied onto the textile before its use as a textile drug delivery system.

Table 1. Percentage of dry extract weight and EHMC content of the liposome and microcapsule formulations.

	% Dry weight	% EHMC \pm % CV
Liposomes	27.2	1.01 \pm 0.02
Microcapsules	41.5	37.32 \pm 2.37

In order to establish an accurate methodology to quantify the amount of active agent incorporated into the fabric, the sun filter encapsulated into microcapsules or liposomes was applied onto different fabrics, cotton (CO), polyamide (PAM), acrylic (PAC), and polyester (PES). Traditionally, the fixation of microcapsules onto textiles is achieved by applying a binder with capsules as the fabric passes through a thermal curing process (Monllor, Bonet, & Cases, 2007; Monllor, Capablanca, et al., 2009; Rodrigues et al., 2009). In this process the fabric is subjected to high temperatures (130–170°C) between 1 and 10 minutes during which the components in the binder are converted into a tough polymer that forms a network on the fabric to retain the capsules. However, it is possible that high temperatures occasionally damage the active agents with the result that their functionality is diminished. For this reason, no binder was used in the present work when microcapsules were applied. Apart from acting as vehicles, liposomes could also be beneficial to skin (Patravale & Mandawgade, 2008; Wachter et al., 2005). Any binder could interact with the liposomes, depriving them of skin contact and impeding their passage to the outermost layers of skin. Bhatia, Mangat, Jain, Bhupinder, and Katara (2008) studied the phospholipid-structured as a possible solution in the formulation of coal tar creams to help stain removal on textiles (cotton/polyester blends) due to its high desorption properties. Moreover, the fibre-care effect of liposome applied to textiles has been patented given their more enduring effect on the skin than conventional application methods (Wachter et al., 2005).

The application of the active agent vehiculated in liposomes (27.2% of dry product and 1.01% EHMC) or in a microencapsulated formulation 20% diluted (8.3% of dry product and 7.5% EHMC) on the textile substrates was performed by foulard in an attempt to achieve an approximately 80% pick-up. The impregnation technology used is the most efficient microcapsule application methodology (Monllor et al., 2007). The percentages of pick-up for the different textiles, the percentage of theoretical product present in the fabric taking into account the composition of liposomes (27.2% product/72.8% water) (see Table 1) and microcapsules (8.3% product/91.7% water), and the percentage of dry product applied calculated by weight difference between dry initial fabric and dry fabric after Pad-Dry process are shown in Table 2.

When liposomes were applied onto the fabrics, there were differences of about 4% between the calculated amount of product impregnated (\approx 22%) and the product found in the fabric after heating at the Stenter (\approx 18%). This could mean that the liposomes showed a slightly lower tendency to be incorporated into the fibres than the water content in the formulation. It seems that cotton

Table 2. Results of the finishing process of several textile fabrics: percentage pick-up and the theoretical percentage of product present in the wet fabrics after impregnation; and percentage o.w.f. (on weight of fibres) of product applied, calculated by weight difference between dry non-treated textile and dry textile after Pad-Dry process.

Textile	Liposomes		Microcapsules	
	% Pick-up (% theoretical product)	% o.w.f. product applied	% Pick-up (% theoretical product)	% o.w.f. Dry product applied
CO	80.87 (21.99)	16.99	80.21 (6.65)	30.39
PAM	80.45 (21.88)	18.39	80.94 (6.72)	55.40
PAC	85.71 (23.31)	19.93	79.75 (6.62)	62.88
PES	84.31 (22.93)	18.76	81.17 (6.74)	37.73

fabric incorporates a lower percentage of liposomes whereas the other synthetic textiles (polyamide, acrylic and polyester) have similar percentages of product applied (on weight of fibres [o.w.f.]). Other authors have shown that lecithin liposomes have a higher affinity with polyamide than with cotton (Baptista, Countinho, Real Oliveira, & Rocha Gomes, 2004). In the case of microcapsule application, the differences between the calculated amount of the impregnated product ($\approx 6.7\%$) and the product in the fabric after heating at the Stenter ($\approx 30\text{--}60\%$) were much higher and depended on the textile material. The high affinity of this microcapsule formulation with respect to water with all the processed textiles should be noted. Both microcapsules and liposomes were applied to the fabrics at pH around 4.0 at which acrylic was anionic, cotton and polyester were neutral and polyamide had a cationic character. At pH 4.0, the liposomes applied had cationic polar heads and the microcapsules applied had silicic acid with an anionic character in their external wall. It could therefore be inferred that cationic liposomes have a slightly high affinity for PAC and the anionic microcapsules had a high tendency to be incorporated into the cationic fibres, which is the special case of polyamide.

However, this would not explain the highest affinity for the microcapsules to the PAC. A higher diffusion of the microcapsules into the PAC fibre would explain this highest absorption (Lis et al., 2008).

A number of works have been based on the increased adhesion of microcapsules to the fabrics by adding a binder or a resin which usually required a thermal process to be fixed (Li et al., 2005; Li, Lewis, Stewart, Qian, & Boyter, 2008; Monllor, Sánchez, Cases, & Bonet, 2009; Nelson, 2002). As stated above, this falls outside the scope of our study given that our aim is to achieve a high EHMC textile desorption to favour skin penetration. The different affinity of microcapsules with textiles used must be studied in depth. In order to determine the amount of product incorporated into the fibres, two extraction methodologies were tested after several trials to optimise the solvent, the time and the bath ratio.

The samples treated with liposomes or microcapsules applied by foulard were extracted with isopropanol in an ultrasound bath and with isopropanol/water, using a soxhlet extractor (see section Materials and methods).

Figure 1 shows the results obtained by the weight difference of the impregnated sample and the extracted

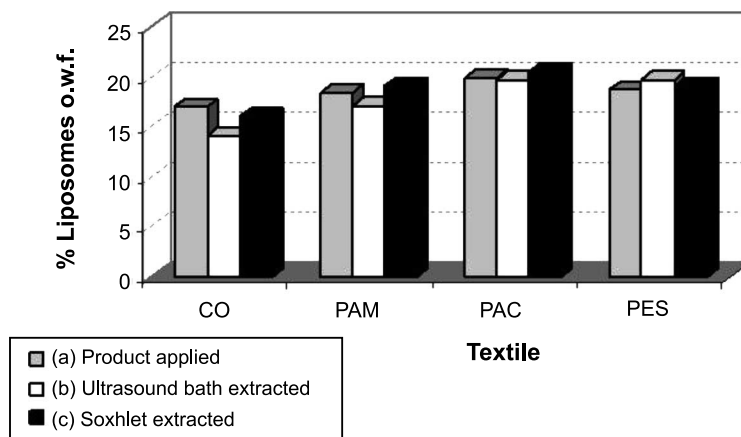


Figure 1. Assessment of liposome application on textiles: percentage o.w.f. of liposomes obtained by weight difference (a) initial and applied fabrics, (b) applied and ultrasound bath extracted fabrics, and (c) applied and soxhlet extracted fabrics.

sample using both methodologies when liposomes were applied onto several textiles. Figure 2 shows the results obtained when microcapsules were applied onto different textiles.

Similar results of the amount of product (liposomes or microcapsules with EHMC) applied and extracted by both methodologies were obtained in all cases although the degree of microcapsule incorporation into the textiles exceeded that of liposome application. These results confirm the different degree of liposomes ($\approx 18\%$) and microcapsules ($\approx 30\text{--}60\%$) to be incorporated into the different textiles. In order to determine the efficiency of both extraction methodologies, the percentage of extracted product related to the applied product was calculated for the liposome and microcapsule-treated fabrics (Figure 3). As shown in the figure, most of the fibres yielded a high percentage (between 90% and 105%) of the extracted product. Only the liposome applied onto cotton fibre and extracted with ultrasound yielded a lower extraction percentage ($\approx 83\%$). In general, it can be deduced that the soxhlet extraction with isopropanol/water at high temperatures is more

suitable for cotton and polyamide fabrics. However, the ultrasound extraction with only isopropanol is more appropriate for the more hydrophobic synthetic fibres such as acrylic and polyester in which an extraction percentage around 100% was obtained.

The EHMC content of the different extraction baths was determined either by HPLC-UV when the ultrasound bath was used (see Figure 4) or by UV-Vis spectrophotometry when soxhlet was used. The results obtained are shown in Figures 5 and 6 for liposome and microcapsule-treated fabrics, respectively. The percentage of EHMC present in the treated fibres was first calculated from the percentage o.w.f. of the product applied (calculated by weight difference between dry non-treated textile and dry textile after Pad-Dry processes). For this calculation, liposomes were considered to have a 3.71% EHMC of their total dry weight and microcapsules were considered to have a 90.58% EHMC of their total dry weight. The results obtained using both extraction and analysis methods of the different treated fabrics were compared with the % EHMC calculated from the total amount of applied product.

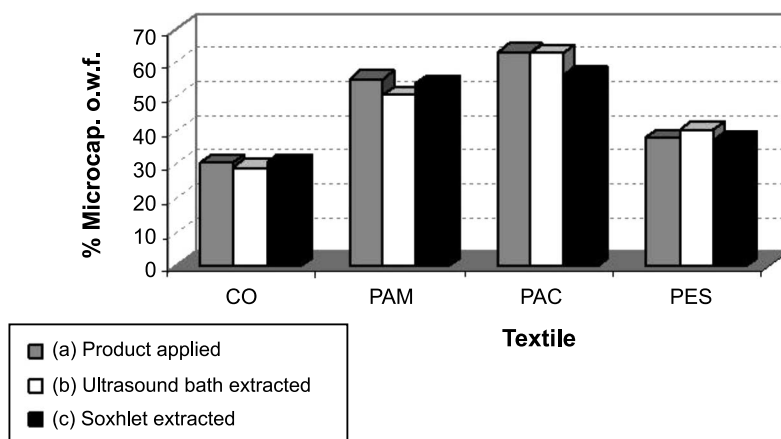


Figure 2. Assessment of microcapsules application on textiles: percentage o.w.f. of microencapsules obtained by weight difference (a) initial and applied fabrics, (b) applied and ultrasound bath extracted fabrics, and (c) applied and soxhlet extracted fabrics.

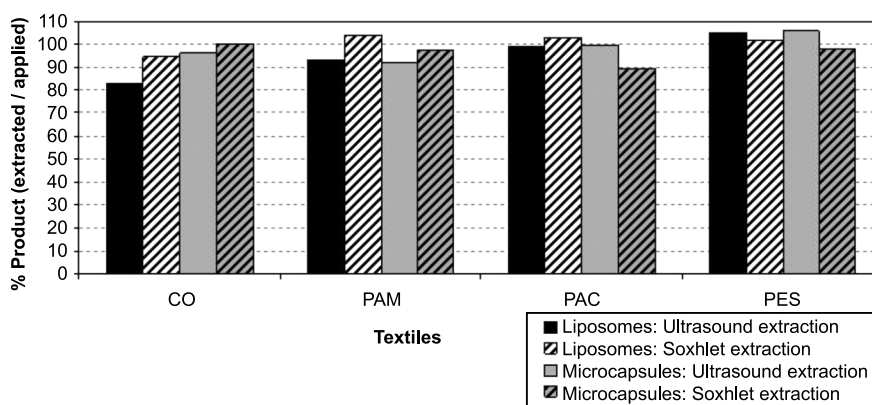


Figure 3. Percentages of extracted product (liposomes or microcapsules) related to the applied product.

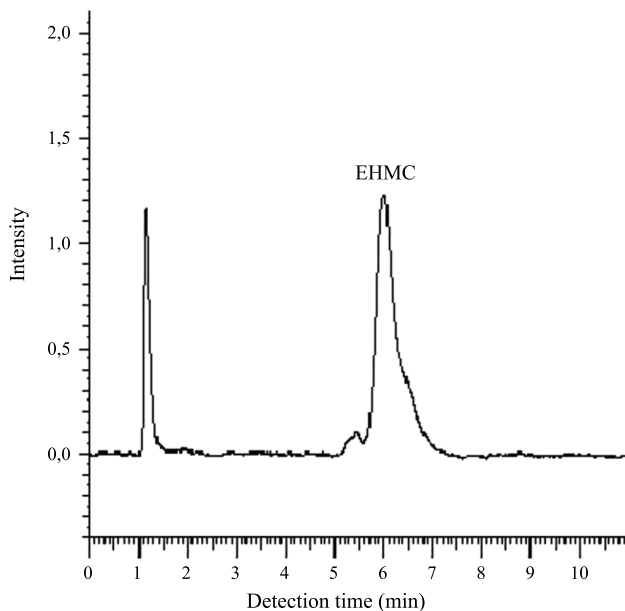


Figure 4. HPLC chromatogram of extract from cotton treated with EHMC microcapsules – (a) solvent peak, and (b) EHMC peak.

In Figures 5 and 6, there was a mark difference between the percentages of EHMC applied and extracted, the latter being much lower in the extraction baths. EHMC analysed by HPLC in the isopropanol ultrasound extracted baths was markedly lower for all applied fabrics. The efficiency of the methodologies used (extraction + detection) was determined by calculating the percentage of extracted EHMC versus the percentage of applied EHMC for the liposome and microcapsule-treated fabrics (Figure 7).

Comparison of the results plotted in Figures 3 and 7 shows that the percentages of EHMC extracted versus

the applied ones are not as high as the percentages obtained for the total products absorbed using liposomes or microcapsules. This could be due to low extraction or some analytical detection problems of the EHMC or to a difference in the absorption characteristics of the products (liposomes or microcapsules). It should be borne in mind that the amount of EHMC present in the fibres is calculated by considering the same availability of the product and the EHMC to be incorporated onto the fibres.

In this case, the extraction and detection of EHMC ranges between 70% and 105%. For all fibres, the HPLC detection of EHMC in the isopropanol ultrasound extracted baths is lower than the UV detection of EHMC in isopropanol/water soxhlet extracted baths. Again this extraction methodology with soxhlet seems to be more suitable than the one with the ultrasound bath. However, it should be pointed out that whereas 100% of extraction can be achieved for cotton or polyester, this should not be applied to polyamide and acrylic. Moreover, the higher absorption of the total product obtained for these two fibres, mainly in the case of microcapsule application, is not reflected in the EHMC analysis. Samples subjected to two different discharge mechanisms show differences in the amount of EHMC released to the media. Depending on the chemical characteristics of the textile substrate, there is adhesion of certain amount of the active agent that is more marked for microcapsules than for liposomes.

In summary, the results obtained from the EHMC extraction and analytical detection indicated that the soxhlet extraction with isopropanol/water at high temperatures followed by UV spectrophotometer detection is more suitable for all fibres than ultrasound extraction with only isopropanol using HPLC-UV

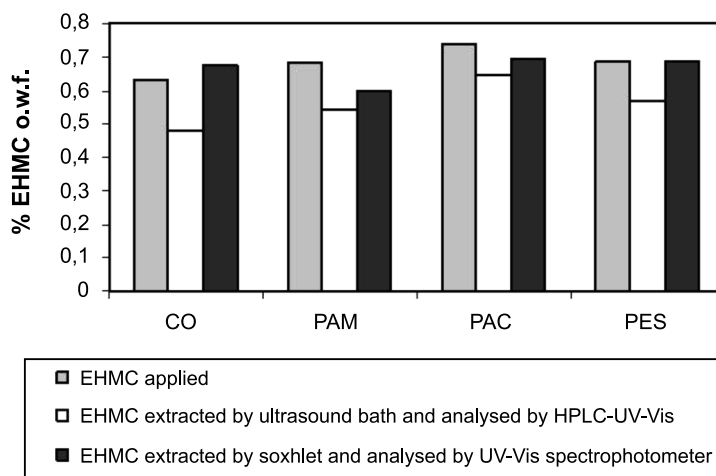


Figure 5. Evaluation of EHMC present in textiles with liposomes: calculated from product applied, EHMC extracted by ultrasound bath and analysed by HPLC-UV-Vis and EHMC extracted by soxhlet and analysed by UV-Vis spectrophotometer.

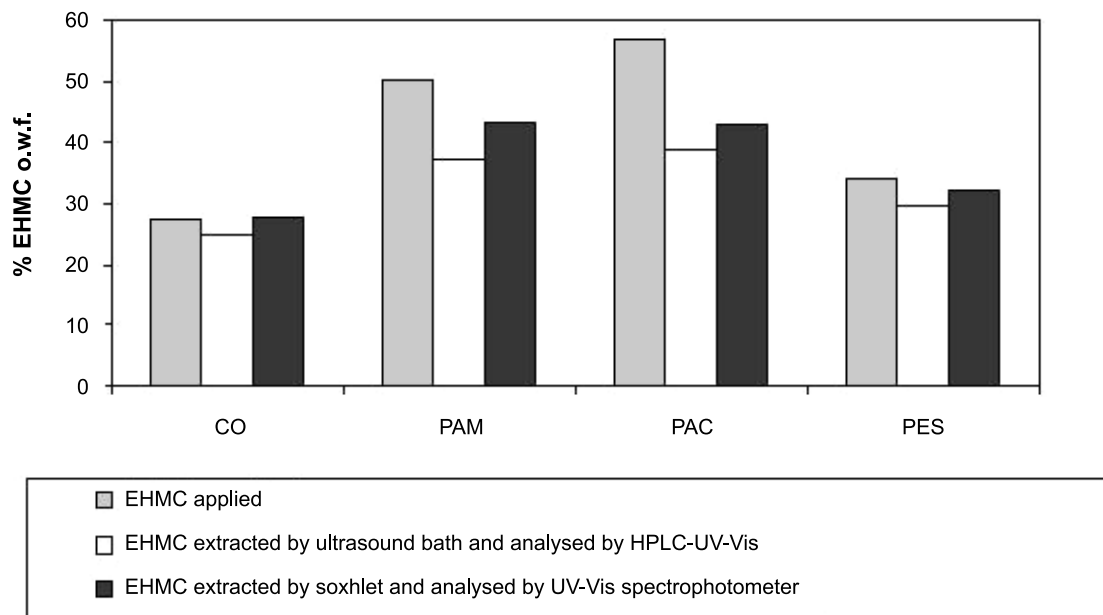


Figure 6. Evaluation of EHMC present in textiles with microcapsules: calculated from product applied, EHMC extracted by ultrasound bath and analysed by HPLC-UV-Vis and EHMC extracted by soxhlet and analysed by UV-Vis spectrophotometer.

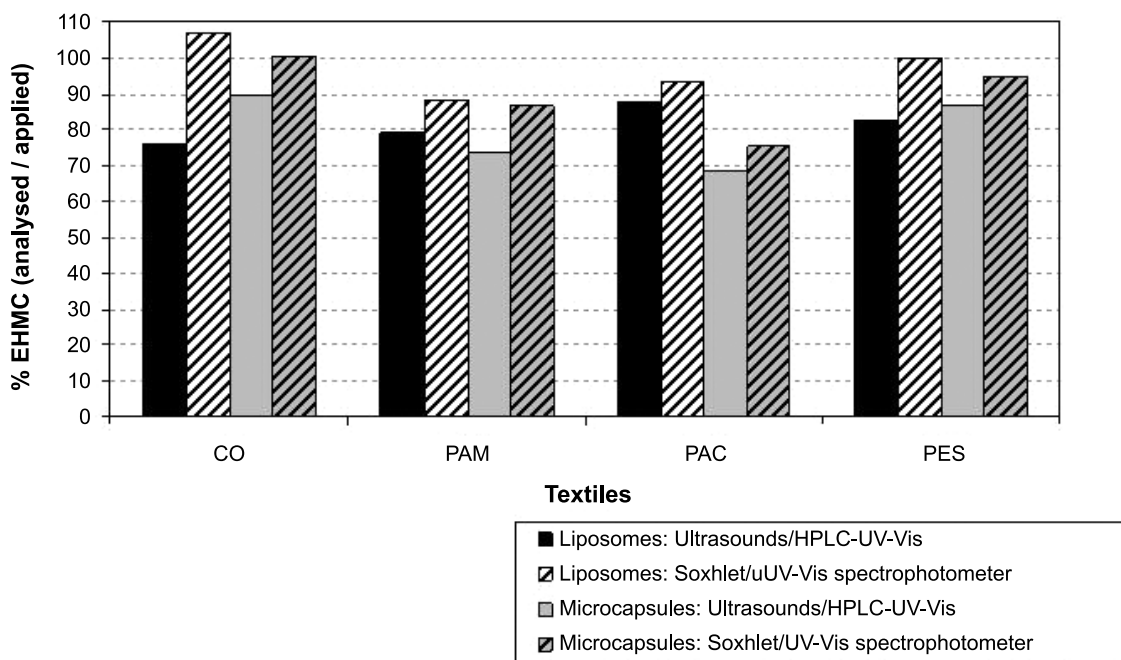


Figure 7. Percentage of extracted EHMC versus the percentage of applied EHMC.

detection. Moreover, it can be confirmed that EHMC has the highest tendency to be incorporated into the fibre when microcapsules are applied, especially in the case of acrylic and polyamide. Different methodologies have been described in the literature to assess the presence of microcapsules in textiles (Monllor et al., 2007;

Monllor, Capablanca, et al., 2009; Monllor, Sánchez, et al., 2009; Rodrigues et al., 2009; Sarier & Onder, 2007). These are based on the use of sophisticated and expensive equipment, SEM, DSC, FTIR, etc., which do not always yield quantitative results. This study presents two extraction and detection procedures that

may be readily adopted by textile manufactures to quantify microcapsules and active agents in textiles.

Conclusions

This study demonstrates that the amount of the EHMC applied onto different textile substrates depends on the way the active agent has been encapsulated, the ionic character of the fibres and the vehicles. Liposomes with cationic polar head groups have a lower absorption than expected onto fibres, the lowest absorption being for cotton. Microcapsules with an anionic character in their external wall (because of silicic acid composition) have higher amounts of product incorporated into textiles than expected, the highest absorption being for polyamide (cationic fibre).

Two extraction methodologies were assayed: with isopropanol in an ultrasound bath and with isopropanol/water using a soxhlet extractor. Similar results of the amount of product (liposomes or microcapsules with EHMC) applied and extracted by the two methodologies were obtained in all cases. These results confirm the absorption found for liposomes ($\approx 18\%$ pick-up) and microcapsules ($\approx 30\text{--}60\%$ pick-up) in different textiles. However, it can be deduced that the soxhlet extraction with isopropanol/water at high temperatures is more suitable for cotton and polyamide and that the ultrasound extraction with only isopropanol is the most appropriate extraction for the more hydrophobic synthetic fibres such as acrylic and polyester.

EHMC from the different extraction baths was determined by HPLC-UV when the ultrasound bath was used or by UV-Vis spectrophotometry when soxhlet was used. There was a marked difference between the EHMC applied and extracted percentages, the lowest amount of this active agent being detected in the extraction baths. Again, the extraction methodology with soxhlet is more suitable than the one with ultrasound bath. However, it should be pointed out that a 100% of extraction can be achieved for cotton or polyester, whereas the extraction is lower than 100% for polyamide and acrylic fibres.

In the present work, a methodology to detect the amount of active agent applied onto several fabrics was established taking into account the influence of the chemical characteristics of vehicles and fibres on EHMC incorporation. Absorption and desorption behaviour of EHMC embedded into different biofunctional textiles must be considered in order to determine the amount of active agents incorporated, and to understand the delivery mechanism when the textile is in contact with human skin. Thus, the methodology used should be verified when an active agent is encapsulated into a new device given that the chemical substances employed in the preparation of capsules can exert a

marked influence on specific doses of active agents that are released to the skin.

Acknowledgements

The authors acknowledge financial support by the National Project from Ministerio de Educación y Ciencia (Spain), Ref. CTQ2006-15404-C03-01. Thanks are also due to the Lipotec Group for supplying microcapsules and liposomes. The authors are indebted to Dr Cebrián and Dr Viladot from the Lipotec Group for their technical support and to Mrs I. Yuste and Mrs V. Martínez for their technical work in the IQAC laboratories.

References

- Aggarwal, A., Dayal, A., & Kumar, N. (1998). Microencapsulation processes and application in textile processing. *Colourage*, 45(8), 15–24.
- Badulescu, R., Vivod, V., Jausovec, D., & Voncina, B. (2008). Grafting of ethylcellulose microcapsules onto cotton fibres. *Carbohydrate Polymers*, 71, 85–91.
- Baptista, A.L.F., Countinho, P.J.G., Real Oliveira, M.E.C.D., & Rocha Gomes, J.I.N. (2004). Lipid interaction with textile fibres in dyeing conditions. *Progress in Colloid and Polymer Science*, 123, 88–93.
- Betz, G., Aeppli, A., Menshutina, N., & Leuenberger, H. (2005). In vivo comparison of various liposome formulations for cosmetic application. *International Journal of Pharmaceutics*, 296, 44–54.
- Bhatia, A., Mangat, P., Jain, B., Bhupinder, S., & Katare, P. (2008). Washability and fabric-staining properties of a novel phospholipids-structured coal tar formulation. *Journal of Dermatological Treatment*, 19, 105–110.
- Guarducci, M. (2006). Textile product having particular functional properties for the skin and process for the preparation thereof. Patent No. WO/2006/106546. Italy: Massimo Guarducci s.r.l.
- Li, S., Boyter, H., & Qian, L. (2005). UV curing for encapsulated aroma finish on cotton. *Journal of the Textile Institute*, 96(6), 407–411.
- Li, S., Lewis, J.E., Stewart, N.M., Qian, L., & Boyter, H. (2008). Effect of finishing methods on washing durability of microencapsulated aroma finishing. *Journal of the Textile Institute*, 99, 177–183.
- Lian, T., & Ho, R.J.Y. (2001). Trends and developments in liposome drug delivery systems. *Journal of Pharmaceutical Sciences*, 90, 667–680.
- Lis, M., Valldeperas, J., Martí, M., Ramírez, R., Cebrián, J., Navarro, J.A., Coderch, L., & Parra, J.L. (2008, May). *Assessment of active principle in microcapsules applied by Pad-Dry Systems*. Paper presented at the 21st IFATCC International Congress, Barcelona.
- Monllor, P., Bonet, A., & Cases, F. (2007). Characterization of the behaviour of flavour microcapsules in cotton fabrics. *European Polymer Journal*, 43, 2481–2490.
- Monllor, P., Capablanca, L., Gisbert, J., Díaz, P., Montava, I., & Bonet, A. (2009). Improvement of microcapsules adhesion to fabrics. *Textile Research Journal*. DOI: 10.1177/0040517509346444.
- Monllor, P., Sánchez, L., Cases, F., & Bonet, A. (2009). Thermal behaviour of microencapsulated fragrances on cotton fabrics. *Textile Research Journal*, 79, 365–380.
- Montazer, M., Validi, M., & Toliyat, T. (2006). Influence of temperature on stability of multilamellar liposomes

- in wool dyeing. *Journal of Liposome Research*, 16(1), 81–89.
- Nelson, G. (2002). Application of microencapsulation in textiles. *International Journal of Pharmaceutics*, 242, 55–62.
- Nierstrasz, V.A. (2007). Textile-based drug delivery systems. In L. Van Langenhove (Ed.), *Smart textile for medicine and healthcare* (pp. 50–73). Cambridge: CRC Press.
- Patravale, V.B., & Mandawgade, S.D. (2008). Novel cosmetic delivery systems: An application update. *International Journal of Cosmetic Science*, 30, 19–33.
- Ramón, E., Alonso, C., Coderch, L., de la Maza, A., López, O., & Notario, J. (2005). Liposomes as alternative vehicles for sun filter formulations. *Drug Delivery*, 12, 83–88.
- Rodrigues, S.N., Martins, I.M., Fernández, I.P., Gomes, P.B., Mata, V.G., Barreiro, M.F., & Rodrigues, A.E. (2009). Scentfashion: Microencapsulated perfumes for textile application. *Chemical Engineering Journal*, 149, 463–472.
- Sarier, N., & Onder, E. (2007). The manufacture of microencapsulated phase change materials suitable for the design of thermally enhanced fabrics. *Thermochimica Acta*, 452, 149–160.
- Teschke, O., & de Souza, E.F. (2002). Liposome structure imaging by atomic force microscopy: Verification of improved liposome stability during absorption of multiple aggregated vesicles. *Langmuir*, 18, 6513–6520.
- Wachter, R., Weuthen, M., Panzer, C., & Paff, E. (2005). Use of liposomes for the finishing of fibres and textiles. Patent Nos. EP1510619-A2, DE10339358-A1, US2005058700-A1. Germany: Cognis IP Management GmbH.

TO BE SUBMITTED

Drug release system of ibuprofen in PCL-microspheres

Carreras¹, N., Acuña¹, V., Martí², M., Lis³, M.J.

(1) Polytechnic University of Catalonia – Department of Chemical Engineering, Colom 1, 08222 Terrassa, Barcelona, Spain.

(2) Institut de Química Avançada de Catalunya, (IQAC-CSIC), Jordi Girona 18-26, 08034 Barcelona, Spain

(3) INTEXTER-UPC. Polquitex Research Group. Colom, 15, 08222 Terrassa, Barcelona, Spain

Corresponding Author: Núria Carreras Parera

E-mail address: nuria.carreras@gmail.com

Telephone: 0034 93 739 80 45

FAX: 93 739 82 25

ABSTRACT

Today, the technology of microencapsulation of active principles is on top of biomedical advances, because through it we can solve many of the problems caused by current methods of taking medication. By active principle microencapsulation not only solve the problems of drug intake but also controlled it's dosage.

In this study has carried out the development of a protocol for the microencapsulation of ibuprofen by solvent evaporation method. A subsequent application of those microencapsulates to biofunctional textile substrates (cotton, polyamide, acrylic and polyester) using a finishing process, and finally a study of the release of active principle in two different media (deionised water and physiological serum) has been carried out using samples of the treated fabrics that were submerged into thermostated vessel at semi infinite bath conditions. The determination of active principles released to the bath was determined by UV-Spectrophotometer. These experimental results have been analyzed and evaluated, therefore have allowed to define a controlled drug release system by Fickian diffusion in different medias.

Keywords: Microcapsules, biofunctional textile substrates, drug release, ibuprofen.

1. INTRODUCTION

Currently, biomedical advances are emerging faster and faster, one of these new methods is microencapsulation. Microencapsulation has become one of the best ways of taking medicines, because slow absorption through the skin prevents from the side

effects that the medicine can cause. By the application on bio-textile substrates let us to get a support for the microspheres formed during the process and it also allows microspheres to be placed on the skin [1-7].

Due to its great versatility, the polymer's family is the most used in the microencapsulation of active principles. Within it are the natural, the semi-synthetic and the synthetic polymers. Natural polymers are mainly polysaccharide, animal and plant origin. The alginate, dextran, gum arabic and chitosan are highlighted. Semi-synthetic polymers comprise cellulose derivatives, of which there is a wide variety with different solubility characteristics. The most widely used synthetic polymers are the acrylic derivatives and polyesters. Among the acrylic derivatives are insoluble polymers with different degrees of permeability and also with different solubilities depending on pH. Polyesters are polymers with character biodegradable. Among them, the most known are poly- ϵ -caprolactone (PCL), the poly-lactic acid (PLA) and its derivatives such as L-PLA, and the copolymers of lactic acid and glycolic acid (PLGA).

Poly- ϵ -caprolactone (PCL) behaves as a biocompatible material and used as biodegradable sutures. Therefore, it is a suitable material for the transport of drugs, such as ibuprofen [2].

Ibuprofen is an anti-inflammatory steroid. It is used to relieve symptoms of arthritis, primary dysmenorrhoea, fever, and as an analgesic, especially where there is an inflammatory component. Ibuprofen appears to have the lowest incidence of gastrointestinal reactions adverse of all non-selective NSAIDs (Non-steroidal anti-inflammatory drug). However, this only occurs at lower doses of ibuprofen, because it's usually advisable a maximum daily dose of 1,200 mg. Adverse effects include dyspepsia, nausea, ulcers / bleeding gastrointestinal, hepatic enzymes increased, diarrhea, constipation, epistaxis, headache, dizziness, priapism, rash, retention salt and fluid, and hypertension. A 2010 study has shown that the use regular NSAID was associated with increased hearing loss. Uncommon side effects include, oesophageal ulceration, heart failure, hyperkalemia, renal failure, confusion, and bronchospasm. Currently, it requires that drug delivery systems be precise in their control of drug distribution and reduce the side effects of the drug. Therefore, drug delivery systems based on a polymeric matrix can allow to have control of the drug release during a period of time until reaching the expected effect in the right target. [8].

Release of core material from a non-erodible microcapsule can happen in different ways. Four theoretical curves (A, B, C and D) that describe four types of diffusion kinetics are contained in Fig 1 [9].

Curve A represents the type of release of a seamless, non-erodible, spherical microsphere encapsulated material released by the state balance of diffusion through a coating of uniform thickness. Rate release remains constant as long as the

concentrations inner and outer core material and the concentration gradient through the membrane are constant. If the beginning is to establish need a finite time, the concentration gradient is constant that is on the wall of the membrane, and then there is a delay release of the core material. Curve A of Fig 1 shows system without delay. If some of the encapsulated materials migrate through of the microsphere membrane during storage happens effect of "burst" (initial burst release), represented by curve B. If the microsphere acts as a matrix of inert particles in the core material is dispersed (a bead), the Higuchi model is valid up to 60% release. In this case, the percentage of drugs released according to the square root of time is linear, as indicated by curve C in Fig 1. The release of the first order is represented by curve D. The curve is linear if it represents the logarithm of the percentage of core material remaining in the capsule versus time [9].

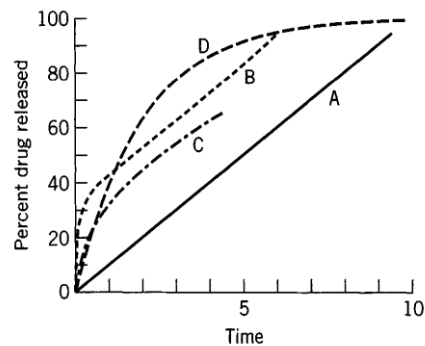


Fig 1. Theoretical curves of release behaviour. A, Membrane reservoir-type free of lag time and burst effects; B, same as A, with burst effects; C, matrix or monolithic sphere with square root time-release; D, system with first-order release [7].

During the study various semi-empirical equations were used, such as the “power law” used to describe the release of the drug from the polymeric system [10-12]:

$$\frac{M_t}{M_\infty} = k \cdot t^n \quad (1)$$

where $\frac{M_t}{M_\infty}$, is the percentage of drug released at each interval of time relative to the percentage of release at the equilibrium, “K” is the constant of drug release, t is time measured and finally “n” is the diffusion exponent.

The equation of power law, gives the diffusion exponents which are classified by this Table 1.

Table 1. Drug delivery models based on the parameter n.

Exponent n			
Plane surface	Cylinder	Sphere	Drug Delivery Systems
0,5	0,45	0,43	Fickian Diffusion Mechanism
0,5 < n < 1,0	0,45 < n < 0,89	0,43 < n < 0,85	Anomalous Diffusion
1,0	0,89	0,85	Non-Fickian Diffusion Mechanism

From Equation 1, when the exponent “n” is set to 1, the rate of drug released is independent of time. This case corresponds to zero order kinetics. For films, the mechanism that creates zero-order release is known among experts such as case II transport. Here the relaxation of macromolecules process happens over the imbibitions of water in the system that is the stage of speed control. Water acts as a plasticizer and decreases the glass transition temperature (T_g) of the polymer. Once the T_g is equal to the set temperature, the polymer chains pass from the glassy state to rubbery state, with an increase of the mobility of macromolecules and volume expansion.

Thus, Equation 1 has two different physical realistic meanings in the two special case of n = 0,5 (indicating the diffusion controlled release of active principles). The values of “n” between 0,5 and 1 can be considered as an indicator for the superposition of both phenomena (anomalous transport). It must always be clear that the two extreme values for the exponent n, 0,5 and 1, are only valid for flat sheet geometry.

The transport in swelling systems can be described by Fick’s second Law, because of this, the diffusion of the active principle can be studied as a plane surface for short times of liberation, from the Korsenmeyer-Peppas equation approximation [10-12].

$$\frac{M_t}{M_\infty} = 4 \sqrt{\frac{D \cdot t}{\pi \cdot \delta^2}} = K' \cdot \sqrt{t} \quad (2)$$

where D is the diffusivity of the active principle in the polymeric system, and δ is the thickness of the lamina.

The model to describe the release drug release from polymeric matrices is derived from the equation of Higuchi for planar films [10-12]:

$$\frac{M_t}{M_\infty} = K \cdot \sqrt{t} \quad (3)$$

In this study, we have tried to apply those drug delivery models to the microencapsulation of ibuprofen and its subsequent applications on biofunctional textiles in order to know the pattern of drug release corresponding to ibuprofen.

2. EXPERIMENTAL

2.1. MATERIALS

PCL (poly(ϵ -caprolactone)) with a molecular mass (M_n) of 60,000 from Aldrich. Ibuprofen in powder with a molecular mass (M_r) of 206.28, supplied by Sigma-Aldrich. PVA (Poly(vinyl alcohol)), 87-89% hydrolyzed, with a (M_w) range of 31,000-50,000 from Aldrich. Dichloromethane stabilized with 20 ppm of amylene, supplied by Panreac were used to prepare microspheres.

The standard woven fabrics used were: Cotton fabric (COT) (Style, ISO 105 - F02) Polyamide fabric (PA) (Style 361, ISO 105-F03), Polyester fabric (PET) (Style 777, ISO 105-F04), and Acrylic fabric (PAC) (Style 864, ISO 105-F05) from Test Fabrics Inc (USA).

All chemicals used were of analytical grade.

2.2 PREPARATION OF IBUPROFEN MICROSPHERES

The solvent evaporation method is used to obtain the microspheres and by it form a microemulsion ($o_1/o_2/w$ double emulsion).

Briefly, the polymer (PCL) and the active principle (ibuprofen) were separately dissolved in methylene chloride and in isopropyl alcohol, respectively.

The simple emulsion (o_1/o_2) was generated by mechanical agitation (Ultra-turrax T25, IKA) for several minutes. Afterwards, this simple emulsion was added to a continuous phase, constituted of 150 ml aqueous solution of PVA (dispersant) (2% w/w) and emulsified for several minutes resulting in a double emulsion ($o_1/o_2/w$). The mixture was maintained under constant agitation until total evaporation of the solvent in order to obtain the corresponding microsphere. The method used was carried out at room temperature. [13-17]

2.3 CHARACTERIZATION

For the characterization of the obtained microspheres, 4 tests were done: Scanning Electron Microscopy (SEM), Encapsulation Efficiency, Fourier Transform Infrared Spectroscopy (FTIR) and Particle Size Distribution.

2.3.1 ENCAPSULATION EFFICIENCY

The encapsulation efficiency (EE) of active compound in microspheres was detected indirectly in the liquid phase by UV/Vis Spectrophotometer (Shimadzu UV-2401 PC)

after centrifugation of dissolution for several minutes. The percentage of caffeine entrapped in the dispersion was calculated by following equation:

$$EE (\%) = \frac{C_t - C_d}{C_t} \cdot 100 \quad (4)$$

where C_t is the theoretical concentration of microencapsulated drug, C_d is the drug concentration remaining in the bath solution corresponding to the amount of drug that has not been microencapsulated.

2.3.2 FOURIER TRANSFORM INFRARED SPECTROSCOPY (FTIR)

A Fourier-transform infrared spectrometer FTIR (Avatar System 320) was used to identify the chemical structure of the formulation of microspheres which were prepared by grinding the powder sample with KBr (wave-numbers $500-4000 \text{ cm}^{-1}$, at a resolution of 4 cm^{-1} and by coadding 20 scans). The goal has been to investigate the possible interactions that can be produced between the polymer and the active agent [18-20].

2.3.3 PARTICLE SIZE DISTRIBUTION

Particle size distribution of microspheres was carried out at Malvern Nanosizer (Model Nano-ZS Series, Malvern). Microspheres samples were introduced into a DTS1060C – Clear disposable zeta cell and water was used as a dispersant at 25°C . The results were reported as intensity of size distribution.

2.3.4 SCANNING ELECTRON MICROSCOPY (SEM)

The treated fabrics were analyzed by SEM (model JSM-5610, JEOL, Tokyo, Japan) in order to detect the existence of microspheres as well as analyze their morphology (shape and surface).

2.4 FINISHING PROCESS

The application of microcapsules onto the fabrics was carried out by foulard process using a Pad-Dry technique of 30 cm width (ERNST BENZ AG KLD-HT and KTF/m250) and followed by a process of drying at room temperature, with the padding pressure to obtain a pick-up of $80\pm 5\%$, from the microencapsulation formulations. The treated fabric samples were finally conditioned at $20\pm 2^\circ\text{C}$ and $60\pm 5\%$ relative humidity for 24 hours before weighting and proceeding to perform subsequent experiments.

2.5 DRUG RELEASE

To analyze the kinetic release of ibuprofen, samples of 1 g of the treated fabric were submerged into the thermostated vessels filled with deionized water and physiological saline at semi-infinite bath conditions at a temperature of 37°C. The semi-infinite bath is called to the system which has one limited direction and extends infinitely in the other, therefore it can be considered that the diffusion into the edges can be neglected. This analysis aims to study the environmental effects on the drug release systems, for instance the effect of saline medium (physiological saline), simulating the skin's sweat. The amount of active principle released to the bath was determinate by UV/Vis Spectrophotometer at different times (from 0 to 200 hours).

3 RESULTS AND DISCUSSION

Microspheres of ibuprofen were prepared following the method of experimental part. Then, those microspheres were characterized using several techniques outlined in the experimental part.

3.1 ENCAPSULATION EFFICIENCY

After 20 hours of stirring the microspheres preparation at room temperature, the encapsulation efficiency was analyzed.

Table 2 shows the ibuprofen encapsulation efficiencies obtained by triplicates, the overall average was about 84%.

Table 2. Encapsulation efficiency of the ibuprofen microspheres.

Sample	Encapsulation efficiency (%)
1	88.00
2	82.00
3	82.00

According to the literature [21-23], the efficiency results obtained are very high. Thus, it may ensure us that the designed method for preparation of ibuprofen microspheres has been very efficient.

3.2 FTIR - MICROSPHERES OF IBUPROFEN

FTIR analysis were carried out to see structural changes between different microspheres components.

Two types of FTIR spectra were obtained. The first one (Fig 2) corresponds to a comparison between the polymer and empty microspheres, and the second one (Fig 3)

compares the structural changes detected between ibuprofen, microspheres of ibuprofen and empty microspheres.

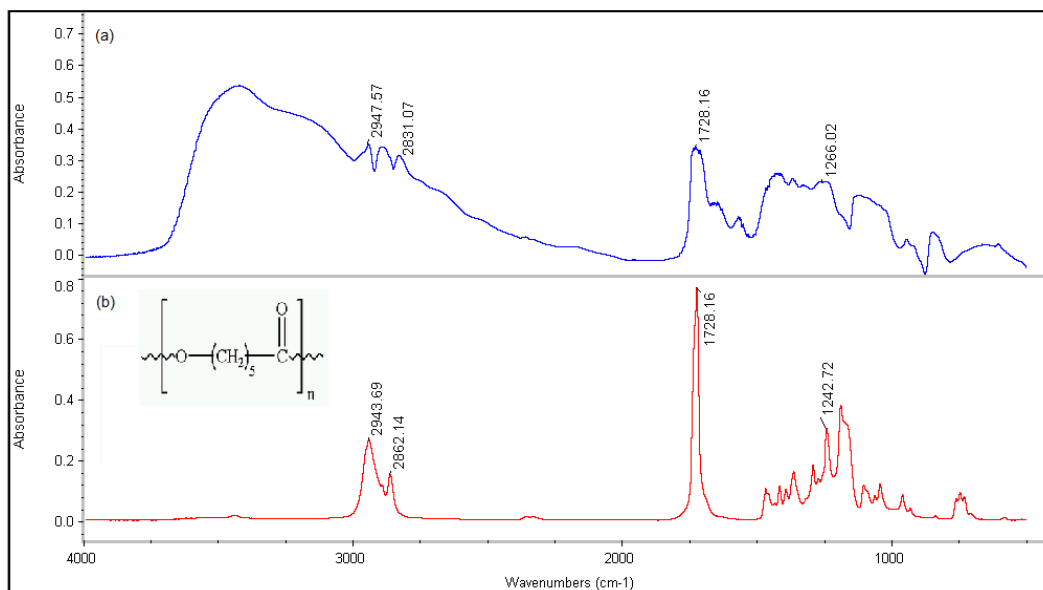


Figure 2. FTIR spectrum of (a) PCL-microspheres without ibuprofen and (b) PCL polymer.

Movements of the characteristic groups in the formation of microspheres are discussed: 1725 cm⁻¹ (carbonyl stretching) shows a shift of the peak corresponding to the movement of the carbonyl group to 1731,63 cm⁻¹. The 1269,58 cm⁻¹ is a shift due to an asymmetric movement to 1269,58 cm⁻¹ of the asymmetric COC stretching. Also notes the displacement of the peaks 2944,23 and 2865,46 cm⁻¹ corresponding to the CH₂ group tension movement.

These movements that occur during the process, may be crucial to justify optimal formation of the microspheres. As it can be seen, PCL polymer has changed from a linear chain to a polymeric matrix form.

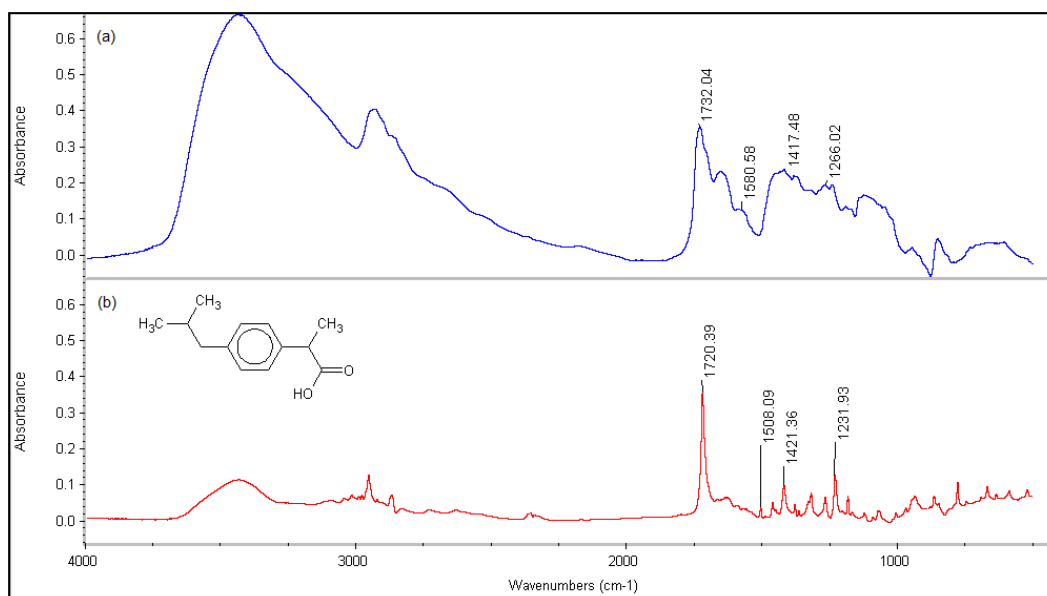


Figure 3. FTIR spectrum of (a) PCL-microspheres with ibuprofen and (b) ibuprofen.

As shown in the image of the different spectra, it can be appreciated the disappearance of one of the characteristic peaks $1231,19 \text{ cm}^{-1}$ corresponding to C-O stretching (COOH) and O-H bending. Also, it can be observed an increased frequency range corresponding to the movement of carbonyl group ($1731,63 \text{ cm}^{-1}$ (carbonyl stretching)), in the case of microspheres corresponds to the structure of the polymer containing more carbonyl groups than the active principle. Moreover, ibuprofen presents a certain steric hindrance due to its aromatic group. This movement could give an idea about a possible interactions due to hydrogen bonds.

3.3 PARTICLE SIZE DISTRIBUTION - MICROSPHERES OF IBUPROFEN

Another parameter studied to characterize the ibuprofen microspheres was particle size. The size of microspheres could be easily affected by a variety of processing factors such as volume and viscosity of inner and external aqueous phase [24].

The particle size distribution of microspheres in terms of intensity is shown in Fig 4.

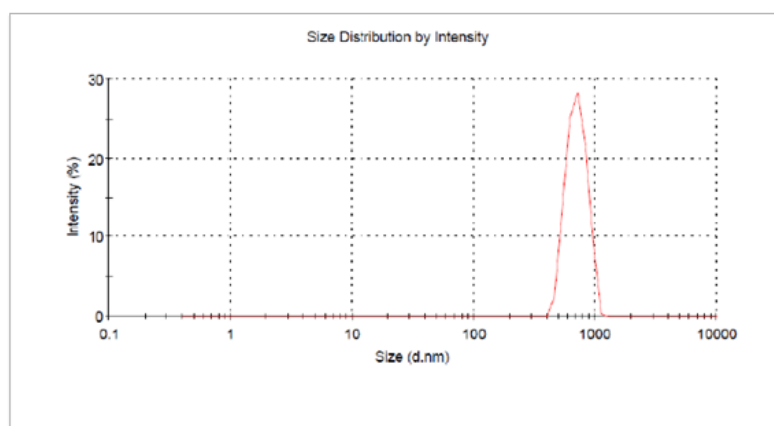


Fig 4. Size distribution by intensity of ibuprofen microspheres.

The average particle diameter is $846.9 \pm 64,95$ nm. As a consequence, the particles obtained can be considered as microspheres, because their particle sizes meaning that are about $1 \mu\text{m}$.

The polydispersity (PDI) value is about 1.000 meaning there are many microspheres with a very different sizes. The PDI values range from 0 to 1 and a higher value indicates a less homogeneous particles size distribution. Therefore, the results indicate that microparticles generated have low homogeneity in size distribution.

3.4 FINISHING PROCESS

The application of the ibuprofen encapsulated on the textile substrates was performed by pad-dry. The percentages of pick up for the different textiles, and percentages of dry product applied calculated by weight difference between dry initial fabric and dry fabric after Pad-dry process are indicated in Table 3.

Table 3. Results of the finishing process of several textile fabrics.

Textile	% Pick-up* (% theoretical product)	% o.w.f.* Dry product applied
COT	76.13	4.30
PA	80.20	35.06
PAC	81.79	18.24
PET	77.65	75.65

* % pick-up and the theoretical percentage of product present in the wet fabrics after impregnation; and % o.w.f. (on weight of fibres) of product applied, calculated by weight difference between dry non-treated textile and dry textile after Pad-Dry process.

It can be seen that depending on each fabric, the results obtained were quite different. Above all we must mention that the cotton has been reduced importantly dry impregnation on the wet; however the changes were observed in the case of polyester,

had remained practically the same permeation rate in both dry and wet. These results should be understood taking into account the efficiencies and the affinities of the fabric with the polymer in terms of hydrophilicity/hydrophobicity.

3.5 SCANNING ELECTRON MICROSCOPY (SEM)

Treated fabrics (only cotton fabric) with ibuprofen microspheres have been analyzed by SEM and the micrographs are shown bellow.

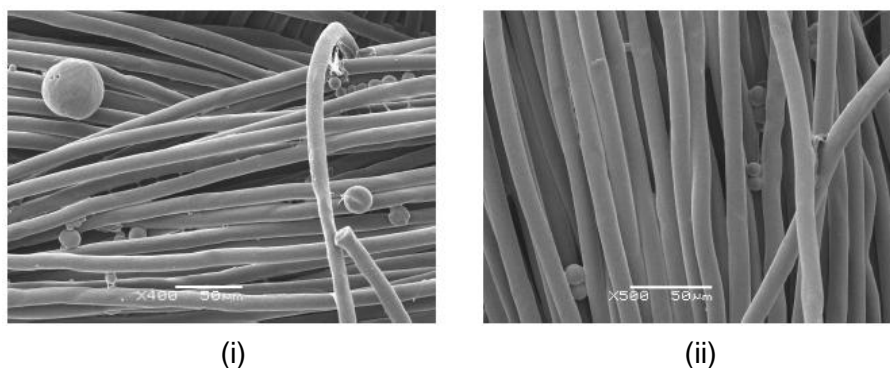


Fig 5. Scanning electron micrographs of microspheres on cotton fabric. (i) microspheres with ibuprofen (x400). (ii) microspheres without ibuprofen (x500).

These two micrographs (Fig 5) show that microspheres were formed with a spherical shape smooth surface, composed of PVA, but internally are porous (although it is not appreciated in these micrographs). The surfaces layer of PVA acts as a binder between microspheres and fabric. It can be observed that all cases the microspheres maintain the same characteristics, thus the process may not be affected by active compound.

3.6 DRUG RELEASE

Afterwards, from the experimental results obtained, we proceed to apply two type of analysis, qualitative (Theoretical Mechanisms of Drug Release) and quantitative (Semi-empirical Equations), in order to know the mechanism of drug release for each kind of fabric.

3.6.1 DRUG RELEASE – THEORETICAL MECHANISMS OF DRUG RELEASE

The ibuprofen release from PCL-microspheres of all treated fabric samples (COT, PA, PAC and PET) are characterized by a bimodal behaviour depending on the type of fabric as shown in the following Figures.

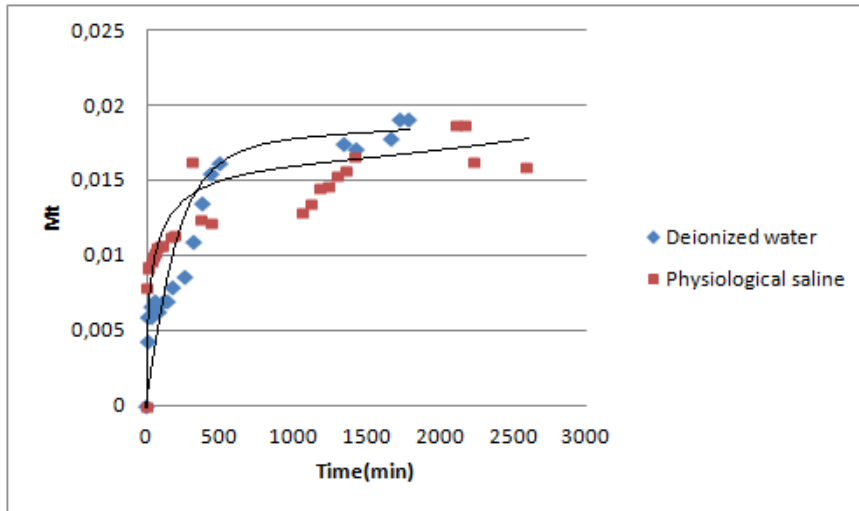


Fig 6. Kinetic release of ibuprofen microspheres applied onto cotton fabric at 37°C according to the experimental media used. M_t (g ibuprofen/ g fabric).

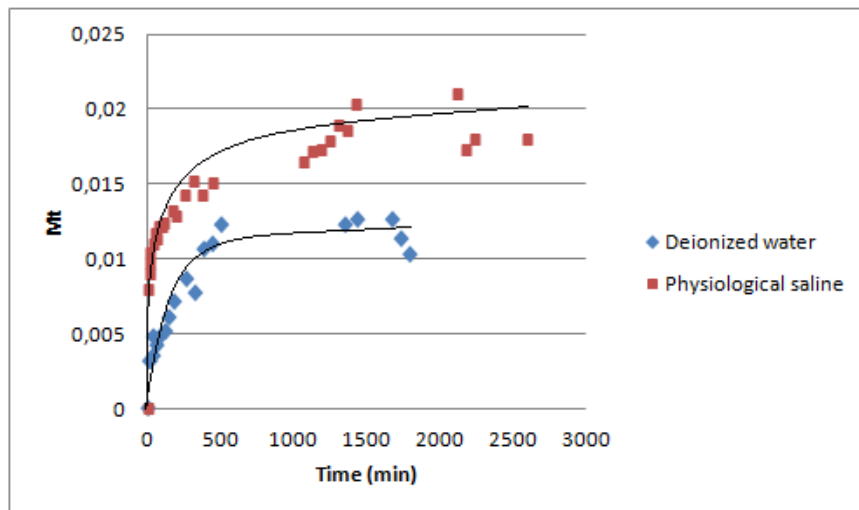


Fig 7. Kinetic release of ibuprofen microspheres applied onto polyamide fabric at 37°C according to the experimental media used. M_t (g ibuprofen/ g fabric).

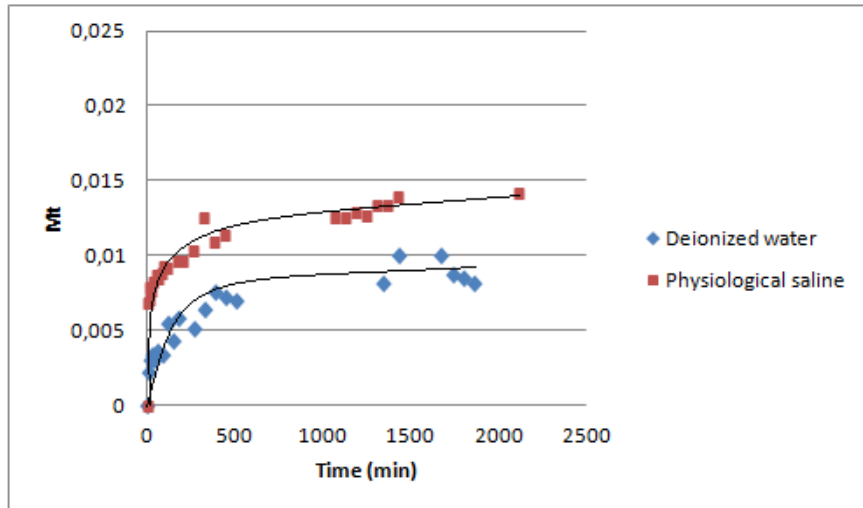


Fig 8. Kinetic release of ibuprofen microspheres applied onto acrylic fabric at 37°C according to the experimental media used. M_t (g ibuprofen/ g fabric).

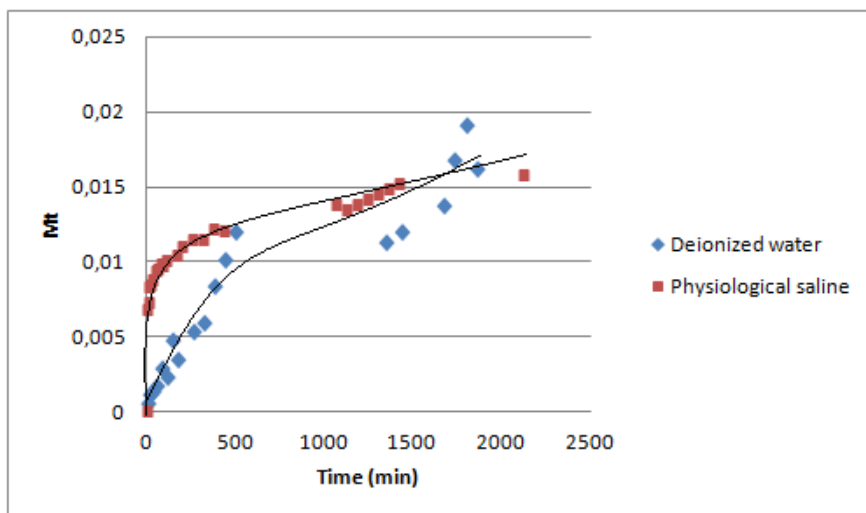


Fig 9. Kinetic release of ibuprofen microspheres applied onto polyester fabric at 37°C according to the experimental media used. M_t (g ibuprofen / g fabric).

Comparing the kinetic profiles obtained with the theoretical curves (A, B, C and D) illustrated in Fig 1 it can be deduced that the behaviour of the fabrics in water medium is similar to the theoretical curve D whereas in saline medium the fabrics behave like a theoretical curve between B/C. In general, burst effect happens, and it can be seen more differences in the case of cotton and polyester than in the others regarding to the type of medium.

3.6.2 DRUG RELEASE – SEMIEMPIRICAL EQUATIONS

Using Eq. (1), the value of the exponent n , indicative of mass transport mechanism was calculated and the results are shown below (Table 4).

Table 4. Estimated parameters, (K) and n values obtained from fitting drug release experimental data to Power Law (Eq. (1)).

Fabric type	T (°C)	Classification (Fig 1)	Experimental media	K	n	Drug Delivery System
COT	37	D	Deionized water	0,0860	0,2948	Fickian diffusion
	37	B	Physiological saline	0,3313	0,1288	Fickian diffusion
PA	37	D	Deionized water	0,0567	0,3805	Fickian diffusion
	37	B/C	Physiological saline	0,3159	0,1368	Fickian diffusion
PAC	37	D	Deionized water	2,9424	0,3109	Fickian diffusion
	37	B/C	Physiological saline	0,3734	0,1258	Fickian diffusion
PET	37	D	Deionized water	2,8987	0,3034	Fickian diffusion
	37	B/C	Physiological saline	0,3474	0,1335	Fickian diffusion

Considering the results obtained for all systems, it is very clear that the ibuprofen release is governed by a Fickian diffusion.

As the release mechanism of active principle follows a Fickian diffusion, the Higuchi Equation (3) governed by this mechanism and the approach of Korsenmeyer-Peppas (2) for plane surfaces have been assumed.

Using Eq. (2) and Eq. (3), it main parameters (expressed as apparent diffusion coefficients), K_H and D/δ^2 , respectively, have been calculated and are shown in Table 5.

Table 5. Estimated parameters applying Higuchi Equation (Eq. (3)) and Korsmeyer-Peppas equation approximation (Eq. (2)).

Fabric type	T (°C)	Experimental media	D/δ ²	K _H
COT	37	Deionized water	0.0002	0.0355
	37	Physiological saline	0.0036	0.1346
PA	37	Deionized water	0.0003	0.0383
	37	Physiological saline	0.0030	0.1240
PAC	37	Deionized water	0.1158	0.7678
	37	Physiological saline	0.0042	0.1460
PET	37	Deionized water	0.1031	0.7246
	37	Physiological saline	0.0037	0.1373

It can be observed that cotton and polyamide have a similar trend, because in both cases the apparent diffusion coefficient and the constant K_H have similar values in deionized water. In contrast, in the case of acrylic and polyester the results observed were quite distant from cotton and polyamide but being similar to each other. It seems that saline medium has not an influence in the different systems, because the results obtained were similar in all cases.

4. CONCLUSIONS

It has been demonstrated that the microencapsulation of ibuprofen it's possible, and it can be done by a procedure with a high percentage of efficiency, which had never been reported before.

Frequencies movements detected by FTIR could give an idea on the possible interactions between microspheres and ibuprofen by hydrogen bonds.

It can be demonstrated that the system has low homogeneity in particle size distribution and with the particle size average of 846,9 nm therefore they are microspheres.

The use of a Pad – dry technique promoted a desired permeation. However, in different fabrics, the pick-up obtained in dry conditions were different; it seems that the chemical affinity there is an important factor to be considered. The kinetic study carried out has allowed to determine the same drug delivery behaviour for all systems in each medium. All samples are governed by Fickian diffusion. In the case of cotton and polyamide have a similar trend, the mass transport has resulted similar in deionized water for both. In contrast, in the case of acrylic and polyester the results observed were quite distant from cotton and polyamide but being similar to each other. As a result, it has

been demonstrated that there is no influence of saline medium in the different systems because it was obtained similar results in all cases.

5. ACKNOWLEDGEMENTS

The authors wish to thank the Spanish National Project (Ministerio de Educación y Ciencia) CTQ-PPQ2009-13967-C03-01 for the financial support.

6. REFERENCES

- [1] Wang B, Siahaan T, Soltero R (2005) Drug delivery: principles and applications. Wiley-Interscience, New Jersey.
- [2] Saez V, Hernández J. R, Peniche C (2007) Las Microesferas como sistemas de liberación controlada de péptidos y proteínas. *Biotecnología Aplicada* V 24 98-107.
- [3] Bertram J. P, Jay S.M, Hynes S.R, Robinson R, Criscione J.M, Lavik E.B (2009) Functionalized poly(lactic-co-glycolic acid) enhances drug delivery and provides chemical moieties for surface engineering while preserving biocompatibility. *Acta Biomaterialia* V 5 2860-2871.
- [4] Sáez V, Hernáez E, Angulo L.S (2004) Mecanismos de liberación de fármacos desde materiales polímeros. *Revista Iberoamericana de Polímeros* V 5 55-69.
- [5] Sáez V, Hernáez E, Angulo L.S (2002) Sistemas de liberación controlada de medicamentos. *Revista Iberoamericana de Polímeros* V 3 1-17.
- [6] Sáez V, Hernández J.R, Peniche C (2007) Las Microesferas como sistemas de liberación controlada de péptidos y proteínas. *Biotecnología Aplicada* V 24 98-107.
- [7] Sáez V, Hernáez E, Angulo L.S, Katime I (2004) Liberación controlada de fármacos. Micropartículas. *Revista Iberoamericana de Polímeros* V 5 87-101.
- [8] Kantor, T.G (1979) Ibuprofen. *Ann. Intern. Med* V 91 877–882.
- [9] Mathiowitz E (1999) Pharmacy – Encyclopedia Of Controlled Drug Delivery V 1&2. Wiley-Interscience, Providence, Rhode Island.
- [10] Siepmann J, Peppas N.A (2001) Modeling of drug release from delivery systems based on hydroxypropyl methylcellulose (HPMC). *Advanced Drug Delivery Reviews* V 48 139-157.

[11] Siepmann J, Kranz H, Bodmeier R, Peppas N. A (1999) HPMC – Matrices for Controlled Drug Delivery: A new Model Combining Diffusion, Swelling, and Dissolution Mechanisms and Predicting the Release Kinetics. *Pharmaceutical Research* V 16 n 11 1748- 1756.

[12] Abdekhodaie M. J, Cheng Y-L (1997) Diffusional release of a dispersed solute from planar and spherical matrices into finite external volume. *Journal of Controlled Release* V 43 175-182.

[13] Guisado García E.I, Gil Alegre M.E, Camacho Sanchez M.A, Torres Suárez A.I (2001) Estudio de solubilidad de ibuprofeno en medio acuoso: Elaboración de una formulación líquida de uso pediátrico. 162 VI Congreso SEFIG y tercera jornada Tecnología Farmacéutica 161-164.

[14] Galindo-Rodríguez S, Allémann E, Fessi H, Doelker E (2005) Versatility of three techniques for preparing ibuprofen-loaded methacrylic acid copolymer nanoparticles of controlled sizes. *Journal of Drug Delivery Science and Technology* V 15 n 5 347-354.

[15] Kawashima Y, Niwa T, Handa T, Takeuchi H, Iwamoto T, Itoh K (1989) Preparation of controlled-release microspheres of ibuprofen with acrylic polymers by a novel quasi-emulsion solvent diffusion method. *Journal of Pharmaceutical Science* V 78 68–72.

[16] Fu X, Ping Q, Gao Y (2005) Effects of formulation factors on encapsulation efficiency and release behavior in vitro of huperzine A-PLGA microspheres. *Journal of Microencapsulation* V 22 705-714.

[17] Wang C, Ye W, Zheng Y, Liu X, Tong Z (2007) Fabrication of drug-loaded biodegradable microcapsules for controlled release by combination of solvent evaporation and layer-by-layer self-assembly. *International Journal of Pharmaceutics* V 338 165-173.

[18] Matkovic S. R, Valle G. M, Galle M & Briand L. E (2004) Desarrollo y Validación del Análisis Cuantitativo de Ibuprofeno en Comprimidos por Espectroscopia Infrarroja. *Acta Farmacéutica Bonaerense* V 23 527-32.

[19] Garrigues S, Gallignani M and De La Guardia M (1993) FIA-FT-IR determination of ibuprofen in pharmaceuticals. *Talanta* V40 89-93.

[20] Sádecká J, Cakrt M, Hercegorá A, Polonsk J and Skaáni I (2001) Determination of ibuprofen and naproxen in tablets. *Journal of Pharmaceutical and Biomedical Analysis* V 25 881-891.

[21] Sheikh Hasan A, Socha M, Lamprecht A, El Ghazouani F, Sapin A, Hoffmana M, Maincent P, Ubrich N (2007) Effect of the microencapsulation of nanoparticles on the reduction of burst effect. *International Journal of Pharmaceutics* V 344 53–61.

[22] Leo E, Forni F, Bernabei M. T (2000) Surface drug removal from ibuprofen-loaded PLA microspheres. *International Journal of Pharmaceutics* V 196 1–9.

[23] Baruch L, Benny O, Gilert A, Ukobnik M, Ben Itzhak O, Machluf M (2009) Alginate-PLL cell encapsulation system Co-entrapping PLGA-microspheres for the continuous release of anti-inflammatory drugs. *Biomed Microdevices* V 11 1103–1113.

[24] Yang Y. Y, Chia H.H, Chung T.S (2000) Effect of preparation temperature on the characteristics and release profiles of PLGA microspheres containing protein fabricated by double-emulsion solvent extraction/ evaporation method. *Journal of Controlled Release* V 69 81-96.

TO BE SUBMITTED

CONTROLLED RELEASE SYSTEM OF CAFFEINE IN PLGA MICROSPHERES

Carreras¹, N., Parés¹, I., Martí², M., Lis³, M.J.

(1) Polytechnic University of Catalonia – Department of Chemical Engineering, Colom 1, 08222 Terrassa, Barcelona, Spain.

(2) Institut de Química Avançada de Catalunya, (IQAC-CSIC), Jordi Girona 18-26, 08034 Barcelona, Spain

(3) INTEXTER-UPC. Polquitex Research Group. Colom, 15, 08222 Terrassa, Barcelona, Spain

Corresponding Author: Núria Carreras Parera

E-mail address: nuria.carreras@gmail.com

Telephone: 0034 93 739 80 45

FAX: 93 739 82 25

ABSTRACT

At the present time, there is a great interest in pharmaceutical technology focused on the development of biodegradable microparticles as a controlled release system. In this study, PLGA-microspheres containing caffeine were prepared using a water-in-oil-in-water (w/o/w) solvent evaporation procedure with poly(vinyl alcohol) as surfactant in the external aqueous phase. The microspheres obtained were characterized by the measure of encapsulation efficiency. The surface morphology and chemical structure of the microparticles were investigated using scanning electron microscopy (SEM) and Fourier transform infrared spectroscopy (FT-IR). For particle size distribution Zetasizer was used. The drug release system was analyzed, through samples of the treated textile fabric (cotton, polyamide, acrylic and polyester) by Pad-Dry technique. The fibers were submerged into thermostated vessels filled with two different mediums: deionized water and physiological saline. Release data were examined kinetically and the ideal kinetic models were estimated for caffeine release. The results showed a bimodal behavior by comparing the different media (water and saline) . It could only be assumed a Fickian Diffusion for short times.

Keywords: Microspheres; PLGA; caffeine; Drug release; Biomaterials.

1. INTRODUCTION

Poly(lactide-co-glycolide) (PLGA) is a biodegradable, biocompatible, non-toxic polymer that can be used as a functional material in studies in the field of life sciences. PLGA particles have been used commercially in the preparation of drug delivery system formulations [1,2].

In the last 20 years, biodegradable microspheres of biocompatible polymers as delivery systems for active agent have been studied. Generally, the drug is distributed in the polymer matrix and is released by two fundamental mechanisms: by diffusion through matrix, and polymer degradation, which leads to erosion of the particles. This has been used natural and synthetic polymers, among the latter highlights the copolymers of lactic acid and glycolic acid (PLGA) [3,4].

The term biomaterial includes all materials introduced into the body tissues for specific therapeutic purposes, diagnostic purposes or prevention. These materials must be biocompatible, which means that they should not cause any significant adverse response from physiological media that damage the biomaterial; after interaction with tissues and body fluids should biodegrade to nontoxic components, chemically and physically, or a combination of both [5,6].

The design and implementation of systems for controlled drug dosing and management systems located in the activity of a given drug is currently one of the most important aspects in the development of new forms of medication [7]. The main objective of the controlled release is simple: get the right amount of active agent, at the right time and right place. This release method is commonly used to prolong the therapeutic dose of effectively using a single dose, and to eliminate or minimize the concentrations exceeding the therapeutic requirements [8].

Release of core material from a non-erodible microparticle can occur in several ways. Fig 1 contains four theoretical curves (A, B, C and D) that describe four types of release behavior. All curves are plotted as percent drug released versus time.

Curve A represents the release behaviour of a perfect, non-erodible, spherical microcapsule which releases the encapsulated material by steady-state diffusion through a coating of uniform thickness. The rate of release remains constant as long as the internal and external concentrations of core material and the concentration gradient through the membrane are constant. If a finite time is needed to establish the initial, constant concentration gradient in the capsule wall membrane then there is a time lag in core material release. Curve A in Fig 1 displays a system with no time lag. If some of the encapsulated material migrates through the microcapsule membrane during storage, a burst effect occurs, as represented by Curve B. If the microcapsule acts as an inert matrix particle in which core material is dispersed (a microsphere), the Higuchi model is valid up to 60% release (3). In this case, a plot of percent drug released versus square-root time is linear, as shown by Curve C in Fig 1. First-order release is represented by Curve D. The curve is linear if log percent core material left in the capsule is plotted versus time [9].

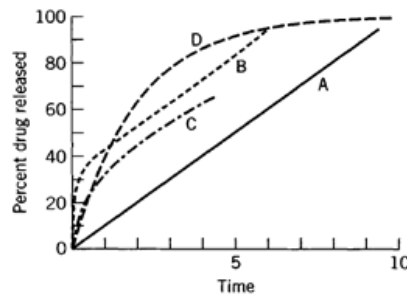


Fig 1. Theoretical release curves expected for different types of non-erodible delivery systems. A, Membrane reservoir-type free of lag time and burst effects; B, same as A, with burst effect; C, matrix or monolithic sphere with square root time-release; D, system with first-order release.

To predict the kinetics of release of a drug, it is necessary to know the exact mechanism of mass transport involving this release. Thus, several semi-empirical equations to describe the controlled release rate of a drug in a matrix system have been formulated. Power Law (1) combines two apparently independent processes, one due to the transport of the drug that obeys Fick's laws and the other to the swelling of the fiber, which involves the transition from a state semi-rigid (glass) to a more flexible (rubber),

$$\frac{M_t}{M_\infty} = k \cdot t^n \quad (1)$$

where M_t amount of drug released at time t , M_∞ the maximal amount of the released drug at infinite time, k is a constant incorporating structural and geometric characteristics of the device, and n is the release exponent, indicative of the mechanism of drug release, as can be seen in the table below:

Table I. Drug delivery models based on the parameter n

Exponent n			
Plane surface	Cylinder	Sphere	Drug Delivery Systems
0,5	0,45	0,43	Fickian Diffusion Mechanism
$0,5 < n < 1,0$	$0,45 < n < 0,89$	$0,43 < n < 0,85$	Anomalous Diffusion
1,0	0,89	0,85	Non-Fickian Diffusion Mechanism

Higuchi published the probably most famous and most often used mathematical equation (2) to describe the release rate of a drug in a planar system for short periods of release time:

$$\frac{M_t}{M_\infty} = K \cdot \sqrt{t} \quad (2)$$

The mass transport in swelling systems can be described by Fick's second Law, so the diffusion of the active principle can be studied as a plane surface for short time of liberation; through the Korsenmeyer-Peppas equation approximation (3), where D is the diffusion coefficient of drug release, and δ is the diffusional distance [10,11,12].

$$\frac{M_t}{M_\infty} = 4 \sqrt{\frac{D \cdot t}{\pi \cdot \delta^2}} \quad (3)$$

2. EXPERIMENTAL

2.1. Materials

PLGA had a copolymer ratio (lactic acid/glycolic acid) of 75/25 and a molecular mass (M_r) range of 5,000-15,000 from Aldrich. Caffeine anhydrous in powder with (M_r) 194.20 from Fluka. PVA (Poly(vinyl alcohol)), 87-89% hydrolyzed, with a (M_w) range of 31,000-50,000 from Aldrich. Dichloromethane stabilized with 20 ppm of amylene, supplied by Panreac.

Standard woven fabrics were used: Cotton fabric (COT) (Style 400, ISO 105-F02), polyamide fabric (PA) (Style 361, ISO 105-F03), acrylic fabric (PAC) (Style 864, ISO 105-F05) and polyester fabric (PET) (Style 777, ISO 105-F04).

All chemicals used were of analytical grade.

2.2. Preparation of microspheres

The microspheres were performed by a $w_1/o/w_2$ emulsion using the conventional solvent evaporation method. Briefly, PLGA and caffeine (3:1) were separately dissolved in methylene chloride and water, respectively. The simple emulsion (w/o) was generated by mechanical agitation (Ultra-turrax T25, IKA) for several minutes at 24000 rpm. Afterwards, this simple emulsion was added to a continuous phase, constituted of 150 ml aqueous solution of PVA (2% w/w) and emulsified for several minutes at 24000 rpm, resulting in a double emulsion (w/o/w). The mixture was maintained under agitation at 400 rpm (8h) leading to the solvent evaporation and consequently the microsphere formation. The method used was carried out at 4°C [13,14,15].

2.3. Characterization of caffeine loaded-microspheres

For the characterization of the obtained microspheres, 4 tests were done: Scanning Electron Microscopy (SEM), Encapsulation Efficiency, Fourier Transform Infrared Spectroscopy (FTIR) and Particle Size Distribution.

2.3.1. Encapsulation efficiency

The encapsulation efficiency of caffeine in PLGA-microspheres was detected indirectly in the liquid phase by UV/Vis Spectrophotometer (Shimadzu UV-2401 PC) after centrifugation for several minutes. The ratio of amount of caffeine entrapped in the dispersion was calculated.

2.3.2. Fourier transform infrared spectroscopy (FTIR)

FTIR spectra were collected on a FTIR Avatar System 320 by preparing KBr pellets using a sample concentration of 1% (w/w). Spectra were recorded between 500 and 4000 cm^{-1} at a resolution of 4 cm^{-1} and by coadding 20 scans.

2.3.3. Scanning electron microscopy (SEM)

The analyzed samples correspond to the treated fibers. The morphology of microspheres was investigated using a SEM (Model JSM-5610 Series, JEOL, Tokyo, Japan). Samples were coated with a thin layer of sputtered gold prior to examination.

2.3.4. Particle size distribution

The size distribution of microspheres was measured using a Zetasizer (Model Nano-ZS Series, Malvern). Microsphere samples were introduced into a DTS1060C – Clear disposable zeta cell and water was used as a dispersant at 25°C. The results were reported as an intensity size distribution.

2.4. Impregnation of microspheres on textile substrates

Microspheres were applied onto fabrics 25x40 cm^2 using Pad-Dry technique (ERNST BENZ AG KLD-HT and KTF/m250) and followed by a process of drying at room temperature, with the padding pressure to obtain a pick-up of 80±5%, from the microencapsulation formulations. The treated fabric samples were finally conditioned at 20±2°C and 60±5% relative humidity for 24 hours. The conditions required for this procedure are shown in the table below:

Table II. Conditions of textile impregnation process

FINISHING CONDITIONS	
SUBSTRATE	Fabric Cotton/Polyamide/Acrylic/Polyester

FABRIC DIMENSIONS	25 x 40 cm ²
LIQUOR RATIO	3 – 5 L/Kg
PICK-UP	80-90%
DRYING CONDITIONS	Room temperature

2.5. Drug Release study

To analyze the kinetic release of active compounds, samples of 1 g of the treated fabric were submerged into the thermostated vessels filled with deionized water and physiological saline at infinite bath conditions at a temperature of 37°C. This analysis aims to study the environmental effects on the drug release systems, for instance the effect of saline medium (physiological saline), simulating the skin's sweat. The amount of active principle realized to the bath was determinate by UV/Vis Spectrophotometer at different times.

3. RESULTS AND DISCUSSION

After loaded-microspheres preparation with caffeine, different parameters were analyzed to characterize the microspheres.

3.1. Scanning Electron Microscopy (SEM)

Treated fabrics with microspheres have been analyzed by SEM. SEM micrographs confirmed that the adhesion between fabrics and, either caffeine microspheres or empty microspheres was effective, as can be observed in Fig 2. Both kind of microspheres have a spherical shape with a smooth surface composed of polyvinyl alcohol (PVA).

The cross-sectional picture as shown in Fig 2, it is clear that although internally the microspheres are all highly porous, thus causing an increase in the control of the dosage of the active principle, there are no distinct hollow cores. Porosity of microspheres is known to vary with numerous factors such as polymer molecular mass, co-solvent concentration, dispersed phase to continuous phase (DP/CP) ratio, active principle concentration, solvent removal rate as well as method. The absence of core formation could be due to the presence of emulsifier in the inner aqueous phase, which prevents coalescence of the internal water droplets [16].

There is variety of sizes of microparticles because is not possible to control, over the experimental procedure, the drop size at the time of the addition of an emulsion in another. This causes the particle size obtained is random and not get a uniform size.

The non-presence of caffeine crystals attached to fabric, leading to consider that the methodology used to encapsulate caffeine is perfect.

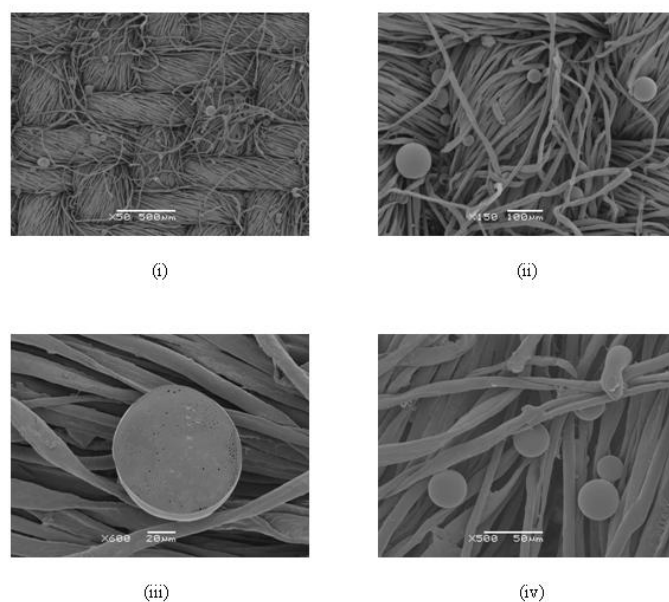


Fig 2. Scanning electron micrographs of microspheres on cotton fabric. (i) microspheres with caffeine (x50) (ii) microspheres with caffeine (x50). (iii) cross-sectional picture of caffeine microspheres (x600). (iv) microspheres without caffeine (x500).

3.2. Encapsulation efficiency

Table III shows the results of caffeine encapsulation efficiencies after centrifugation and the overall average is about 28%. Encapsulation efficiencies achieved are remarkably low [15,17,18] and there is no literature to compare them with other encapsulation efficiencies and to establish whether methodology followed is optimal or not.

Table III. Encapsulation efficiency of the microspheres

Sample	Encapsulation efficiency (%)
1	27,97
2	27,89
3	27,97

Therefore, further studies are needed to achieve stabilization of the caffeine in the polymer matrix, because of the greater affinity of this with the medium than with the polymer.

3.3. FTIR Analysis

FTIR analysis was carried out to verify the microsphere formation, to see if structural changes occur in these microspheres and to justify the possible interactions that can be to inside of them.

Fig 3 shows the FTIR spectrum of (a) PLGA polymer and (b) microspheres without caffeine. Several structural differences are apparent both characteristic frequencies movements of the components as defined in the characteristic peaks. The frequency of 1758.54 cm^{-1} belonging to the strain carbonyl group (C=O stretching) is part of PLGA, have a displacement and an increase in the bandwidth of the frequency (1736.53 cm^{-1}) in the spectrum of microspheres without caffeine. Similarly, the frequencies of the methyl group (1456.10 cm^{-1}) of PLGA moves and increases the bandwidth in the frequency of 1438.86 cm^{-1} for microspheres without caffeine. Also, note the minimum frequency shift of 1090.64 cm^{-1} (C-O-C asymmetric stretching) and 1272.84 cm^{-1} (C-H) belonging to the PLGA regarding frequencies of 1092.54 cm^{-1} (C-O-C asymmetric stretching) and 1273.84 cm^{-1} (C-H) microspheres without caffeine. Finally, the disappearance of the frequency of 1420.30 cm^{-1} (C-H deformation caused by the link -O-CH₂) of PLGA in the spectrum of the microspheres without caffeine.

These structural changes suggest that the PLGA polymer goes being a linear chain to close and thus form a polymer matrix.

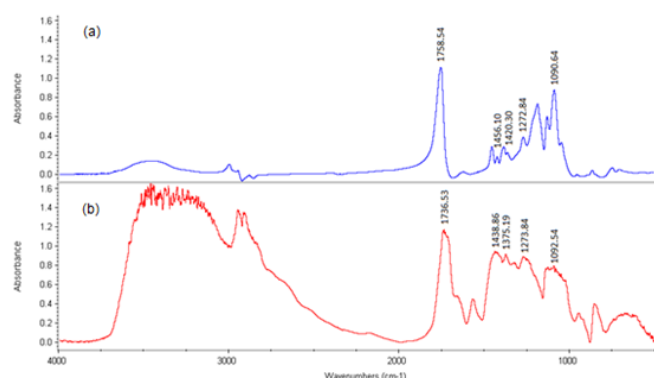


Fig 3. FTIR spectrum of (a) PLGA polymer and (b) microspheres without caffeine.

Fig 4 shows the FTIR spectrum of (a) caffeine microspheres and (b) caffeine. Comparing the spectrum of caffeine with caffeine microspheres encapsulated in PLGA, many structural differences represented by the displacements of the characteristic frequencies of the components can be seen. In the frequency of 1701.53 cm^{-1} , belonging to the tension of the carbonyl group (C=O stretching) as part of caffeine, there is a movement and an increased bandwidth of the frequency (1736.28 cm^{-1}) in the spectrum microspheres containing caffeine. Another import peak to note is 1661.58 cm^{-1} (C = N stretching) in the spectrum of caffeine is very significant on the

microspheres with caffeine. Moreover, the latter suffers a slight shift to a frequency of 1654.67 cm^{-1} . This move could give an idea of the possible interaction in the form of bridges between the oxygen atoms of carbonyl groups and nitrogen that has caffeine. Most important frequencies to emphasize that are part of the structure of caffeine and, as in previous cases, identify the peaks corresponding displacements, such as: CH_3 asymmetric bend (1456.4 cm^{-1} , 1431.23 cm^{-1} and 1359.64 cm^{-1}), the C-N stretching (1286.53 cm^{-1}) and cyclic C = N tension (1550.29 cm^{-1}).

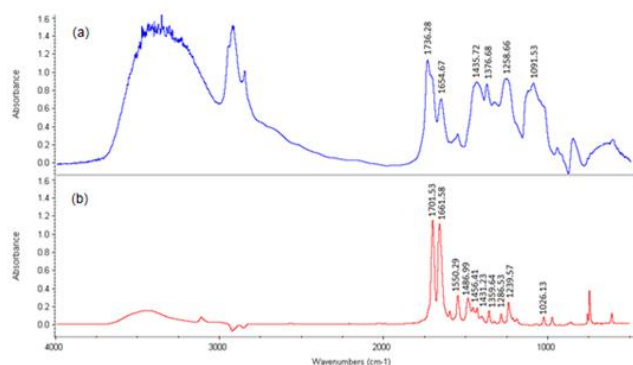


Fig 4. FTIR spectrum of (a) caffeine microspheres and (b) caffeine.

3.4. Particle size distribution

The size of microparticles can be easily affected by a variety of processing factors, such as volume of inner and external aqueous phase and the viscosity of inner and external aqueous phase. Increase in the molecular mass of polymer also leads to the size of microspheres increases [16].

Fig 5 shows three different size distributions belonging to caffeine microspheres. The most important of them is about 87.5% intensity and the average particle diameter is 159.1 nm.

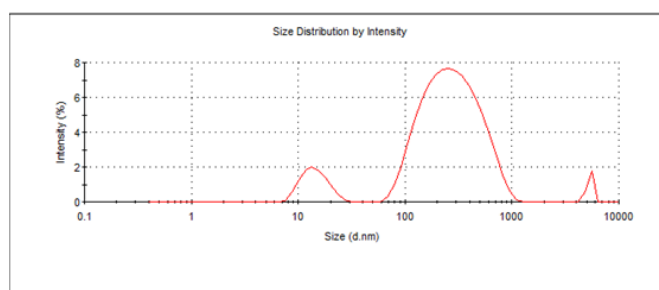


Fig 5. Size distribution by intensity of caffeine microspheres.

About microspheres without caffeine (Fig 6), two similar intensities were obtained, 47.8 and 43.6%. The average particle diameter is 760.4 nm.

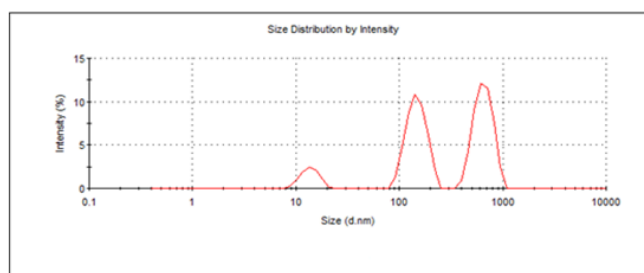


Fig 6. Size distribution by intensity of microspheres without caffeine.

These results show that both of them are less than 1 μm , this implies that the achieved microspheres are not microspheres, but nanospheres.

3.5. Impregnation of microspheres on textile substrate

Microspheres solution was applied onto fabrics 25x40 cm^2 using Pad-Dry technique. The results belonging to % by weight (dry) of various treated fabrics differ significantly compared with the % permeation of these in the solution of microspheres, as shown in Table IV.

Table IV. Results of the finishing process of several textile fabrics: % pick-up and the theoretical percentage of product present in the wet fabrics after impregnation; and % o.w.f. (on weight of fibres) of product applied, calculated by weight difference between dry non-treated textile and dry textile after Pad-Dry process.

Textile	% Pick-up* (% theoretical product)	% o.w.f.* Dry product applied
COT	83.37	2.37
PA	80.94	1.75
PAC	82.49	1.98
PET	81.21	1.26

This implies that the fabrics absorb the solution of microspheres. However, in dry, few microspheres remain attached to them, probably caused by a lack of affinity in the system. Another important fact can be the influence of medium due to such low encapsulation efficiencies obtained.

Fabric has a higher percentage by weight (dry) is the cotton. Cotton is a hydrophilic fiber with the same ability as to absorb as to desorb. The polyester fabric is the contrary of cotton because is the most hydrophobic synthetic fabric. Lastly, there are the fabrics of polyamide and acrylic, although the last has a higher weight percent (dry) than the polyamide fabric, it is the most hydrophobic of each other.

3.6. Theoretical mechanisms of Drug Release

The results obtained on the kinetic release profiles for all treated fabric samples (PA COT, PA, PAC and PET) in deionized water and physiological saline are graphically plotted in Figures 7 to 10.

The caffeine release from PLGA-microspheres of all treated fabric samples (COT, PA, PAC and PET) are characterized by a bimodal behavior depending on the medias as shown in following figures.

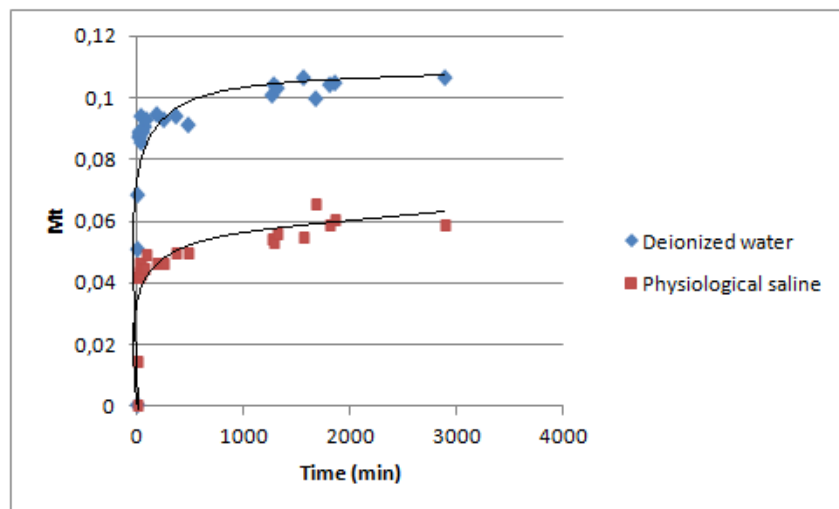


Fig 7. Kinetic release of caffeine microspheres applied onto cotton fabric at 37°C according the experimental media. M_t (g caffeine/ g fabric).

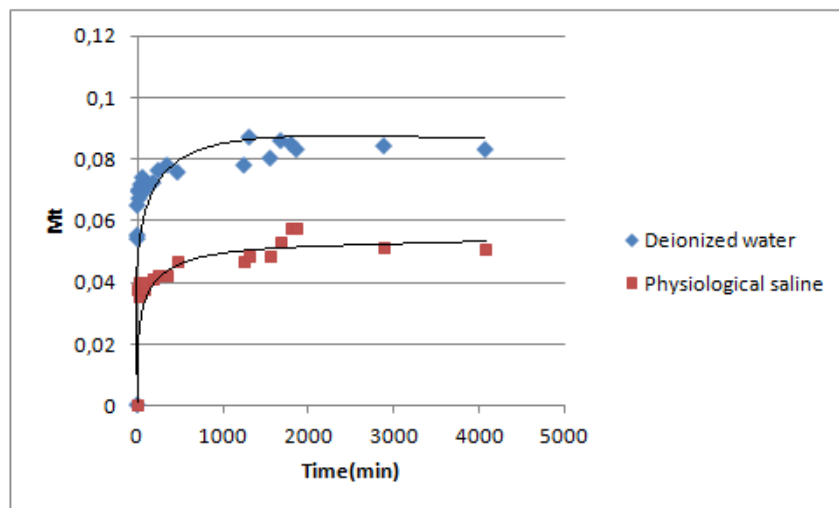


Fig 8. Kinetic release of caffeine microspheres applied onto polyamide fabric at 37°C according the experimental media. M_t (g caffeine/ g fabric).

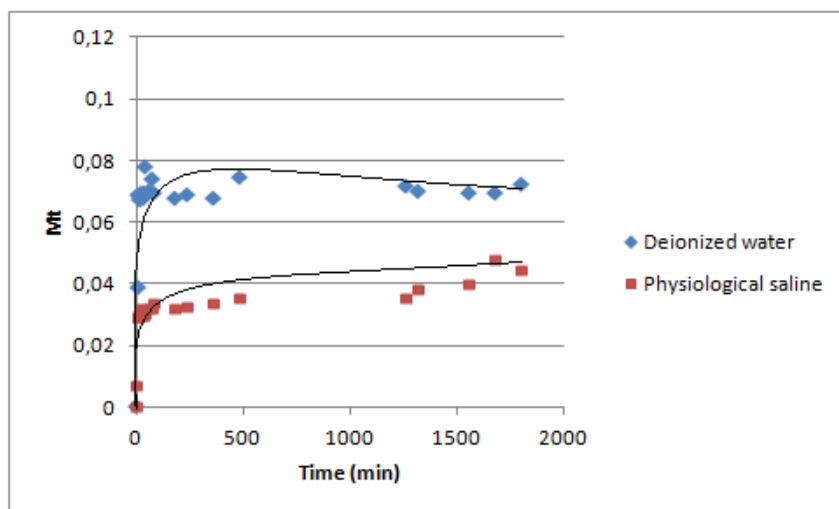


Fig 9. Kinetic release of caffeine microspheres applied onto acrylic fabric at 37°C according the experimental media. M_t (g caffeine/ g fabric).

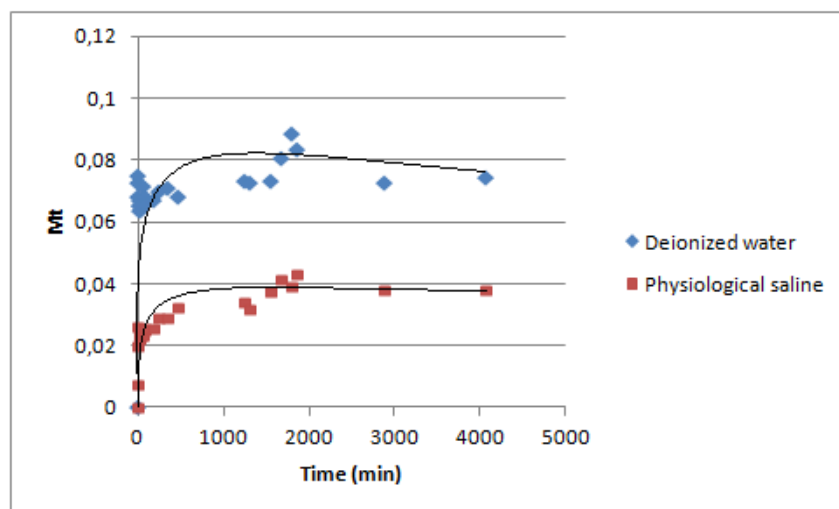


Fig 10. Kinetic release of caffeine microspheres applied onto polyester fabric at 37°C according the experimental media. M_t (g caffeine/ g fabric).

It can be demonstrated that there are big differences in the amount of active principle released. In the case of cotton the released active principle was higher than in the other fabrics, in both mediums. However, synthetic fabrics showed released amounts of active principle were similar between each other, therefore it can be considered that the nature of fabrics may influence on the delivery system.

In all different textiles the caffeine release to deionized water are faster than to physiological saline. This may be due to saline ions that interact with the system causing it to behave differently in each case.

Comparing the kinetic profiles from the theoretical curves (A, B, C and D) illustrated in Fig 1. The behavior of the different fabrics, regardless the mediums were similar to the

theoretical curve B/D. This bimodal kinetic profile could be explained by a burst effect and a part of the drug entrapped in the polymeric matrix, which requires a longer time for degradation [17,19].

Several semi-empirical equations to describe the controlled release rate of caffeine in deionized water and physiological saline were analyzed.

3.7. Power Law

As mentioned in the Introduction, fabrics have two behaviors and were treated in two steps, short times (K_1) and long times (K_2). Using Eq. (1), the value of the exponent n , indicative of mass transport mechanism was calculated. Therefore, the most release mechanism of caffeine from PLGA-microspheres of all samples was governed by Fickian diffusion, as shown in Table V. Except for acrylic that is an anomalous delivery in physiological saline medium.

Table V. Estimated parameters, short times (K_1) and n values obtained from fitting drug release experimental data to Power Law (Eq. (1)).

Fabric type	T (°C)	Classification (Fig 1)	Experimental media	K_1	n_1	Drug Delivery System
COT	37	B/D	Deionized water	0.4676	0.2273	Fickian diffusion
	37	B/D	Physiological saline	0.2371	0.4909	Fickian diffusion
PA	37	B/D	Deionized water	0.5981	0.0881	Fickian diffusion
	37	B/D	Physiological saline	0.4826	0.0913	Fickian diffusion
PAC	37	B/D	Deionized water	0.5064	0.2588	Fickian diffusion
	37	B/D	Physiological saline	0.1467	0.6825	Anomalous diffusion
PET	37	B/D	Deionized water	0.6786	0.0265	Fickian diffusion
	37	B/D	Physiological saline	0.3929	0.1070	Fickian diffusion

Table VI. Estimated parameters, long times (K_2) and n_2 values obtained from fitting drug release experimental data to Power Law (Eq. (1)).

Fabric type	T (°C)	Classification (Fig 1)	Experimental media	K_2	n_2	Drug Delivery System
COT	37	B/D	Deionized water	0,7276	0,0382	Fickian diffusion
	37	B/D	Physiological saline	0,5487	0,0620	Fickian diffusion
PA	37	B/D	Deionized water	0,6979	0,0390	Fickian diffusion
	37	B/D	Physiological saline	-	-	-
PAC	37	B/D	Deionized water	0,8270	0,0142	Fickian diffusion
	37	B/D	Physiological saline	0,4953	0,0642	Anomalous diffusion
PET	37	B/D	Deionized water	-	-	-
	37	B/D	Physiological saline	0,1902	0,4714	Fickian diffusion

In long times, the mechanism of caffeine delivery is governed by Fickian diffusion as shown Table VI. And again, except for acrylic that is an anomalous delivery in physiological saline medium.

3.8. Korsenmeyer-Peppas equation approximation and Higuchi model for a planar matrix

As the release mechanism of active principle follows a Fickian diffusion, the Higuchi equation governed by this mechanism and the approach of Korsenmeyer-Peppas for plane surfaces have been proposed. The parameters were obtained from these equations for each treated fabric, and according to the experimental media are shown in Table VII.

Table VII. Estimated parameters applying Higuchi's equation (Eq. (2)) and Korsmeyer-Peppas equation approximation (Eq. (3)).

Fabric type	T (°C)	Experimental media	D/δ^2	K_H
COT	37	Deionized water	0.0116	0.2429
	37	Physiological saline	0.0162	0.2875
PA	37	Deionized water	0.0084	0.2072
	37	Physiological saline	0.0070	0.1893
PAC	37	Deionized water	0.0289	0.3836
	37	Physiological saline	0.0137	0.2639
PET	37	Deionized water	0.0264	0.3663
	37	Physiological saline	0.0079	0.2004

The results from Table VII show that in the case of PAC and PET fabrics, the experimental medium most conducive to the mass transport of caffeine, and the constant K, is deionized water. The PAC fabric has the high mass transfer coefficient, closely followed by PET fabric. Therefore, one can say who have a behavior and a similar trend as seen in the qualitative analysis of the same, being the two most hydrophobic tissue while COT and PA the most hydrophilic. COT and PA do not follow the same trend as those of PAC and PES. As PA deionized water medium in the middle of the mass transfer coefficient and the constant K is greater than in saline, although much lower values than those of PAC and PES for COT is quite the opposite. The effect of mediums is important because the kinetic parameters are different. The mass transfer coefficient is lower in deionized water than physiological saline. The release of caffeine may be inhibited, due to some interactions between fiber carboxyl groups and ions of physiological saline [20], like is the case of PA and PET. This makes sense in COT and PAC have higher values than others, because do not have carbonyl groups in their chemical structures.

4. CONCLUSIONS

PLGA microspheres containing caffeine were obtained by a w/o/w double-emulsion solvent evaporation technique. The encapsulation efficiency of caffeine was low, leading to further studies to improve these efficiencies. Frequencies movements could give an idea of the possible interaction in form of bridges between the oxygen atoms of

carbonyl groups and nitrogen that has caffeine. Microspheres have a spherical shape, a smooth surface produced by polyvinyl alcohol (PVA) and are internally highly porous, thus causing an increase in the control of the dosage of the active principle. It is necessary to get a relative homogeneity in the size distribution of particles and so, to achieve efficient results. Pad-dry technique causes a desired permeation control and, therefore, is a simple technique that allows the application of the desired amount of fabric products. The kinetic study determined a bimodal behavior and the medium significantly affects to drug release system.

5. ACKNOWLEDGEMENTS

The authors wish to thank the Spanish National Project (Ministerio de Educación y Ciencia) CTQ-PPQ2009-13967-C03-01 for the financial support.

6. REFERENCES

- [1] F. Ito, Y. Uchida, Y. Murakami. Facile technique for preparing organic-inorganic composite particles: Monodisperse poly(lactide-co-glycolide) (PLGA) particles having silica nanoparticles on the surface, *Colloids and Surfaces A: Physicochemical and Engineering Aspects*, 361 (2010) 109-117.
- [2] R.A. Jain. The manufacturing techniques of various drug loaded biodegradable poly(lactide-co-glycolide) (PLGA) devices, *Biomaterials*, 21 (2000) 2475-2490.
- [3] V. Sáez, J.R. Hernández, C. Peniche. Las Microesferas como sistemas de liberación controlada de péptidos y proteínas, *Biotecnología Aplicada*, 24 (2007) 98-107.
- [4] N. Stivaktakis, K. Nikou, Z. Panagi, A. Beletsi, L. Leondiadis, K. Avgoustakis. PLA and PLGA microspheres of β -galactosidase: Effect of formulation factors on protein antigenicity and immunogenicity, *Wiley Periodicals Inc.*, 3 (2004) 139-148.
- [5] V. Sáez, E. Hernáez, L.S. Angulo, I. Katime. Liberación controlada de fármacos. Micropartículas, *Revista Iberoamericana de Polímeros*, 5 (2004) 87-101.
- [6] J.P. Bertram, S.M. Jay, S.R. Hynes, R. Robinson, J.M. Criscione, E.B. Lavik. Functionalized poly(lactic-co-glycolic acid) enhances drug delivery and provides chemical moieties for surface engineering while preserving biocompatibility, *Acta Biomaterialia*, 5 (2009) 2860-2871.
- [7] V. Sáez, E. Hernáez, L.S. Angulo. Mecanismos de liberación de fármacos desde materiales polímeros, *Revista Iberoamericana de Polímeros*, 5 (2004) 55-69.

- [8] V. Sáez, E. Hernáez, L.S. Angulo. Sistemas de liberación controlada de medicamentos, *Revista Iberoamericana de Polímeros*, 3 (2002) 1-17.
- [9] Pharmacy – *Encyclopedia Of Controlled Drug Delivery*, 1&2 (1999) 495-497.
- [10] J. Siepmann, N.A. Peppas, Modeling of drug release from delivery systems based on hydroxypropyl methylcellulose (HPMC), *Advanced Drug Delivery Reviews*, 48 (2001) 139-157.
- [11] J. Siepmann, H. Kranz, R. Bodmeier, N. A. Peppas, HPMC – Matrices for Controlled Drug Delivery: A new Model Combining Diffusion, Swelling, and Dissolution Mechanisms and Predicting the Release Kinetics, *Pharmaceutical Research*, 16, n 11, (1999), 1748- 1756
- [12] M. J. Abdekhodaie, Y. – L. Cheng, Diffusional release of a dispersed solute from planar and spherical matrices into finite external volume, *Journal of Controlled Release*, 43, (1997) 175-182.
- [13] Y.W. Yang, P. Y.J. Hsu, The effect of poly(D,L-lactide-co-glycolide) microparticles with polyelectrolyte self-assembled multilayer surfaces on the cross-presentation of exogenous antigens, *Biomaterials*, 29 (2008) 2516-2526.
- [14] C. Wischke, D. Lorenzen, J. Zimmermann, H. H. Borchert, Preparation of protein loaded poly(D,L-lactide-co-glycolide) microparticles for the antigen delivery to dendritic cells using a static micromixer. *European Journal of Pharmaceutics and Biopharmaceutics*, 62 (2006) 247-253.
- [15] X. Fu, Q. Ping, Y. Gao, Effects of formulation factors on encapsulation efficiency and release behavior in vitro of huperzine A-PLGA microspheres, *Journal of Microencapsulation*, 22 (2005) 705-714.
- [16] Y.Y. Yang, H.H. Chia, T.S. Chung, Effect of preparation temperature on the characteristics and release profiles of PLGA microspheres containing protein fabricated by double-emulsion solvent extraction/ evaporation method, *Journal of Controlled Release*, 69 (2000) 81-96.
- [17] R.M. Ribeiro-Costa, A.J. Alves, N.P. Santos, S.C. Nascimento, E.C.P. Gonçalves, N.H. Silva, N.K. Honda, N.S. Santos-Magalhaes. In vitro and in vivo properties of usnic acid encapsulated into PLGA-microspheres, *Journal of Microencapsulation*, 21 (2004) 371-384.

[18] C. Wang, W. Ye, Y. Zheng, X. Liu, Z. Tong. Fabrication of drug-loaded biodegradable microcapsules for controlled release by combination of solvent evaporation and layer-by-layer self-assembly, *International Journal of Pharmaceutics*, 338 (2007) 165-173.

[19] B.S. Zolnik, P.E. Leary, D.J. Burgess. Elevated temperature accelerated release testing of PLGA microspheres, *Journal of Controlled Release*, 112 (2006) 293-300.

[20] J.E. Rosas, J.L. Pedraz. Microesferas de PLGA: un sistema para la liberación controlada de moléculas con actividad inmunogénica, *Rev. Colomb. Cienc. Quim. Farm.* 36 (2007) 134-153.

TO BE SUBMITTED

**DRUG RELEASE FROM MICROCAPSULES EMBEDDED IN BIOFUNCTIONAL
TEXTILES**

**Carreras, N.¹, Valldeperas, J., Rodríguez, R., Martí, M., Coderch, L.^{*}, Parra, J.L.^{*}
and Lis, M.J.**

*INTEXTER-UPC. Polquitex Research Group. Colom, 15, 08222
Terrassa.Barcelona.Spain*

()Institut de Química Avançada de Catalunya, (IQAC-CSIC), Jordi Girona 18-26,
08034 Barcelona, Spain*

Corresponding Author ¹: Núria Carreras Parera

E-mail address: nuria.carreras@gmail.com

Telephone: 0034 93 739 80 45

FAX: 93 739 82 25

ABSTRACT

Current technology of microencapsulation has enabled the production of biofunctional textiles. These textiles are able to release drugs or cosmetics to the skin. This technology is based on empirical procedure that are limited to applications high value-added, such as medicine field for drug delivery. A quantitative analysis based on physico-chemical principles can allow the generation of new technologies.

In this work, after the foulard application of a microencapsulated active principle, a sun filter, ethyl hexyl methoxycinnamate (EHMC), into microcapsules, onto different fabrics (polyamide, acrylic, and polyester), the drug delivery system was analyzed, through samples of the treated fiber that were submerged into a thermostated vessels with deionised water at semi infinite bath conditions. The amount of active principle delivered to the bath was determined by UV-Visible Spectrophotometry. The determination of the exact amount of active principle present in the fabric samples was assessed by a previous ultrasound bath extractions and an analytical sun filter detection from the extracted baths by HPLC.

From the results obtained, it can be concluded that the sun filter delivery is clearly related with the existing gradient of concentration in the sample following a mechanism of Fickiag diffusion.

Keywords: Microcapsules; Ethyl hexyl methoxycinnamate (EHMC); Biofunctional textiles; Drug release;

INTRODUCTION

The science of drug release may be described as the application of chemical and biological principles to control the *in vivo* temporal and spatial location of drug molecules for clinical benefit. When drugs are administered, only a very small fraction of the dose actually hits the relevant receptors or sites of action, and most of the dose is actually wasted either by being taken up into the “wrong” tissue, removed from the “right” tissue too quickly, or destroyed en route before arrival. [1, 2]

Today's world requires that drug delivery systems be precise in their control of drug distribution. Moreover, many drugs are difficult to taking because they must be delivered slowly over a prolonged period to have a beneficial effect.

The design and implementation of systems for controlled drug dosing and management systems located in the activity of a given drug is currently one of the most important aspects in the development of news forms o medication [3]. The main objective of the controlled release is simple: get the right amount of active agent, at the right time and right place. This release method is commonly used to prolong the therapeutic dose of effectively using a single dose, and to eliminate or minimize the concentrations exceeding the therapeutic requirements [4].

Actual capsule release data have been plotted for all of the described ways and analyzed in terms of the appropriate model. Good agreement between actual results and assorted model release curves may exist for some portion of the release curve, but significant deviations occur often. Release of core material from a non-erodible microcapsule can occur in several ways. Figure 1 contains four theoretical curves (A, B, C, and D) that describe four types of release behaviour. All curves are plotted as percent drug released versus time.

Curve A represents the release behaviour of a perfect, non-erodible, spherical microcapsule which releases the encapsulated material by steady-state diffusion through a coating of uniform thickness. The rate of release remains constant as long as the internal and external concentrations of core material and the concentration gradient through the membrane are constant. If a finite time is needed to establish the initial, constant concentration gradient in the capsule wall membrane then there is a time lag in core material release. Curve A in Figure 1 displays a system with no time lag. If some of the encapsulated material migrates through the microcapsule membrane during storage, a burst effect occurs, as represented by Curve B. If the microcapsule acts as an inert matrix particle in which core material is dispersed (a microsphere), the Higuchi model is valid up to 60% release (3). In this case, a plot of percent drug released versus square-root time is linear, as shown by Curve C in Figure 1. First-order release is represented by Curve D. The curve is linear if log percent core material left in the capsule is plotted versus time. [5]

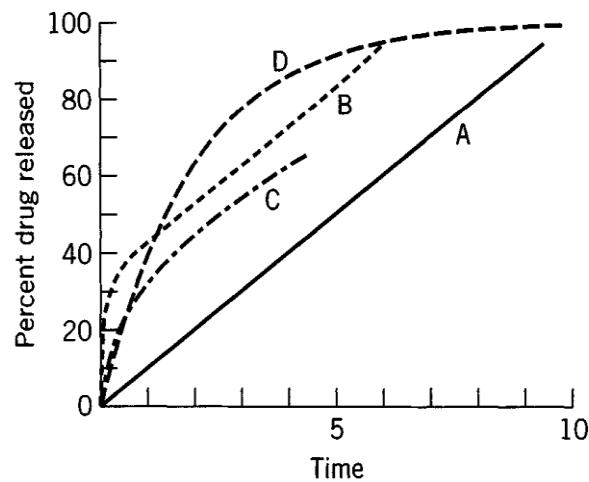


Figure 1. Theoretical release curves expected for different types of nonrodible delivery systems. A, Membrane reservoir-type free of lag time and burst effects; B, same as A, with burst effects; C, matrix or monolithic sphere with square root time-release; D, system with first-order release.

The Korsenmeyer-Peppas equation (1) is used to account for the coupled effects of Fickian diffusion and viscoelastic relaxation in polymer systems, including both processes,

$$\frac{M_t}{M_\infty} = k \cdot t^n \quad (1)$$

where M_t amount of drug released at time t , M_∞ the maximal amount of the released drug at infinite time, k is the rate constant of drug release, n is a diffusional exponent that depends on the system geometry and its value is indicative of the release mechanism of the active principle.

Eq (1) has been used frequently in the literature to describe the relative importance of transport mechanisms as shown in Table I. [5][6][7][8]

Table 1. Drug delivery models based on the parameter n .

N	Drug Delivery Systems
$n \leq 0,5$	Fickian Diffusion Mechanism
$0,5 < n < 1$	Anomalous Diffusion
$n \geq 1$	Non-fickian Diffusion Mechanism (zero-order model)

Higuchi published the probably most famous and most often used mathematical equation to describe the release rate of drugs from matrix systems. Initially valid only for planar matrix was later modified and extended to consider different geometries and matrix characteristics. The classical Higuchi equation was derived under pseudo-steady state assumptions and generally cannot be applied to real controlled release systems. This equation can be expressed as:

$$\frac{M_t}{M_\infty} = K\sqrt{t} \quad (2)$$

In addition, a proportionality between the fractional amount of drug released and the square root of time can as well be derived from an exact solution of Fick's second Law. So the diffusion of the active principle can be studied as a plane surface for short times of liberation, where D is the diffusion coefficient of drug release, and δ is the thickness of thin films under perfect sink conditions, can be expressed as follows [10-12]:

$$\frac{M_t}{M_\infty} = 4 \left(\frac{Dt}{\pi\delta^2} \right)^{1/2} = K\sqrt{t} \quad (3)$$

Thus, a proportionality between the fraction of drug released and the square root of time can also be based on these physical circumstances which are substantially different from those studied by Higuchi for the derivation of his classical equation.

The main objective of this study has been to evaluate the diffusion system with mathematical kinetic models, for the drug release from textiles treated with microcapsules systems which contains an active agent such as Ethyl Hexyl Methoxycinnamate (EHMC).

2. EXPERIMENTAL

2.1 Materials

Standard woven fabrics were used: Polyamide fabric (PA) (Style 361, ISO 105-F03), polyester fabric (PET) (Style 777, ISO 105-F04), and acrylic fabric (PAC) (Style 864, ISO 105-F05) from Test Fabrics Inc (USA).

Microcapsules (38% EHMC, 56.8% water) from Lipotec Group (Gavà, Spain) were prepared by o/w emulsion with a shield of silicic acid and xanthan gum for an external

wall. Principal parameters of the microcapsules were determined by a Zeta-sizer Nano-ZS (Malvern, U.K.), obtaining an average diameter of them of 936.7 nm (Standard deviation 7.3 nm) and an average zeta potential of -37.8 mV (standard deviation 9.2 mV)

All chemicals used were of analytical grade.

2.2 Treatment of the fabrics with microcapsules

All fabrics samples (PA, PAC and PET) were conditioned under standard atmospheric pressure at $20\pm 2^{\circ}\text{C}$ and $60\pm 5\%$ relative humidity for 24 hours prior to application. Microcapsules were applied onto fabrics $25 \times 40 \text{ cm}^2$ at 20% of solution (7.6 % EHMC) and pH 4.1.

The application of microcapsules onto the fabrics was carried out by a pad-dry technique that consists on foulard with diffusion and fixation by dry. It was followed by a process of drying in the Laboratory Stenter (ERNST BENZ AG KLD-HT and KTF/m250), with the padding pressure to obtain a pick-up of $80\pm 5\%$, from the microencapsulation formulations. Then the impregnated and squeezed fabrics were put into an air curing and heat –setting chamber and maintained at 47°C for 10 minutes. The treated fabric samples were finally conditioned at $20\pm 2^{\circ}\text{C}$ and $60\pm 5\%$ relative humidity for 24 hours before weighting and proceeding to other experiments.

2.3 Extraction methodology

Fabric samples about 1g were extracted by a Soxhlet using 100ml isopropanol/water (50/50), using a 1/100 liquor ratio for 1h at its boiling point (82.3°C). After the extraction textile samples were dried 48 hours in the same conditions (20°C and 60% RH) before weighted.

A Cary 300 Bio spectrophotometer (Varian, USA) was used to detect EHMC in an isopropanol/water (50/50 v/v) solution at the wavelength of 310 nm.

Calibration curves were used, employing microcapsules as standards, and the curves showed linearity over the concentration range of 0.05g/l to 0.5g/l in all cases.

2.4 Drug Release

To analyze the kinetic release of EHMC, samples of 1 g of the treated fabric were submerged into thermostated vessels filled with deionized water at semi-infinite bath conditions at a temperature of 37°C . The semi-infinite bath is called to the system which has one limited direction and extends infinitely in the other; therefore it can be considered that the diffusion into the edges can be neglected. The amount of active principle delivered to the bath was determined by UV-Vis Spectrophotometry at different times (from 0 to 200 hours).

3. RESULTS AND DISCUSSION

3.1. Treatment of the fabrics with microcapsules

The application of the active agent vehiculized in a microencapsulated formulation 20% diluted (8.3% of dry product and 7.5% EHMC) on the textile substrates was performed by foulard in an attempt to achieve an approximately 80% pick-up (Product percentage collected in the fabrics after the Pad-Dry stage). The percentages of pick-up for the different fabric treated, the percentages of theoretical product present in each fabric taking into account the composition of microcapsules (8.3% product/91.7% water), as well as the percentages of dry product applied calculated by weight difference between dry fabric after Pad-Dry process and dry initial fabric are shown in Table 2, according to the conclusions of a previous paper [13].

Table 2. Results of the finishing process of several textile fabrics: % pick-up and the theoretical percentage of product present in the wet fabrics after impregnation; and % o.w.f. (on weight of fibres) of product applied, calculated by weight difference between dry non-treated textile and dry textile after Pad-Dry process.

Textile	MICROCAPSULES	
	% Pick-up (% theoretical product)	% o.w.f. Dry product applied
PA	80,94 (6.72)	55,40
PAC	79,75 (6.62)	62,88
PET	81,17 (6.74)	37,73

When comparing the experimental results obtained for the different fibers studied, some comments have to be done:

The amount of bath absorbed by the different samples is very similar (very close to the expected 80%).

Dry matter content determined differs slightly. PET fibre shows less content, probably due to its hydrophobic nature and to the non-existence of ionic groups in its structure

PA, at the impregnation conditions (pH=4.1) must have bigger percentage of terminal amine groups in its ionized ($-\text{NH}_3^+$) form than carboxylic groups. That can suggest the existence of an electrostatic attraction between polymer chains of PA and microcapsules. This can explain the higher content of dry matter detected for PA in respect to PET.

In the case of PAC fibres, at the experimental conditions used, Sulphate groups should be in its ionic form and carboxylic in the neutral one. That is just the contrary than in PA fibres, although PAC shows a higher dry matter content than PA.

Nevertheless, what is common to the three types of fibres is the existence of zeta potential values in each one (PET: -64 to -78 mV, PA: -42 mV and PAC: -47 mV) [14], which are similar between PA and PAC, but not with PET that shows a higher negative zeta potential.

As it can be seen in Table 2, results on dry product applied show a similar amount for PA and PAC (55.40 and 62.88 % owf) and low amount for PET (37.73% owf). We can deduce that zeta potential has a relevant influence on the process of microcapsules retention and, with certain probability, that it is responsible of those experimental results. Nevertheless this phenomenon must be studied much deeper to establish the extent of this influence.

No resin was used to promote the adhesion of microcapsules to the fabrics because one of the main factors in the preparation of a biofunctional textile is the active agent delivery mechanism given that the use of resins could interfere in this release.

3.2 Theoretical mechanisms of Drug Release

The results obtained on the kinetic release profiles for all treated fabric samples (PA, PAC and PET) are graphically plotted in Figure 2 and Table 3. Comparing the kinetic profiles obtained with the theoretical curves (A, B, C and D) indicated in Figure 1, it can be clearly deduced that the behaviour of the different fabrics was similar to the theoretical curve D. This behaviour represents a First-order release system that it corresponds to a controlled release [15, 16].

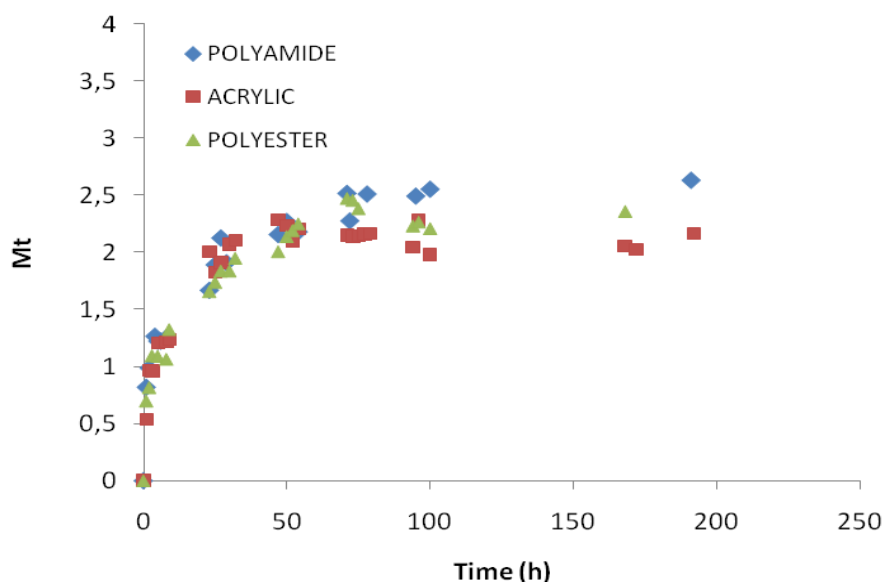


Figure 2. Release of microencapsulated sun filter (EHMC) applied onto polyamide, acrylic and polyester fabrics at 37°C. M_t (g EHC/g fabric)

3.3 Power law

Using Eq. (1), the value of the exponent n , indicative of drug transport mechanism, was calculated. As Table 3 shows, values about 0.25 were obtained, so the transport mechanism observed may be considered as a Fickian diffusion according to the drug delivery models based on the parameter n . [17, 18]

Table 3. Estimated parameters, K and n values obtained from fitting drug release experimental data to Korsmeyer-Peppas model (Eq. (1)).

Fabric type	Temperature (°C)	Classification (Figure I)	K	N	Drug Delivery System
Polyamide	37	D	0,3176	0,24	Fickian
Acrylic	37	D	0,3608	0,23	Fickian
Polyester	37	D	0,3088	0,26	Fickian

3.4 Higuchi equation

As the release mechanism of active principle in our research follows Fickian diffusion and the transport in swelling systems can be described by Fick's second Law, this system can be studied like a plane surface for short times of active principle release. Therefore, parameters were obtained from the Higuchi equation and the solution of Fick's second law for thin films, which are shown in the Table 4.

The results were calculated using release profiles, i.e. percentage of drug release (M_t/M_∞) versus $\sqrt{\text{time}}$, and were plotted for each treated fabric (Fig. 3, Fig. 4 and Fig. 5) [19, 20].

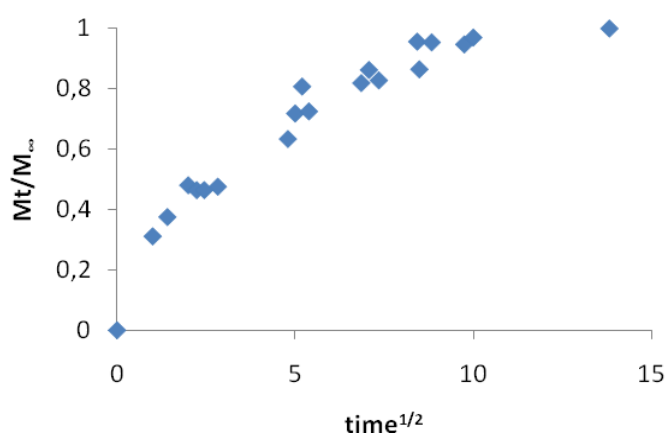


Figure 3. Release percentage of microencapsulated sun filter (EHMC) applied onto polyamide fabric at 37°C.

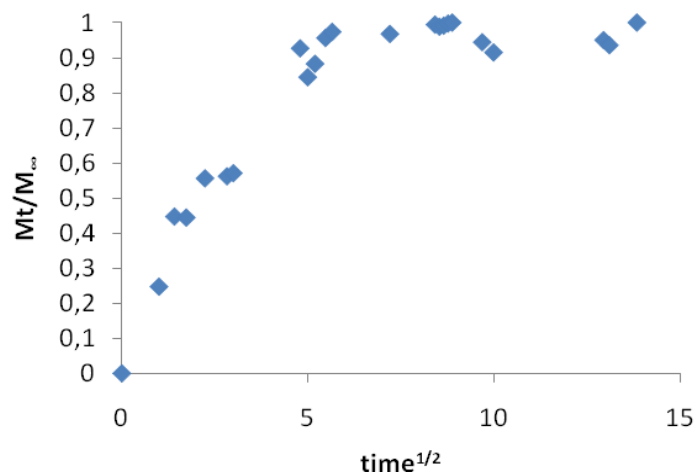


Figure 4. Release percentage of microencapsulated sun filter (EHMC) applied onto acrylic fabric at 37°C.

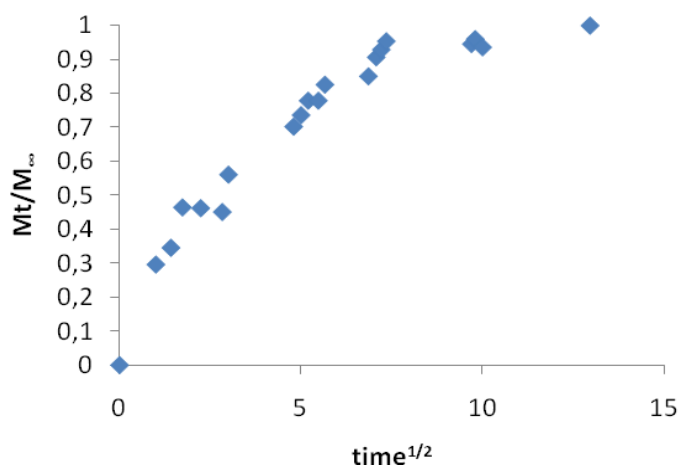


Figure 5. Release percentage of microencapsulated sun filter (EHMC) applied onto polyester fabric at 37°C.

Table 4. Parameters measured and estimated applying the mathematical models (Eq. (2) and Eq. (3)).

Fabric type	Temperature (°C)	D/δ^2	K (Higuchi)
Polyamide	37	0,0460	0,2420
Acrylic	37	0,0513	0,2555
Polyester	37	0,0372	0,2177

Results from Table 4, show the same tendency than the observed from Table 2. The increasing order on diffusion magnitudes detected for PET, PA and PAC indicates that

the rate of EHMC delivering is absolutely related with the existent gradient of concentration (dry matter) in the fiber. That behavior is according with the proposed mechanism of Fickian diffusion.

From the results obtained, it seems that the main factor for kinetic delivery rate is the behavior and capacity of fabrics to absorb more or less microcapsules from the bath. Therefore, when trying to apply to industry, regulation of the delivery rate will depend mainly on the impregnation percentage and on the initial concentration of the microcapsules present in to the pad-liquor bath.

4. CONCLUSIONS

In this study it has been demonstrated that the controlled release dosage of active principle can be possible. The characterization of the mechanism of drug release can be defined using equations of Power Law, when Fickian diffusion is assumed. Higuchi model and the solution of Fick's second law for thin films can be also used to determine the diffusion coefficient of drug release.

For each polymer-based fibre, the delivery action is similar, so the chemical structure of the fabric is not an important parameter in this system. Although, the kinetic models have certain limits on their applicability in different systems, it has been demonstrated that the behaviour of the synthetic fabrics studied, considering their own absorption capacity, follows the same release mechanism, that is a Fickian diffusion.

5. ACKNOWLEDGEMENTS

The authors acknowledge the financial support of the National Projects from Ministerio de Educación y Ciencia (Spain), Ref. CTQ-PPQ2009-13967-C03-01 and MAT2010-20324-C02-02. Thanks are also due to the Lipotec Group for supplying microcapsules.

6. REFERENCES

1. Ijeoma F. Uchegbu, Drug Delivery, *Polymers in Drug Delivery*. Taylor & Francis Group, LLC, (2006) 1-5.
2. Rubio L., Alonso C., Coderch, L., Parra J. L., Martí, M., Cebrián, J., Navarro, J. A., Lis M. and Valldeperas J. Skin Delivery of Caffeine Contained in Biofunctional Textiles. *Textile Research Journal*, 2010: **80**(12): 1215-1221.
3. Sáez, V., Hernáez, E., Angulo L.S. Mecanismos de liberación de fármacos desde materiales polímeros, *Revista Iberoamericana de Polímeros*, 2004: **5**: 55-69.
4. Sáez, V., Hernáez, E., Angulo L.S. Sistemas de liberación controlada de medicamentos, *Revista Iberoamericana de Polímeros*, 2002: **3**: 1-17.
5. Pharmacy - Encyclopedia Of Controlled Drug Delivery, V 1&2, (1999) 495-497.
6. Siepmann, J., Kranz, H., Bodmeier, R., Peppas, N. A. HPMC – Matrices for Controlled Drug Delivery: A new Model Combining Diffusion, Swelling, and Dissolution

Mechanisms and Predicting the Release Kinetics, *Pharmaceutical Research*, 1999: **16**(11): 1748-1756.

7. Abdekhodaie, M. J., Cheng, Y. – L. Diffusional release of a dispersed solute from planar and spherical matrices into finite external volume, *Journal of Controlled Release*, 1997: **43**: 175-182.

8. Siepmann, J., Lecomte, F., Bodmeier, R. Diffusion- controlled drug delivery systems: Calculation of the required composition to achieve desired release profiles, *Journal of Controlled Release*, 1999: **60**: 379-389.

9. Kumari, K., Kundu, P.P. Studies on in vitro release of CPM from semi-interpenetrating polymer network (IPN) composed of chitosan and glutamic acid, *Bulletin of Materials Science*, 2008: **31**(2): 159-167.

10. Siepmann, J., Peppas N.A. Modelling of drug release from delivery systems based on hydroxypropyl methylcellulose (HPMC), *Advanced Drug Delivery Reviews*, 2001: **48**: 139-157.

11. Peppas, N. A., Keys, K. B., Torres – Lugo M., Lowman, A. M. Poly (ethylene glycol) – containing hydrogels in drug delivery, *Journal of Controlled Release*, 1999: **62**: 81-87.

12. Brazel, C.S., Peppas, N. A. Modeling of drug release from swellable polymers, *European Journal of pharmaceuticals and biopharmaceutics*, 2000: **49**: 47-58.

13. Martí, M., Rodríguez, R., Carrera, N., Lis, M., Valdeperas, J., Coderch, L. and Parra, J.L. Monitoring of the microcapsule/liposome application on the textile fabrics. *Journal of Text. Inst.*, 2012: **103**(1):19-27.

14. Cutler W.G and Davies R.C. ed. Detergency Theory and Test Methods, *Surfactant Science Series. Ed. Marcel Dekker Inc. New York*, Parte I, 5, (1972).

15. Serra, L., Doménech, J., Peppas, N.A. Drug transport mechanisms and release kinetics from molecularly designed poly(acrylic acid-g-ethylene glycol) hydrogels, *Biomaterials*, 2006: **27**: 5440-5451.

16. Wang, C., Ye, W., Zheng, Y., Liu, X., Tong, Z. Fabrication of drug-loaded biodegradable microcapsules for controlled release by combination of solvent evaporation and layer-by-layer self-assembly, *International Journal of Pharmaceutics*, 2007: **338**: 165-173.

17. Ranjha, N.M., Mudassir, J., Akhtar, N. Methyl methacrylate-co-itaconic acid (MMA-co-IA) hydrogels for controlled drug delivery, *J Sol-Gel Sci Technol*, 2008: **47**: 23-30.

18. Peppas, N.A., Colombo, P. Analysis of drug release behavior from swellable polymer carriers using the dimensionality index, *Journal of Controlled Release*, 1997: **45**: 35-40.

19. Chevalier, E., Viana, M., Artaud, A., Haddouchi, S., Chulia, D. A novel application of the T-cell for flow-through dissolution: The case of bioceramics used as ibuprofen carrier, *Talanta*, 2009: **77**: 1545-1548.

20. Dredán, J., Antal, I., Rácz, I. Evaluation of mathematical models describing drug release from lipophilic matrices, *International Journal of Pharmaceutics*, 1996: **145**: 61-64.